Regulation of gene expression over cycles of torpor-arousal in thirteen-lined ground squirrels

Shannon N. Tessier

M.Sc. Carleton University, 2010

A thesis submitted to the Faculty of Graduate Studies and Research in partial fulfillment of the requirements for the degree of

Doctor of Philosophy

Department Biology

Carleton University

Ottawa, Ontario, Canada

The undersigned hereby recommend to the Faculty of Graduate Studies and Research acceptance of this thesis

"Regulation of gene expression over cycles of torpor-arousal in thirteen-lined ground squirrels"

submitted by

Shannon Noëlla Tessier, M.Sc.

in partial fulfillment of the requirements for the degree of Doctor of Philosophy

_____
Chair, Department of Biology

_____
Thesis Supervisor

_____
External Examiner

Carleton University

Abstract

Mammalian hibernators undergo profound behavioural, physiological and biochemical changes to cope with hypothermia, ischemia-reperfusion, and finite fuel reserves during days or weeks of continuous torpor. Against a backdrop of global suppression of energy-expensive processes such as transcription and translation, selected genes/proteins are strategically up-regulated to meet challenges associated with hibernation. Hence, hibernation involves substantial transcriptional and post-transcriptional regulatory mechanisms and provides a model to determine how a set of common genes/proteins can be differentially regulated to enhance stress tolerance beyond that which is possible for nonhibernators. The present research analyzed epigenetic factors, signal transduction pathways, transcription factors, and RNA binding proteins that regulate gene/protein expression programs that define the hibernating phenotype. Epigenetic factors alter gene expression programs by influencing the accessibility of DNA promoter regions to the transcriptional machinery. While DNA methylation was not differentially regulated comparing summer and winter animals, posttranslational modifications on histone proteins were responsive to torpor-arousal, possibly providing a mechanism to dynamically alter chromatin structure. Unique posttranslational modifications on H3 and H2B were identified by mass spectrometry; these have never been found in other organisms. Signal transduction pathways such as mitogen-activated protein kinases convert information received at the cell surface to regulatory targets within cells that promote changes in gene expression. Results showed that MAPK regulation is crucial during arousal from torpor in muscle and heart. Important cytoprotective features needed for hibernation are antioxidant defenses; regulation of antioxidant genes is under primary control of transcription factors, such as Nrf2. Data

presented elucidates the regulation of Nrf2 transcription factors by post-translational modifications (e.g. serine phosphorylation, lysine acetylation) and protein-protein interactions with a negative regulator (KEAP1) during hibernation. Finally, a role for RNA binding proteins including TIA-1, TIAR, and PABP-1 is described. Data showed the localization of RNA-binding proteins to subnuclear structures which may represent highly organized storage centers and/or enhance mRNA stability. Taken together, the thesis identifies novel regulatory mechanisms that aid suppression of transcriptional and translational rates, while also coordinating complex pathways that selectively enhance cytoprotective pathways aimed at mitigating stresses associated with torpor-arousal.

Acknowledgements

There are so many people to thank and with so little space. I am one of the luckiest women to be surrounded by so many amazing people who have inspired, encouraged, and supported me in countless ways. First and foremost, I would like to sincerely thank my thesis supervisor and scientific parents Dr. Kenneth B. Storey and Janet Storey. Ken and Jan, you may not realize this but I was watching and learning from everything you both did. I was paying attention. You have both taught me so much and I am sure it won't end here. Thanks for always pushing me to higher levels of achievement, encouraging me to try new things, offering guidance while also leaving room to problem-solve on my own, and offering no shortage of "danger-tunities." I feel tremendously grateful for your great advice in all aspects of my life, but more importantly for the confidence and motivation you have instilled in me. Also, thanks to my committee members, Dr. Maria DeRosa and Dr. Kathleen Gilmour, who have played an active role in my scientific development during both my master's and doctoral studies.

I would also like to thank my family for their unwavering support in everything and anything I do. Thanks to my parents for supporting my insatiable desire to travel the world since these travels ultimately became a huge part of who I am today. To my mother and step-father, thank you for listening to me over breakfast on that fateful day back in 2006. I often look back at those beginnings and feel proud to see how we have grown the charity together. To my father and step-mother, thank you for putting all your trust in me and always rallying behind me when I needed it most. A special thanks to my brothers and best friends Chris, Darren, Marc and Eric. It's hard to imagine the person I would be without your influence, protection, and support. To Denis, you are perfect in my eyes and every day is better with you in my life. Thanks for being there for me during the bad and

celebrating with me throughout the good. Thanks for your patience; it was essential during my studies. Thanks for your advice and guidance; it helped me overcome hills that seemed like mountains. Thanks for the laughter and adventures we shared; I look forward to so many more to come.

A huge thanks to my childhood friends who never missed a moment throughout my life. I am sure we will grow old together just as we have always envisioned. Finally, I would like to thank all Storey lab members (you know who you are) who have made every day enjoyable. I have learned so much from each of you and look forward to endless friendships.

Table of Contents

List of Abbreviations

5-caC	5-carboxylcytosine
5-fC	5-formylcytosine
5-hmC	5-hydroxymethylcytosine
5-mC	5-methylcytosine
13LGS	Thirteen-lined ground squirrel
AB	Amorphous bodies
AP-1	Activator protein 1
APS	ammonium persulfate
ARE	Antioxidant response element
ATF2	Activating transcription factor-2
ATF4	Activating transcription factor-4
ATP	Adenosine triphosphate
BLAST	Basic Local Alignment Search Tool
bp	Base pair
bZIP	Basic leucine zipper domain
CaMKKβ1	Calcium/calmodulin-dependent protein kinase kinase β1
CB	Coiled bodies
CBP	CREB-binding proteins
cDNA	complementary deoxyribonucleic acid
CK2	Casein kinase II
CNK1	Connector Enhancer of KSR-1
Co-IP	Co-immunoprecipitation
CpG	Cytosine-phosphate-guanine

CRE	cAMP response element
CREB1	cAMP responsive element binding protein 1
ddH_2O	distilled deionized-H_2O
DEPC	Diethylpyrocarbonate
DMP	Dimethyl pimelimidate
DNA	Deoxyribonucleic acid
DNMT	DNA methyltransferase
DTT	Dithiolthreitol
EA	Early arousal
EC	Euthermic cold room
EDTA	Ethylenediamine tetraacetic acid
eIF	Eukaryotic translation initiation factor
ELK1	ETS domain-containing protein
ELM	Eukaryotic Linear Motif
EN	Entrance into torpor
ER	Endoplasmic reticulum
ERK	Extracellular-signal-regulated kinases
EST	Expressed Sequence Tags
FGM	Fibro-granular material
FOXO	Forkhead box, class O proteins
GPox	Glutathione peroxidase
GST	Glutathione S-transferase
HCl	Hydrochloric acid
HDAC	Histone deacetylase

Hepes	4-(2-hydroxyethyl)-1-piperazineethanesulfonic acid
HIF-1α	Hypoxia-inducible factor-1 alpha
HO-1	Heme oxygenase-1
HRP	Horse radish peroxidase
HSP	Heat shock protein
IA	Interbout arousal
JIP	JNK-interacting protein
JNK	c-Jun amino-terminal kinase
kDa	Kilodalton
KEAP1	Kelch-like ECH-associated protein 1
KSR	Kinase Suppressor of Ras
LT	Late torpor
MAFbx	Muscle atrophy F box/atrogin-1
MAPK	Mitogen-activated protein kinase
MAPKK	MAP kinase kinase (MAP2K, MEK, or MKK)
MAPKKK	MAPK kinase kinase (also MAP3K or MEKK)
MEF2	Myocyte enhancer factor-2
MEK1	MAP kinase kinase 1 (MAP2K, MAPKK, or MKK)
MEKK	MAPK kinase kinase (also MAP3K or MAPKKK)
MKK	MAPKK, MAP2K, or MEK
MLK	Mixed-lineage kinase family
mRNA	messenger ribonucleic acid
MSK1	Mitogen- and stress-activated protein kinase
MuRF1	Muscle ring finger 1

NaCl	Sodium chloride
NaF	Sodium fluoride
Na_3VO_4	Sodium orthovanadate
NF-κB	Nuclear factor kappa-light-chain-enhancer of activated B cells
NLK	Nemo-like kinase
Nrf2	Nuclear factor (erythroid-derived 2)-like 2
PABP-1	Poly(A)-binding protein
PAGE	Polyacrylamide gel electrophoresis
PBS	Phosphate-buffered saline
PCR	polymerase chain reaction
PERK	Protein kinase RNA-like ER kinase
PGC-1α	PPARγ coactivator 1-alpha
PI3K	Phosphoinositide 3-kinase
PKC	Protein kinase C
PMF-1	Polyamine-modulated factor-1 protein
PMSF	Phenylmethanesulfonylfluoride
POSH	plenty of SH3
PPARγ	Peroxisome proliferator-activated receptor gamma
PRD	Prion-related domain
PTM	Post-translational modification
PVDF	Polyvinylidine fluoride
RBD	RNA-binding domain
RNA	Ribonucleic acid
RNA POL II	RNA Polymerase II

RNF4	RING finger protein 4
RNP	Ribonucleoprotein
ROS	Reactive oxygen species
RRM1-3	RNA recognition motifs
rRNA	ribosomal RNA
RT	Room temperature
SAPK	Stress-activated MAPK
SDS	Sodium dodecyl sulfate/ lauryl sulphate
SIRT1	Sirtuin 1
sMaf	small musculoaponeurotic fibrosarcoma
SOD	Superoxide dismutase
SSC	Sodium chloride and sodium citrate
SSCT	SSC with Tween
ssDNA	single-stranded DNA
SUMO	Sumoylation
TAD	Transactivation domain
TAE	Tris-acetate-EDTA
T_b	Body temperature
TBS	Tris-buffered saline
TBST	TBS-Tween
TEMED	N, N, N', N'-tetramethylethylenediamine
TET	Ten-eleven translocation
TF	Transcription factor

TIA-1	T-cell intracellular antigen 1
TIAR	TIA1-related
TMB	Tetramethylbenzidine
TRE	Tetradecanoyl-phorbol ester response element
Tris	Tris(hydroxymethyl)aminomethane
Ub-E1	Ubiquitin activating enzyme
Ub-E2	Ubiquitin conjugating enzyme
Ub-E3	Ubiquitin ligase
UTR	Untranslated region

List of Figures

List of Tables

List of Appendices

Chapter 1

General Introduction

The expression of mammalian genes is regulated by epigenetic factors, signal transduction pathways, transcription factors and other constituents of the transcriptional machinery, mRNA processing factors, components of the translational apparatus, and the subcellular distribution of each these factors. Epigenetic factors such as DNA methylation influence the binding of transcription factors or corepressors and post-translational modifications of histone tails alter chromatin structure and accessibility, collectively affecting transcriptional competence [Ling and Groop 2009]. The eukaryotic transcriptional machinery consists of RNA polymerase II, transcription factors, and other accessory factors which recognize specific regulatory elements in gene promoter regions in order to implement active transcription [Thomas and Chiang 2006]. During transcription, pre-mRNA is processed by a vast array of proteins which orchestrate 5'capping, constitutive and alternative RNA splicing, and 3' polyadenylation which may also be influenced by regulatory elements present in the 5' and 3' UTR [Bentley 2002]. The journey continues as mRNAs interact with diverse RNA binding proteins and are shuttled from the nucleus to the cytoplasm where they interact with the translational machinery and are subject to intricate regulatory features [Proud 2002]. Also, microRNAs and other non-coding RNAs exert control over translation [Morin et al. 2008a; Liu et al. 2010; Kornfeld et al. 2012]. Finally, overlaid alongside each of these steps are subcellular domains which act to enrich and localize factors into organizational centers for improved efficiency and control of mRNA fate [Mao et al. 2011].

A particularly interesting model for the regulation of gene/protein expression in response to environmental stress is mammalian hibernation. Hibernation is defined as a reversible state of seasonal heterothermy employed as a survival strategy to survive long

winter months with limited food [Wang and Lee 1996]. Seasonal hibernators cycle through multiple periods of profound torpor (where core body temperatures can fall to near ambient 0-5°C) interspersed with intermittent periods of arousal until environmental conditions in the spring return to a state that again can support normal euthermic life [Wang and Lee 1996]. In this capacity, mammalian hibernators endure hypothermia, ischemia-reperfusion, and restricted nutritional resources and yet transition seamlessly to and from the torpid state. The ability to induce a hibernation-like state holds immense clinical promise since it would serve as a means of lowering tissue energy needs and reduce damage caused by ischemia-reperfusion; however, it is also associated with many adverse effects in humans and most mammals. Nonetheless, hypometabolic states have been applied for treatment of stroke, heart attack, multiple organ failure, as well as brain and spinal cord injury [Lee 2008]. Moreover, the ability to induce and maintain a dormant state could improve chances for survival by injured patients during transport to medical facilities or extend the viability of donor organs removed for transplantation. Importantly, it has been proposed that this capacity to survive during severe seasons may rely to a great extent on regulated and coordinated use of common genes/proteins rather than specially evolved ones [Srere et al. 1992]. This principle not only signifies that human cells may one day be able to take advantage of these positive survival strategies for the improvement of human health and disease, but suggests that the principles which define a hibernating cell hold a wealth of knowledge, especially as it pertains to the regulation of gene/protein expression programs.

Mammalian hibernators are an excellent model system for uncovering mechanisms involved in gene/protein expression in response to stress since they display

regulatory mechanisms which act to globally reduce transcription [Morin and Storey 2006] and translation [Frerichs et al. 1998] during torpor, yet a small subset of stress-responsive pathways must be activated in order to overcome the stresses associated with the hibernating phenotype [Hittel and Storey 2001; Eddy et al. 2005; Yan et al. 2008]. Furthermore, many studies of mammalian hibernators have shown that the total pool of mRNA remains stable [Frerichs et al. 1998] but there are many examples of a discord between mRNA and protein expression profiles [Shao et al. 2010]. These data suggest that mRNA substrate availability does not explain the inhibition of protein synthesis nor does it provide a full understanding of the differential regulation of the hibernator proteome. Taken together, mammalian hibernators are subject to substantial transcriptional and post-transcriptional regulation and various mechanisms have been elucidated to date [Storey and Storey 2004b]. For example, work spanning a range of mammalian hibernators has identified epigenetic controls that coordinate the global suppression of transcription [Morin and Storey 2009; Storey 2014], the involvement of signal transduction pathways and their regulatory effect on gene expression [Eddy and Storey 2007; MacDonald and Storey 2005; Abnous et al. 2012], the involvement of transcription factors and their regulation by posttranslational modifications in achieving a directed cellular response to the various stresses faced as a result of hibernation [Carey et al. 2000; Cai et al. 2004; Lee et al. 2007; Mamady and Storey 2008; Morin et al. 2008b; El Kebbaj et al. 2009; Tessier and Storey 2012], and, finally, the regulation of translation via post-translational modifications on ribosomal initiation/elongation factors [Wu and Storey 2012; Van Breukelen et al. 2004] and the disaggregation of polyribosomes during hibernation [Knight et al. 2000; Hittel and Storey, 2002; Pan and Van Breukelen 2011].

Hibernation

The ability to enter a hypometabolic state occurs widely across the animal kingdom and examples of mammalian hibernators include fat-tailed mouse opossums, ground squirrels, little brown bats, hedgehogs, tenrecs, lemurs, and bears (Storey 2010). Hibernation is a response to limited food reserves and decreases in T_b which approach ambient temperatures. Hibernating ground squirrels generally exhibit low body temperatures (~5°C for thirteen-lined ground suiqrrels), while other species such as lemurs may hibernate at relatively higher temperatures. Many species use only body fuel reserves to survive the winter necessitating a phase of hyperphagia prior to hibernation that hugely increases body fat reserves [Storey 2010]. Data from several hibernators suggest a strong preference for lipid catabolism during torpor coupled with mechanisms which mediate carbohydrate sparing [Carey et al. 2003; Dark 2005; Shao et al. 2010]. As shown in Fig. 1.1, hibernation generally consists of multiple bouts of deep torpor, either occurring on the order of days or weeks, with intermittent periods of arousal during which animals rewarm to euthermic body temperature [T_b; Wang and Lee 1996]. The mechanisms utilized to limit energy expenditure involve profound behavioural and physiological changes that can be traced to important molecular "switches" that shut down metabolism and aid in meeting challenges associated with hypometabolism [Storey 2010; Bouma et al. 2012]. For example, mammals limit activity in their burrows as they settle into a deep torpor and this behaviour is matched with the strong downregulation of ATP costly intracellular processes including gene transcription and protein synthesis [Wang and Lee 1996; Storey and Storey 2004]. A secondary, yet equally important component to the hypometabolic state is the selective upregulation of multiple

preservation mechanisms that counteract the otherwise deleterious aspects of surviving hypothermia, ischemia-reperfusion, and restricted ATP availability [Storey and Storey 2004, 2010; Storey 2010].

A torpor bout begins with a process of regulated metabolic suppression which in turn leads to a fall in T_b. This has been documented multiple times. For example, in the liver of ground squirrels, a reduction in mitochondrial metabolism precedes the drops observed in T_b [Chung et al. 2011] and bears demonstrate only minimal changes in T_b yet display a 75% decrease in basal rates [Tøien et al. 2011]. This reduction in T_b further slows metabolic rate allowing some hibernating species to achieve a T_b that approaches 0^oC, with torpor metabolic rates of <1% of their resting euthermic rate [Geiser 2004; Heldmaier et al. 2004; Chung et al. 2011]. Relatively low T_b is not the only challenge hibernators must overcome. In ground squirrels heart rate, respiration rate and cerebral blood flow fall to approximately 1%, 3% and 10% of their normal levels, respectively [Zatzman 1984; McArthur and Milsom 1991; Martin et al. 1999; Dave et al. 2012]. These and other physiological parameters are rapidly returned to euthermic levels during intermittent arousals supported by a 10-20 fold surge in oxygen consumption within minutes as the animal rewarms to 37°C [Storey 2003; Staples 2011]. This surge in oxygen consumption increases the production of reactive oxygen species (ROS) necessitating most organisms that use hypometabolism to possess increased antioxidant defenses, which protect macromolecules from damage by ROS during both extended periods of torpor and the arousal process [Storey 1996].

DNA methylation and histone modifications

The field of epigenetics – the study of heritable changes in gene expression that are not caused by changes in the underlying DNA sequence – is an explosive area of research that has begun to provide valuable insight into the functional specialization of cells containing essentially the same genetic information. Two particularly interesting epigenetic mechanisms of interest in the present thesis are DNA methylation and posttranslational modifications on histone proteins. DNA methylation involves the addition of a methyl group to cytosine residues in DNA, primarily those that are distributed at CpG islands. Occurring near transcription start sites, DNA methylation has a general repressive effect on gene expression. Another epigenetic mechanism associated with the chromosomes on which they act is posttranslational modifications on histone proteins. One of the most commonly studied posttranslational modifications on histone proteins is acetylation which acts to neutralize positively charged amino acid side chains that are attracted to the negatively charged DNA backbone. Therefore, the addition of an acetyl functional group has the general effect of relaxing chromatin to a more accessible structure. Epigenetic modifications play a role in transcriptional regulation by modifiying how transcription factors interact with DNA regulatory elements [Medvedeva et al. 2014]. DNA methylation at transcription factor binding sites prevents their interaction with DNA and transcription factors recruit coregulators such as p300/CBP (a histone acetyltransferase) into complexes which catalyze histone modifications.

The control of gene expression is vital to surviving mammalian hibernation since metabolic rate depression relies on coordinated decreases in energy-consuming processes such as transcription [Morin and Storey 2006; Storey 2014]. It may be suggested, therefore, that one possible mechanism to achieve global controls on gene expression

may include epigenetic factors such as DNA methylation and posttranslational modifications on histone proteins. Preliminary work has already identified a potential regulatory role for epigenetic factors during hibernation, although the data are very sparse. Morin and Storey (2006) identified two forms of covalent modifications on histone H3 that are associated with active transcription and that were both significantly reduced in muscle during hibernation. Consequently, these data suggest that epigenetic factors may play an important role during hibernation and has fueled further advances in the area of metabolic rate depression.

Signal transduction

Cellular responses to various stimuli rely on the coordination of complex signal transduction pathways and their interaction with a range of effector targets aimed at mitigating exogenous and endogenous perturbations. Conserved from yeast to humans, the family of mitogen-activated protein kinases (MAPK) has entered the spotlight as an important regulator of gene expression, cell survival and apoptosis, among many others. MAP Kinases contain a three-tiered signal relay in which an activated MAP kinase kinase kinase (MAPKKK or MEKK) activates a MAP kinase kinase (MAPKK or MEK), which then activates a MAP kinase (extracellular-signal-regulated kinases, ERK; c-Jun N-terminal kinases, JNK; p38) [MacDonald, 2004]. One type of particularly relevant downstream target are transcription factors since these signals change the transcriptional program with influences in all aspects of cellular survival and physiological responses. In many ways, therefore, transcription factors represent the bridge point between sensing external cues and directing the transcription of genes which will ultimate allow a cell to

survive adverse conditions. Another central channel of MAPK regulation includes the regulation of heat shock protein 27 (HSP27) which is a chaperone protein that also plays an established role in the regulation of translation and influences stress-induced apoptosis [Cuesta et al. 2000; Zheng et al. 2006].

Signal transduction pathways and their regulatory effects on gene expression have been shown to be pivotal in meeting challenges associated with hibernation in ground squirrels and bats [Tessier and Storey 2012, Mamady and Storey 2006; Eddy and Storey 2007; Morin et al. 2008]. Furthermore, the actions of transcription factors have been shown to play a role in enhancing stress tolerance including the activation of the unfolded protein response by ATF4 [Mamady and Storey 2008; Eddy and Storey 2007], modulating antioxidant capacity by Nrf2 and NF-κB [Morin et al. 2008; Allan and Storey 2012; Carey et al. 2000], protecting and readjusting cellular metabolism by HIF-1α [Morin and Storey 2005; Maistrovski et al. 2012], and playing a role in the regulation of lipid metabolism by PPARγ and PGC-1α [Eddy et al. 2005], amongst many other examples [Tessier and Storey 2010; Tessier and Storey 2012; Brooks et al. 2011]. Furthermore, data from multiple studies with hibernators suggest that heat shock proteins play an important role during torpor-arousal [Carey et al. 2003; Eddy et al. 2005; Epperson et al 2010]. Consequently, studies which trace the activation of signal transduction networks and their effector molecules (e.g. transcription factors, HSPs) would help to bridge connections between signaling and gene expression, while also developing our understanding of the stress response. Analysis of these pathways in a hibernating animal with higher resistance to various forms of stress would increase our

understanding of the mechanisms of adaptation and compensation that are available to nonhibernating mammals.

Nrf2 and antioxidant defenses

Attack by ROS is a major cause of damage to cellular macromolecules (e.g. DNA, protein, lipids) and therefore, all organisms maintain robust antioxidant defenses that can nonetheless be overwhelmed in a variety of stress and disease states [Halliwell and Gutteridge 2007]. Adaptation of antioxidant defenses is widespread as a response to physiological or environmental challenges and, in fact, the first evidence of this actually came from hibernators. In 1990, Buzadzic et al. showed that antioxidant defenses were elevated seasonally to very high levels in brown adipose tissue of hibernating ground squirrels to counter ROS produced in association with the extreme rates of oxygen consumption needed to power thermogenesis during arousal. The expression of antioxidant enzymes at the optimal time, concentration and in the optimal cellular compartment is the key to the maintenance of redox homeostasis. Regulation of antioxidant genes is under the primary control of redox-sensitive transcription factors which rescue cells by the upregulation of key antioxidant enzymes [Chan and Kan, 1999; Storey, 2010]. One of these is Nrf2 (Nuclear factor (erythroid-derived 2)-like 2, also known as NFE2L2), a basic leucine zipper transcription factor that regulates a number of antioxidant/detoxification enzymes [Giudice and Montella, 2006].

There are many signals known to regulate transcription factors (TFs), and certainly more to be uncovered. It is estimated that the majority of transcription factors do not operate alone but rather in complexes. These associations, whether they act to

enhance, inhibit, or selectively direct transcription are extremely dynamic and stress responsive. The signals which initiate complex formation or, conversely, promote complex dissociation are regulated by signal transduction pathways and a multitude of post-translational modifications (PTMs). While phosphorylation plays pivotal roles in the control of transcription factor regulation, other understudied PTMs, such as acetylation, methylation, sumoylation, ubiquitination, etc, are also beginning to be recognized as having important regulatory roles. Over 80 transcription factors as well as their accessory proteins are now known to possess at least one of these PTMs, aside from phosphorylation, demonstrating the importance of such regulatory mechanisms to the cell [Glozak et al. 2005]. Therefore, it is of interest to map the protein-protein interactions as well identify PTMs on Nrf2 transcription factors over a time course of torpor and arousal in order to elucidate new mechanisms of TF regulation.

RNA binding proteins and nuclear dynamics

One prominent feature of eukaryotic cells is the ability to organize discrete subcellular compartments, enabling more efficient systems with enhanced control. To date, numerous subcellular compartments and the microenvironments therein have been identified as playing a role in the post-transcriptional regulatory program including several stress-responsive nuclear (e.g. fibro-granular material, amorphous bodies, Cajal bodies) and cytoplasmic bodies (e.g. stress granules). Vast networks of RNA-protein and protein-protein complexes are recruited to specific sites of transcription, splicing, processing, storage, and transport [Zimber 2004], resulting in their enrichment and improving the efficiency of mRNA processing. In contrast, limiting components of these

large regulatory complexes may be sequestered in compartments such as the nucleolus rendering them unavailable, and effectively inhibiting unwanted cellular functions [Audas et al. 2012]. With the growing list of environmental stress conditions and disease states that are related to changes in cellular compartmentation, it is becoming increasingly important to understand these changes in the context of gene/protein expression programs. Mammalian hibernators present a unique opportunity to explore these concepts and these are relevant to the hypometabolic state because this form of control allows mRNA/proteins to be regulated without changes in their total expression.

The presence of nuclei containing structural components that form in response to torpor/hibernation has been observed in several tissues of the hazel dormouse (*Muscardinus avellanarius*) and the edible dormouse (*Glis glis*) [Zancanaro et al. 1993; Malatesta et al. 1994a, b, 1995, 1998, 1999, 2000; Tamburini et al. 1996]. For example, structures including coiled bodies (CBs) and amorphous bodies (ABs) are suggested to represent storage sites for splicing factors that can be rapidly used upon arousal [Malatesta et al. 2001]. The presence of these nuclear structures is correlated with reduced metabolic rate and their reversal occurs within a few minutes of arousal, providing a mechanism for the rapid resumption of protein synthesis [Malatesta et al. 2001]. Additionally, using linear sucrose gradients aimed at separating monosome versus polyribosome fractions, protein constituents that regulate ribosome transitions have also been studied [Hittel and Storey 2002]. In this study, a redistribution of PABP-1 (a protein known to be associated with cytoplasmic stress granules) from monosome fractions (fractions 8–10) to fractions 4, 5, and 7 occurred during torpor. Although not confirmed by immunofluorescence, fractions 4, 5, and 7 were suggested to represent mRNA

sequestered into stress granules during hibernation. Therefore, there is compelling evidence to suggest that nuclear and cytoplasmic structures may play a critical role in torpor-arousal transitions. Since knowledge of the exact functional role and interplay of each structure is in its infancy, it is of interest to identify the role of RNA binding proteins known to be involved in posttranscriptional regulation and the formation of subcellular structures in the hibernating mammal.

Objectives and hypotheses

Since mammalian hibernators are subject to substantial transcriptional and post-transcriptional regulation as they transition to and from the torpid state, I chose for my Ph.D. thesis to explore multiple regulatory mechanisms that can guide gene/protein expression and provide the hibernating cell with the means to survive the stresses associated with cycles of torpor-arousal (e.g. hypothermia, ischemia-reperfusion). I chose to approach this task at multiple levels including the analysis of global epigenetic controls on gene expression including DNA methylation and histone modifications (Chapter 2), the link between signal transduction pathways and gene expression (Chapter 3), expanding the known types of regulatory factors that influence transcription factor activity to under-studied PTMs (e.g. acetylation, ubiquitination, and sumoylation) and protein-protein interactions (Chapter 4), and analysis of the involvement of RNA-binding proteins and subcellular compartmentation in post-transcriptional regulation (Chapter 5). Each of these biochemical themes were analyzed in three major tissues (muscle, heart, liver) of the hibernating thirteen-lined ground squirrel (*Ictidomys tridecemlineatus*). Muscle was selected for its importance in shivering thermogenesis during arousal, while

the heart must maintain function at low body temperatures. Finally, liver was chosen since it plays an established role in metabolism and in the maintenance of homeostasis during hibernation. While each chapter is aimed at deepening the understanding of established themes in the field of hibernation, the present thesis also utilizes novel approaches and makes significant advances.

Objective 1: Epigenetic regulation, histones and DNA methylation.

As mentioned above, metabolic rate during torpor can fall to <1% of resting euthermic rate when animals are hibernating at low ambient temperatures, necessitating molecular controls which provide the cell with the means to virtually shut down all but the most vital metabolic processes, thereby lowering metabolic rate and conserving precious fuel/energy. One such mechanism may involve controls which act to globally reduce transcription. Initial studies in thirteen-lined ground squirrels evaluated the involvement of RNA polymerase activity, histone deacetylase activity (HDAC), and two forms of covalently modified histone H3 (phosphorylated Ser 10 and acetylated Lys 23) as mechanisms of transcriptional suppression; all were consistent in indicating an overall decrease in transcriptional activity during torpor [Morin and Storey 2006]. In this thesis, I greatly extended the analysis of epigenetic mechanisms as methods of achieving global reductions on gene expression, focusing particularly on direct controls on DNA via cytosine methylation and chromatin modification by PTM controls on histone proteins H3, H2A, H2B, and H4.

Hypothesis 1: Epigenetic mechanisms including DNA methylation and posttranslational modifications on histone H3, H2A, H2B, and H4 will provide a means

of reducing transcriptional rates during torpor and this response will be reversed during arousal.

Chapter 2 tests this hypothesis by exploring DNA modifications including methylation at the 5 position of cytosine (5-mC) which has the specific effect of reducing gene expression. Recently, additional DNA cytosine modifications have been identified including 5-hydroxymethylcytosine (5-hmC), 5-formylcytosine (5-fC) and 5-carboxylcytosine (5-caC) which are intermediates in an oxidative demethylation pathway. Levels of 5-mC, 5-hmC, and 5-caC were assessed in the muscle of thirteen-lined ground squirrel comparing summer, late torpor, and interbout arousal using a technique called DNA dot blots. Furthermore, chromatin is composed of DNA wrapped around nucleosomes consisting of two copies of each H2A, H2B, H3, H4. These core histone proteins carry epigenetic information in the form of posttranslational modifications (PTMs) and Chapter 2 focuses on the best characterized of these including acetylation (associated with relaxed chromatin), methylation (variable effects on transcription) and phosphorylation. While acetylation may be viewed as having the general effect of increasing access to DNA, the "histone code" hypothesis suggests that specific histone modifications or combinations of modifications confer unique biological functions [Strahl and Allis 2000]. Using western blots, the modifications assessed include acetylation of H3 at lysine residues K9, 14, 18, 23, 27, and 56 and phosphorylation of H3 at serine 10, as well as acetylation of H2A and H2B at K5, and H4 at K8. Finally, histone purification followed by mass spectrometry was used to identify novel PTMs on histones that are associated with the hibernation phenotype in thirteen-lined ground squirrel.

Objective 2: Linking signaling pathways to gene expression.

Signal transduction pathways and transcription factors play a vital role in hypometabolism of all model organisms assessed to date, yet the underlying molecular mechanisms that connect signaling to gene expression are not always well understood. Initial studies have shown that MAP kinases are differentially regulated in select tissues of Richardson's ground squirrels (*Spermophilus richardsonii*) comparing control and torpid conditions [MacDonald and Storey, 2005; Abnous et al. 2012]. However, the responses of MAPKs over cycles of torpor-arousal have not been assessed over the multiple stages of the full torpor-arousal cycle. MAPKs regulate a vast array of downstream substrates, although the present chapter focuses on their regulation of transcription factors and heat shock proteins. These are of particular interest because transcription factors mediate changes in the expression of specific genes, and heat shock proteins are a conserved feature of hypometabolism. Hence this thesis examines the differential regulation of MAPKs, transcription factors, and heat shock proteins since they have been attributed to overcoming ischemia-reperfusion, cold T_b, and metabolic rate depression.

Hypothesis 2: MAPK family members will be differentially regulated over the torpor-arousal cycle and this regulatory mechanism will play a role in activating select transcription factors and heat shock proteins involved in surviving hibernation.

Chapter 3 tests this hypothesis by exploring the relative expression of extracellular-signal-regulated kinases (ERK), c-Jun N-terminal kinases (JNK), and p38 in their phosphorylated active forms since these provide a convenient signature for the activation of MAPK pathways. Additionally, phosphorylated transcription factors

including CREB1, ELK1, c-Jun, ATF2, and p53 as well as total and phosphorylated forms of heat shock proteins HSP27, HSP60, HSP70 (HSP72) and HSP90α are assessed. This chapter uses multiplex Luminex® assays which are extremely sensitive - using as little as 130 ng of total protein per well. The method uses color-coded microspheres that are coated with antibodies specific for given protein targets. The microsphere-antibody captures the target from complex biological samples. Detection of the analyte is based on flow cytometry and excitation of the dyes measures the amount of analyte bound. Finally, some additional western blots are performed in order to add additional targets not available in the multiplex format.

Objective 3: Nrf2 regulation by posttranslational modifications and protein-protein interactions.

As mentioned above, transcription factors play a vital role during hibernation. Against a backdrop of global decreases in transcription/translation, select pathways must be strategically enhanced and transcription factors are vital to this response. Particularly important targets that are enhanced in hibernation are antioxidant defenses. This is needed because arousal from torpor requires a massive increase in heat production that is fueled by a 10–20-fold surge in oxygen consumption and lipid oxidation by the thermogenic organs (brown adipose and skeletal muscle). The surge in oxygen use causes a corresponding overproduction of damaging reactive oxygen species (ROS). Nrf2 is a basic leucine zipper transcription factor responsible for regulating a variety of antioxidant and detoxification enzymes, although initial studies of Nrf2 indicated that total protein levels did not change over the torpor-arousal cycle [Morin et al. 2008]. Consequently,

Nrf2 was chosen for its established role in regulating antioxidant defense genes, but also because it exhibits complex regulatory patterns that could provide an interesting model for seeking hibernation-responsive adaptations. Known regulatory mechanisms that control Nrf2 include phosphorylation which releases the inhibitor protein KEAP1, acetylation which regulates its association with its transcriptional partner MafG (thus facilitating DNA binding capacity), and ubiquitination which targets Nrf2 for degradation.

Hypothesis 3: Nrf2 transcription factors will be differentially regulated by posttranslational modifications and protein-protein interactions aimed at modifying Nrf2 activity/action during hibernation in a manner that does not require the large inputs of energy that would otherwise be needed to regulate Nrf2 via de novo synthesis of the protein.

Chapter 4 tests this hypothesis by performing co-immunoprecipitation studies that purify Nrf2 along with its binding partners across the torpor-arousal cycle in skeletal muscle of thirteen-lined ground squirrels. With Nrf2 purified samples, western blots using antibodies directed against posttranslational modifications including serine phosphorylation, lysine acetylation, ubiquitination and sumoylation are assessed. Additionally, antibodies directed against a known inhibitor of Nrf2 activity, KEAP1, are employed in order to assess the involvement of protein-protein interactions in the regulation of Nrf2.

Objective 4: RNA binding proteins and cellular compartmentation.

RNA-binding proteins such as TIA-1/R and PABP-1 play critical roles in posttranscriptional regulation with influences on transcription and mRNA splicing as well as the localization, stability, and association of mRNA transcripts with the translation machinery. Moreover, these RNA binding proteins have an established function in the formation of cytoplasmic stress granules which have been previously suggested to play roles during hibernation in thirteen-lined ground squirrels [Hittel and Storey 2002]. Additionally, TIA-1 and TIAR are expressed as two major isoforms (TIA-1a/TIA-1b, TIARa/TIARb) which display distinct functional properties and may be differentially regulated during hibernation.

Hypothesis 4: RNA binding proteins will play a role in the enhancement of mRNA stability, act as sites of transcript storage and/or play a role in pre-mRNA processing and this response will support the overall suppression of translation during torpor and its rapid resumption during arousal.

Chapter 5 will test this hypothesis by performing computational analysis in order to obtain the full TIA-1/R and PABP-1 sequences, PCR in order to identify TIA-1/TIAR isoforms, immunofluorescence and fluorescence microscopy matched with subcellular fractionation in order to determine the subcellular distribution of these factors in response to torpor, and solubility tests that distinguish soluble versus insoluble forms of TIA-1/TIAR that are typically associated with specific functions. Since RNA-binding proteins play a role in mRNA processing, these proteins could provide a framework for the global suppression of translation and selective regulation of key cellular networks during torpor, as well as facilitate the arousal from torpor and return to euthermic metabolism.

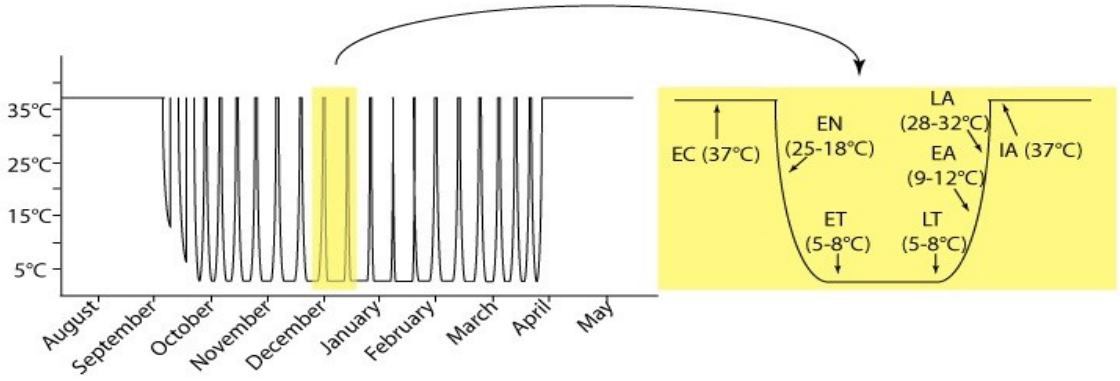

Figure 1.1: Body temperature (T_b) of a thirteen-lined ground squirrel as a function of time over one hibernation season. Highlighted in yellow is one torpor-arousal cycle. The different stages are: (1) euthermic, cold room (EC), (2) entrance (EN), (3) early torpor (ET), (4) late torpor (LT), (5) early arousal (EA), and (6) interbout arousal (IA). Modified from Hindle et al. 2011.

Chapter 2

The role of DNA methylation and histone protein modifications in achieving global controls on gene expression during mammalian hibernation.

Introduction

It was once believed that the underlying DNA sequence of our genes represented our sole mechanism of heritability. All of this changed as researchers discovered that environmental factors could alter traits without changing the nucleotide sequence of genes and this information could be passed through generations. Researchers began an active pursuit to elucidate this secondary genetic code and it soon became apparent that epigenetic regulatory mechanisms were involved in an overwhelming number of physiological and pathological processes [Jirtle and Skinner 2007]. Core epigenetic mechanisms are DNA methylation and post-translational modifications on histone proteins. Collectively, these alter gene expression programs by influencing the accessibility of DNA promoter regions to the transcriptional machinery [Ling and Groop 2009]. Since the molecular response to environmental changes require coordination of the transcriptional program [Hittel and Storey 2001; Eddy et al. 2005; Morin and Storey 2006; Yan et al. 2008], the present chapter aimed to deepen our understanding of the epigenetic factors which may contribute to global changes in gene expression during hibernation. More specifically, this chapter focuses on epigenetic factors which are physically associated with the chromosomes on which they act including DNA methylation and histone modifications.

DNA methylation is a core factor in chromatin structure and plays an important role in numerous cellular processes including embryonic development, genomic imprinting, X-chromosome inactivation, suppression of mobile genetic elements, and gene transcription regulation [Martin-Subero 2011]. In mammals, methylation located at CpG islands (regions with a high frequency of cytosine-guanine dinucleotides) are the

most important in regulatory terms and tend to be near transcription start sites [Caiafa and Zampieri 2005]. DNA methylation at the 5 position of cytosine has the specific effect of reducing gene expression and involves the transfer of a methyl group by DNA methyltransferase (DNMT) enzymes to the carbon 5 position of cytosine to produce 5-methylcytosine (5-mC) [Xu et al. 2010]**.** The field of DNA methylation analysis has expanded recently with the identification of multiple 5-methyl cytosine variants. Research has shown that the Tet family of cytosine oxygenase enzymes is involved in oxidizing 5-methylcytosine into 5-hydroxymethylcytosine (5-hmC)**,** 5-formylcytosine (5-fC) and 5-carboxylcytosine (5-caC) [Kohli and Zhang 2013]**.** The exact function of these 5-methyl cytosine variants is still not fully elucidated; however, one hypothesis suggests that they are intermediates of an oxidative demethylation pathway [Kohli and Zhang 2013].

DNA is packaged in the nucleus via interactions with positively charged histone proteins organized into nucleosomes and forming the main building blocks of eukaryotic chromatin. DNA is wrapped around nucleosomes which are composed of an octamer core containing two copies of each of histone H2A, H2B, H3, and H4 and each nucleosome is separated by linker DNA which is organized by H1. Core histone proteins carry epigenetic information in posttranslational modifications (PTMs) including acetylation, methylation, phosphorylation, ubiquitination, and sumoylation [Bönisch and Hake 2012]. PTMs occurring on histone proteins can influence histone:DNA and histone:histone interactions, especially those in the N- and C-terminal tails. Of the posttranslational modifications present on histones proteins, acetylation is one of the best characterized and is almost invariably associated with relaxed chromatin and the activation of

transcription [Shahbazian and Grunstein 2007]. In most mammals, H2B is primarily acetylated at Lys5, 12, 15, and 20, H2A at Lys5, 9, 13, and 15, H3 at Lys9, 14, 18, 23, 27, and 56, and H4 at Lys5, 8, 12, 16, and 20 [Cheung et al. 2000; Strahl and Allis 2000]. Additionally, phosphorylation at Ser10 of histone H3 is tightly correlated with chromosome condensation [Goto et al. 1999].

While epigenetic changes occur in response to various stimuli, DNA methylation patterns and histone modifications have a direct effect on the accessibility of chromatin to transcription factors thereby playing a critical role in gene expression programs. Since DNA methylation is a fairly long-term, stable modification, I hypothesized that global changes in DNA methylation contribute to the overall inhibition of transcription during the torpor phases of mammalian hibernation. Furthermore, I hypothesized that broad changes in histone acetylation and phosphorylation also contribute to gene silencing by chromatin compaction during torpor. The data in the present chapter analyze and compare DNA methylation and histone modifications in summer and winter animals and between aroused versus torpid animals during the winter season. In this capacity, a dot blot technique was used to measure relative changes in 5-mC, 5-hmC, and 5-caC in skeletal muscle of thirteen-lined ground squirrels. Additionally, previous studies on thirteen-lined ground squirrels made initial analyses of covalently modified histone H3 (phosphorylated Ser 10 and acetylated Lys 23) finding significantly reduced levels in muscle during deep torpor [Morin and Storey 2006]. In order to expand on these measurements, western blotting was used to assess Ac-H3K23 and p-H3S10 over a range of other time points in the torpor-arousal cycle. In addition, the effects of hibernation on additional acetylation sites on histone H3, H2A, H2B, and H4 were also assessed (H3 K9,

14, 18, 27, 56; H2A and H2B K5; H4 K8). In general, I predicted that acetylation and phosphorylation levels would be reduced during deep torpor and these would be reversed during arousal from torpor. Finally, I tested the idea that ground squirrel specific PTMs may occur by using a histone purification technique and mass spectrometry. As a result, well known PTMs on histone proteins were identified as well as novel modifications.

Materials and Methods

Animals

Thirteen-lined ground squirrels (*Ictidomys tridecemlineatus*), weighing 130-180 g, were wild-captured in August by a United States Department of Agriculture-licensed trapper (TLS Research, Bloomingdale, IL). Animals were transported to the Animal Hibernation Facility, National Institute of Neurological Disorders and Stroke, NIH, Bethesda, MD. Hibernation experiments were conducted by the laboratory of Dr. J.M. Hallenbeck. Thirteen-lined ground squirrels for the summer experimental condition were sampled during July and had been in the NIH colony since the previous August. They were maintained at room temperature and had hibernated the previous winter. Thirteen-lined ground squirrels were individually housed in shoebox cages in a holding room with an ambient temperature of 21°C under a 12/12-hour light/dark cycle. Animals were fitted with a sensor chip (IPTT-200; Bio Medic Data Systems, Seaford, DE) injected subcutaneously while the squirrels were anesthetized with 5% isofluorane. Animals were fed standard rodent diet and water *ad libitum* until they gained sufficient lipid stores to enter hibernation; weight typically plateaued at 220-240 g. To induce hibernation, animals were transferred to cold chambers at 4-6ºC and 60% humidity in cages containing wood shavings. Body temperature (T_b), time and respiration rate were

monitored and used to determine the stage of hibernation. Experiments were done during the winter months of December-March, and all animals (except summer animals) had been through a series of torpor-arousal bouts prior to sampling. Animals were sampled at different points over torpor-arousal cycles. They were removed from the hibernation chamber, anesthetized with isoflurane and sacrificed by decapitation within 2 minutes. Tissue samples were quickly excised and immediately frozen in liquid nitrogen. Samples were delivered to Carleton University on dry ice and stored at -80ºC until use. Tissue samples were retrieved from the following conditions: (1) EC designates euthermic, cold room; these euthermic squirrels had a stable Tb (~37°C) and high metabolic rate for at least three days. EC animals were capable of entering torpor but had not entered torpor in the past 72 hours. (2) EN designates entrance; animals that are in the entrance phase of the hibernation bout (Tb = 25-18°C) characterized by decreasing T_b (at least two successive temperature readings showed a decreasing T_b). (3) LT designates late torpor; animals that have remained in the deep torpor phase of the hibernation bout for 5 days and have not begun a periodic arousal (Tb = 5-8°C). (4) EA designates early arousal animals; characterized by an increased respiratory rate of more than 60 breaths per minute accompanied by a rising body temperature with sampling between Tb = 9-12°C. (5) IA designates interbout arousal; animals were naturally aroused after the torpor phase of the hibernation bout and reached the respiratory rate, metabolic rate, and body temperature of fully aroused animals for up to 18 hours after being in torpor for up to 5 days.

DNA extraction

Samples of frozen skeletal muscle from three time points (Summer, LT, IA) were separately extracted (N=4). DNA extraction used small amounts of tissue (25 mg) and followed manufacturer's instructions (Zymo Research Genomic DNA Tissue Prep, Cat#D3050). Briefly, a solution containing 95 µl H_2O, 95 µl 2X digestion buffer, and 10 µl Proteinase K (20 mg/ml Proteinase K in buffer) was added to each tissue sample. Samples were then vortexed, incubated at 55°C for 3 hours, and 700 µl of Genomic Lysis Buffer (containing 0.5% β-mercaptoethanol) was added. After thorough vortexing, samples were centrifuged at 10,000 x g for one minute to remove insoluble debris. The supernatant was transferred to a Zymo-Spin™ IIC Column in a Collection Tube and centrifuged at 10,000 x g for one minute. DNA Pre-Wash Buffer (200 µl) was then added to the spin column in a new Collection Tube and centrifuged at 10,000 x g for one minute. The g-DNA Wash Buffer was added (400 µl) to the spin column and centrifuged at 10,000 x g for one minute. The spin column was transferred to a clean microcentrifuge tube and 200 µl of distilled deionized-H_2O (ddH_2O) was added. After an incubation of 5 min at room temperature, the DNA was eluted from the column by centrifuging at top speed for 30 seconds. DNA concentrations were determined by reading absorbance at 260 nm on a GeneQuant Pro spectrophotometer (Pharmacia) using the ratio of absorbance at 260/280 nm as an indicator of DNA purity. DNA was standardized to 2 ng/µl with ddH_2O and stored at -40 °C until use.

DNA dot blots

Pieces of positively charged nylon membrane were cut into the appropriate size, submerged in distilled water, and then placed on a rocker. DNA samples were diluted to the desired concentration using 1 M NaOH and 200 mM EDTA (pH 8.2) to give a final

concentration of 0.4 M NaOH/10 mM EDTA. The samples were then heated for 10 min in a water bath at 100°C, quickly centrifuged to collect the condensate, and placed on ice. The nylon membrane was placed in the Bio-Dot Apparatus (Cat# 170-6545) and assembled according to manufacturer's instructions. The membrane was then prewashed with 500 µl of distilled water per well by switching on the suction of the manifold device and allowing the water to filter through. The DNA samples were then applied to the wells (total of 100-200 ng/well, as determined by dilution curves) and filtered through by gravity. After all the samples had filtered through, each well was rinsed with 500 µl of 0.4 M NaOH, the manifold suction was briefly applied, the manifold was dismantled, and the membranes was allowed to air dry. The DNA was cross-linked to the nylon membrane by placing the membrane between two pieces of filter paper and placing in the oven for 2 hours. Following DNA crosslinking, the membrane was treated similar to a basic western blot; the membranes were washed three times (5 min each wash) in 2X SSCT (3M NaCl, 0.3 M sodium citrate, 0.05% Tween-20), blocked with milk diluted in 2X SSCT, and incubated with primary/secondary antibody diluted in 2X SSCT.

The total amount of DNA loaded per well ranged from 100 ng (5-hmC) to 200 ng (5-mC, 5-caC). Membranes to be incubated with antibodies recognizing 5-mC (Cat#61256), 5-hmC (Cat#39792), or 5-caC (Cat#61230) were blocked for 60 min with 10% milk, 40 min with 5% milk, and 60 min with 5% milk, respectively. Primary antibody dilutions were 1:2000 v/v for 5-mC, 1:7500 v/v for 5-hmC, 1:2500 v/v for 5-caC and all were incubated overnight at 4°C. HRP-linked anti-rabbit IgG secondary antibody dilutions were 1:14000 v/v (30 min) for 5-mC and 1:12000 v/v (40 min) for 5-hmC and 5-caC. All membranes were washed three times (5 min/wash) prior to

visualization by enhanced chemiluminescence. Dot blots were then restained using methylene blue (0.02% methylene blue in 1X Tris-acetate-EDTA; recipe for 50X TAE 40 mM Tris, 20 mM acetic acid, 1 mM EDTA, pH of 8.4) and, finally, destained using 20% ethanol in order to visualize total genomic DNA.

Total protein extraction

Samples of frozen skeletal muscle from five time points in the torpor-arousal cycle (EC, EN, LT, EA, IA) were separately extracted (N=4). Briefly, samples of skeletal muscle were quickly weighed, crushed into small pieces under liquid nitrogen, and then homogenized 1:2 w:v using a Polytron PT10 in ice-cold homogenizing buffer (20 mM Hepes, 200 mM NaCl, 0.1 mM EDTA, 10 mM NaF, 1 mM Na_3VO_4, 10 mM β-glycerophosphate) with 1 mM phenylmethylsulfonyl fluoride (Bioshop), and 1 µl protease inhibitor cocktail (Sigma Genosys) added immediately before homogenization. Each sample was centrifuged at 10,000 x g (10 min, 4°C) before removing the supernatant containing soluble proteins. Protein concentration was quantified by the Coomassie blue dye-binding method using the BioRad reagent (BioRad Laboratories, Hercules, CA) with absorbance read at 595 nm on a MR5000 microplate reader. Samples were adjusted to a constant 10 µg/µl by addition of small amounts of homogenizing buffer and then aliquots were combined 1:1 v/v with 2X SDS loading buffer (100 mM Tris-base pH 6.8, 4% w/v SDS, 20% v/v glycerol, 0.2% w/v bromophenol blue, 10% v/v 2-mercaptoethanol) and boiled. The final protein samples (5 µg/µl) were stored at -40°C until use.

Western Blotting

Equal amounts of protein from each sample were loaded onto SDS-polyacrylamide gels or Tris-tricine gels and separated on a BioRad Mini Protean III apparatus. The appropriate amount of protein loaded was determined using protein dilution curves. For Tris-tricine gels, the stacking gel was composed of 375 µl 3.0 M Tris-HCl/SDS (pH 8.45), 253 µl 30% acrylamide, 875 µl water, 15 µl 10% APS, 1:5 µl TEMED whereas the 15% resolving gel contained 1.875 mL 3.0 M Tris-HCl/SDS (pH 8.45), 2.875 mL 30% acrylamide, 316 µl water, 112 µl 10% APS, 3.5 µl TEMED. The Tris-tricine 10X anode buffer was 2 M Tris-HCl, pH 8.8 and the 10X running buffer was 1 M Tris-HCl, 1 M tricine, 1% w/v SDS, pH 8.3. Samples loaded on 15% Tris-tricine gels were run at 30 V for 1 h followed by ~2 h at 150 V. Other proteins were separated by standard SDS-PAGE and run at 180 V for 45-60 min in 1X Tris-glycine SDS running buffer (25 mM Tris, 192 mM glycine, 0.1% SDS, pH 8.3). SDS-polyacrylamide gels were made based on a discontinuous gel system; stacking gel pH 6.8 (130 µl 1.0 M Tris-HCl, 170 µl 30 % acrylamide, 680 µl water, 10 µl 10% SDS, 10 µl 10% APS, 1 µl TEMED) and conditions for a 10% resolving gel pH 8.8 (1.3 ml 1.5 M Tris-base, 1.7 ml 30% acrylamide, 2.0 ml water, 50 µl 10% SDS, 50 µl 10% APS, 2 µl TEMED). Proteins were then transferred to PVDF membrane (0.2 micron PVDF for transfer of Tris-tricine gels and 0.45 µm PVDF for all others) by electroblotting at 160 mA for 1–1.5 h using a transfer buffer containing 25 mM Tris (pH 8.5), 192 mM glycine and 10% v:v methanol at room temperature.

To evaluate relative protein levels of all targets, 20 µg of protein was loaded into each well. PVDF membranes to be probed with antibodies specific for all targets were blocked with 2.5% w/v non-fat dried milk dissolved in TBST for 30 min. Epitopes

corresponding to all primary antibodies were mapped to sites in the thirteen-lined ground squirrel genome to confirm specificity. Antibodies specific for mammalian p-H3S10 (#3377), Ac-H3K9 (#9649), Ac-H3K14 (#7627), Ac-H3K18 (#9675), Ac-H3K23 (#8848), Ac-H3K27 (#8173), Ac-H3K56 (#4243), Ac-H2AK5 (#2576), Ac-H2BK5 (#12799), Ac-H4K8 (#2594) were all purchased from Cell Signaling Technology. Antibodies for histone H3 cross-reacted with bands on the immunoblots at the expected molecular masses of 17 kDa for the mammalian protein whereas H2A, H2B, and H4 cross-reacted with single bands at 14, 17, and 10 kDa, respectively. Antibodies were all used at 1:1000 v/v dilution in TBST. Membranes were then probed with HRP-linked anti-rabbit IgG secondary antibody (~1:4000 v:v dilution). All membranes were washed three times between incubation periods in TBST for approximately 5 minutes/wash. Bands were visualized by enhanced chemiluminescence and then blots were restained using Coomassie blue to visualize all protein bands. Immunoblot band density in each lane was standardized against the summed intensity of a group of Coomassie stained protein bands in the same lane; these were chosen because they did not show variation between different experimental states and were not located close to the protein bands of interest. Western blots of housekeeping genes (e.g. GAPDH) were also performed in order to confirm total protein levels remained constant.

Histone Purification

The histone purification kit enables the purification of histone proteins while preserving their post-translational modifications including acetylation, methylation, and phosphorylation states (Active Motif, Cat#40025). Histones prepared for mass spectrometry were purified from euthermic controls (EC) and followed manufacturer's

instructions. Skeletal muscle tissue (550 mg) was homogenized 1:3 w:v in ice-cold Extraction Buffer (containing protease inhibitor, 1 mM NaF, and 10 mM β-glycerophosphate) using a Dounce homogenizer and incubated on a rotating platform (overnight, 4°C). After centrifugation at 14,000 × g (10 min, 4°C), the supernatant was transferred to a clean tube. The pellet was neutralized by adding 100 µl 1M Tris HCl pH 8.0 and subjected to western blotting to confirm that histone proteins were not isolated in the pellet. The supernatant containing histones was neutralized and equilibrated with 5X Neutralization Buffer. If still acidic, additional Neutralization Buffer was added until a pH of 8 was achieved. The column was prepared by adding enough purification resin for a packed column of 1 mL and all buffers/samples were added without disturbing the resin bed or introducing air bubbles. The packed column was cleaned with a total of 9 mL sterile water and equilibrated with a total of 9 mL Equilibration Buffer before adding 1.5 mL of sample and washing the column with 9 mL of total histone wash buffer.

All fractions were collected in microcentrifuge tubes by gravity flow (1 mL/ fraction) including the unbound flow through and wash in order to confirm that histones were retained on the column. Histone H2 fractions were collected by adding a total of 10 mL H2A/H2B Elution Buffer (the majority of H2A/H2B proteins were isolated in fractions 2-5). Elution of the H3/H4 tetramers used a total of 4 mL H3/H4 Elution Buffer (H3/H4 proteins were mainly recovered in fractions 1-3). All fractions were combined with 4% perchloric acid overnight (4°C) for precipitation of core histones. The following day, samples were centrifuged 14,000 × g (1 hour, 4°C) and the supernatant transferred to a clean tube (supernatant was kept to verify histone precipitation). The pellet was then washed with 4 % perchloric acid to eliminate salt, washed twice with acetone containing

0.2% HCl, washed twice with 100% acetone, and air dried for 20 minutes until the pellet was completely dry. Fractions were resuspended in sterile water, combined 1:1 v:v with 2× SDS loading buffer and boiled. Final protein samples were stored at -40°C until use.

Mass spectrometry and protein identification

MS experiments were performed by the Proteomics Platform of the Eastern Quebec Genomics Center (Quebec, Canada). After washing with water, tryptic digestion was performed on a MassPrep liquid-handling robot (Waters, Milford, MA, USA) following manufacturer's specifications and the protocol of Shevchenko et al. (1996), with the modifications suggested by Havlis et al. (2003). Peptides were then loaded on a 75 µm C18 PicoFrit column (BioBasic, New Objective, Woburn, MA, USA) and resolved by reversed-phase (RP) nanoscale capillary liquid chromatography (nano LC) using a 30 min 2-50% solvent B (acetonitrile, 0.1% formic acid) gradient at 200 nL/min (obtained by flow-splitting) with a Thermo Surveyor MS pump. The peptides were directly electrosprayed into and analyzed by an LTQ linear ion trap mass spectrometer (Thermo Fisher Scientific, San Jose, CA, USA) equipped with a nanoelectrospray ion source (Thermo Fisher Scientific). Mass spectra were acquired using a data dependent acquisition mode using Xcalibur software version 2.0 (Thermo Fisher Scientific). Each full scan mass spectrum (400 to 2000 m/z) was followed by collision-induced dissociation of the seven most intense ions. The dynamic exclusion (30 seconds) function was enabled, and the relative collisional fragmentation energy was set to 35%.

Database searching

A dataset of peptide assignments was obtained by searching these spectra with the Mascot analysis program (Matrix Science, London, UK; version 2.4.1) using a Rodentia

peptide database (UR13_3_Rodentia_9989_20130403; 207730 entries) and assuming the digestion enzyme trypsin (Perkins et al, 1999) with allowance for two missed cleavages. Mascot was searched with a fragment ion mass tolerance of 0.100 Da and a parent ion tolerance of 0.100 Da. Iodoacetamide derivatives of cysteine were specified in Mascot and X! Tandem as a fixed modification while deamidation of asparagine and glutamine, methylation of lysine and arginine, oxidation of methionine, acetylation of lysine and phosphorylation of serine, threonine and tyrosine were specified in Mascot as variable modifications. Scaffold (version Scaffold_2_01_02, Proteome Software Inc., Portland, OR, USA) was used to validate MS/MS-based peptide and protein identifications. The identification of a protein was confirmed when at least 2 unique peptides are identified with a peptide probability more than 95% for each of the two peptides. Proteins that contained similar peptides and could not be differentiated based on MS/MS analysis alone were grouped to satisfy the principles of parsimony.

Results

Changes in the methylation status of genomic DNA

The global DNA methylation status of skeletal muscle across three experimental conditions (summer, LT, and IA) was assessed using a DNA dot blot technique. These experimental conditions were chosen because only seasonal changes (summer versus winter animals) were hypothesized to involve significant changes in global methylation. Figure 2.1 shows that 5-mC and 5-hmC DNA methylation targets did not change significantly over the three experimental conditions tested. However, 5-caC content was unaffected between summer and late torpor but levels were significantly reduced during interbout arousal, a 45% reduction as compared to LT.

Analysis of Histone posttranslational modifications

Posttranslational modifications on histone H3, H2A, H2B, and H4 protein levels in skeletal muscle were analyzed by immunoblotting comparing muscle from euthermic control animals (EC) with up to four time points on the torpor-arousal cycle: EN, LT, EA, and IA (Fig. 2.2-2.4). Morin and Storey (2006) previously described the relative changes in Ac-H3K23 and p-H3S10 (that are associated with active transcription) comparing EC and LT conditions in thirteen-lined ground squirrel muscle. While the previous study showed a significant decrease for both targets during LT as compared to EC, the present study expanded this analysis to include other time points over the torpor-arousal cycle. However, as Fig. 2.2 shows, the relative acetylation at lysine 23 and phosphorylation at serine 10 of H3 did not change during EN, EA, and IA, as compared to EC values.

Relative changes in the amount of histone H3 protein acetylated at lysine 9, 14, 18, 27, and 56 from thirteen-lined ground squirrel skeletal muscle was also assessed over the torpor-arousal cycle (Fig. 2.3). While there were no statistically significant changes in histone H3 acetylated at lysine 9 or lysine 56, the relative amount of Ac-H3K14 showed a 3.2-fold increase during EA, as compared to controls. A parallel change was also observed for Ac-H3K27 whereby a 1.8 fold increase during EA as compared to EC was observed. Additionally, relative changes in Ac-H3K18 occurred during the transitory phases of the torpor-arousal cycle, showing statistically significant increases during EN (2.9 fold) and EA (2.8 fold) as compared to EC levels.

Relative changes in the amounts of histone H2A and H2B proteins acetylated at lysine 5 and histone H4 acetylated at lysine 8 were also assessed in thirteen-lined ground

squirrel skeletal muscle (Fig. 2.4). There were no statistically significant changes in lysine acetylation on histone H2A, H2B, and H4 over the torpor-arousal cycle.

Identification of Histone posttranslational modifications by mass spectrometry

Following purification of histone proteins from EC muscle, bands were excised and sent for mass spectrometry analysis by the Eastern Quebec Genomics Center (Quebec, Canada). Histone proteins contain gene duplications as well as non-allelic variants with only subtle differences in their primary sequence [Bönisch and Hake 2012]. As a result, the present alignments combined genes with identical sequences and these are only represented once in the figures (Fig. 2.5-2.8). Peptides are assigned to a particular gene variant based on the principles of parsimony; however, it is often unclear which variants were indeed represented since differences in variant sequences may be attributed to just a single amino acid substitution and the peptide containing such a substitution might not have been detected by mass spectrometry. Table 2.1 summarizes the posttranslational modifications on histone peptides obtained from skeletal muscle of thirteen-lined ground squirrel. Additionally, amino acid residue number assignments are influenced by the original published paper describing the site as well as other factors (e.g. the first methionine is sometimes not considered in the numeration). Consequently, amino acid residues corresponding to the thirteen-lined ground squirrel sequence as depicted in Fig. 2.5-2.8 are cross-referenced with those commonly reported in the literature and in the PhosphoSitePlus database (Table 2.1; www.phosphosite.org).

The sequence coverage obtained for mass spectrometry was determined to be 43%, 41%, 75%, and 42% for ground squirrel histone H3, H2A, H2B, and H4, respectively (Fig. 2.5-2.8). Posttranslational modifications on histone H3 were detected at

lysine 19 and 24 (K*QLATK*AAR) (Fig. 2.5) which correspond to Ac-H3K18 and Ac-H3K23 according to commonly reported residues in the literature, respectively. A lysine methylation was also detected on histone H3 at lysine 80. However, no posttranslational modifications were detected for H2A or H4 by mass spectrometry (Fig. 2.6 and Fig 2.8). The sequence coverage was best for histone H2B with many peptides and posttranslational modifications detected by mass spectrometry. Peptides which contained amino acid substitutions relative to the human sequence were also detected and are shown as thirteen-lined ground squirrel peptides (13LGS) (Fig. 2.7). While containing amino acid substitutions relative to the human sequence, the peptide PEPARSAPAPK and SRKESYSVYVYNK (Unit Prot G5BV35) were identical matches to the naked mole rat, a species whose genome has recently been sequenced (Kim et al. 2011). Furthermore, these peptides were found to contain posttranslational modifications including a methylation on arginine 6 (PEPAR*SAPAPK) and an acetylation on lysine 45 (SRKESYSVYVYNK*). With respect to lysine 45 acetylation, this modification has also been found in humans and mice (corresponding to lysine 44), although the present peptide contains an amino acid substitution in the -1 position. Additional posttranslational modifications on H2B included acetylation of lysine 48 (VLK*QVHPDTGISSK), methylation of arginine 74 (AMGIMNSFVNDIFER*), acetylation or methylation of lysine 110 (LLLPGELAK*), and methylation of lysine 118 (HAVSEGTK*AVTKYTSSK). To my knowledge, arginine 6 and 74 methylation represent unique modifications in thirteen-lined ground squirrels which have not been characterized in other animals.

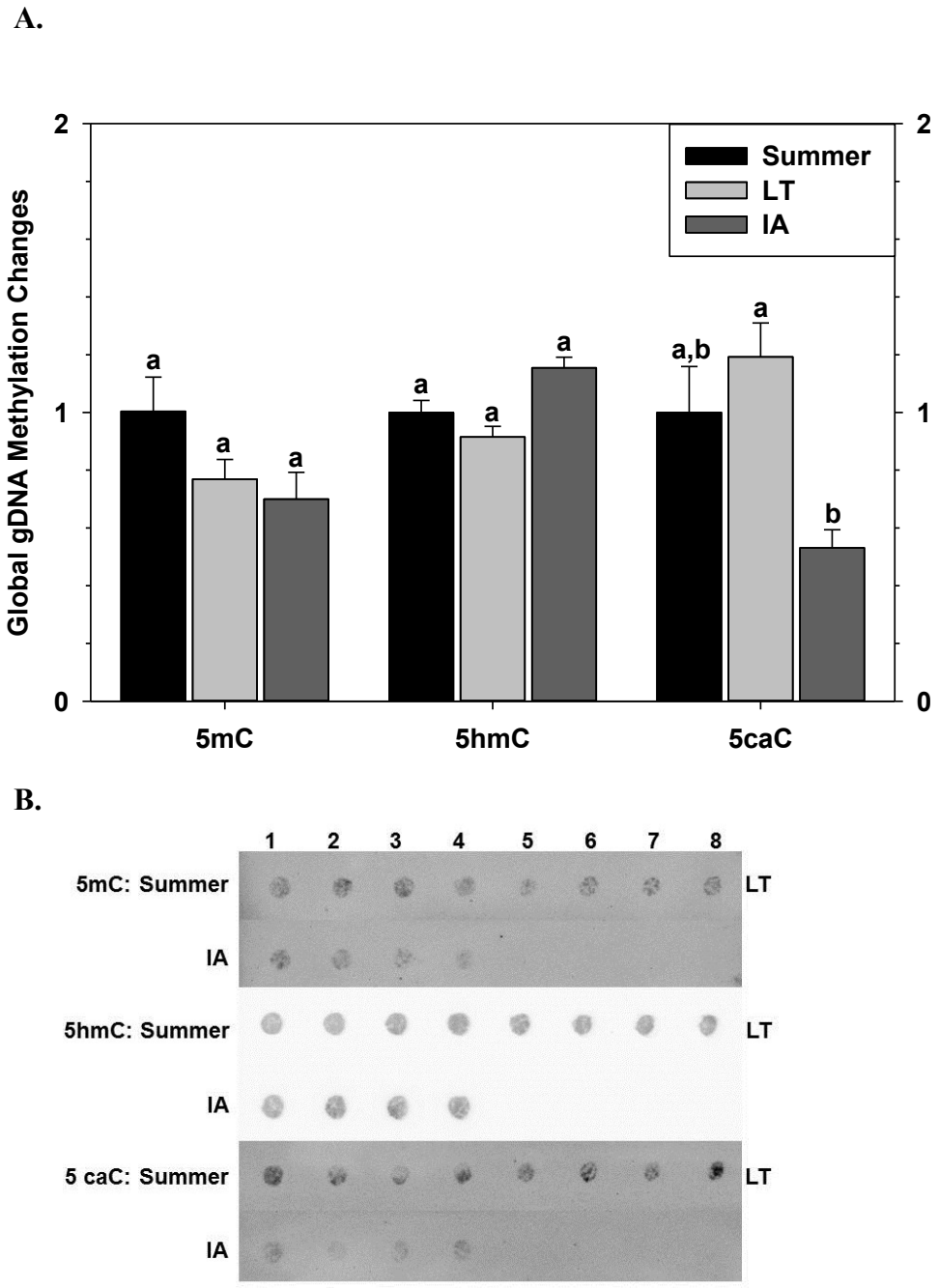

Figure 2.1: Relative changes of DNA modifications in skeletal muscle of thirteen-lined ground squirrel during summer, late torpor (LT), and interbout arousal (IA). A. Histograms show mean relative expression levels (± S.E.M., n=4 independent proteins isolations) for three sampling points. B. Representative DNA dot blots are shown for 5-methylcytosine (5mC), 5-hydroxymethylcytosine (5hmC), and 5-carboxylcytosine (5caC). The DNA modification and experimental conditions are labeled to the left and right while sample numbers (lanes) are labeled along the top indicating 4 samples of one type (e.g., Summer/IA lanes 1, 2, 3, 4) and 4 samples of another (e.g. LT lanes 5, 6, 7, 8). Data were analyzed using analysis of variance with a post-hoc Tukey test ($p<0.05$); values are not significantly different from each other share the same letter notation.

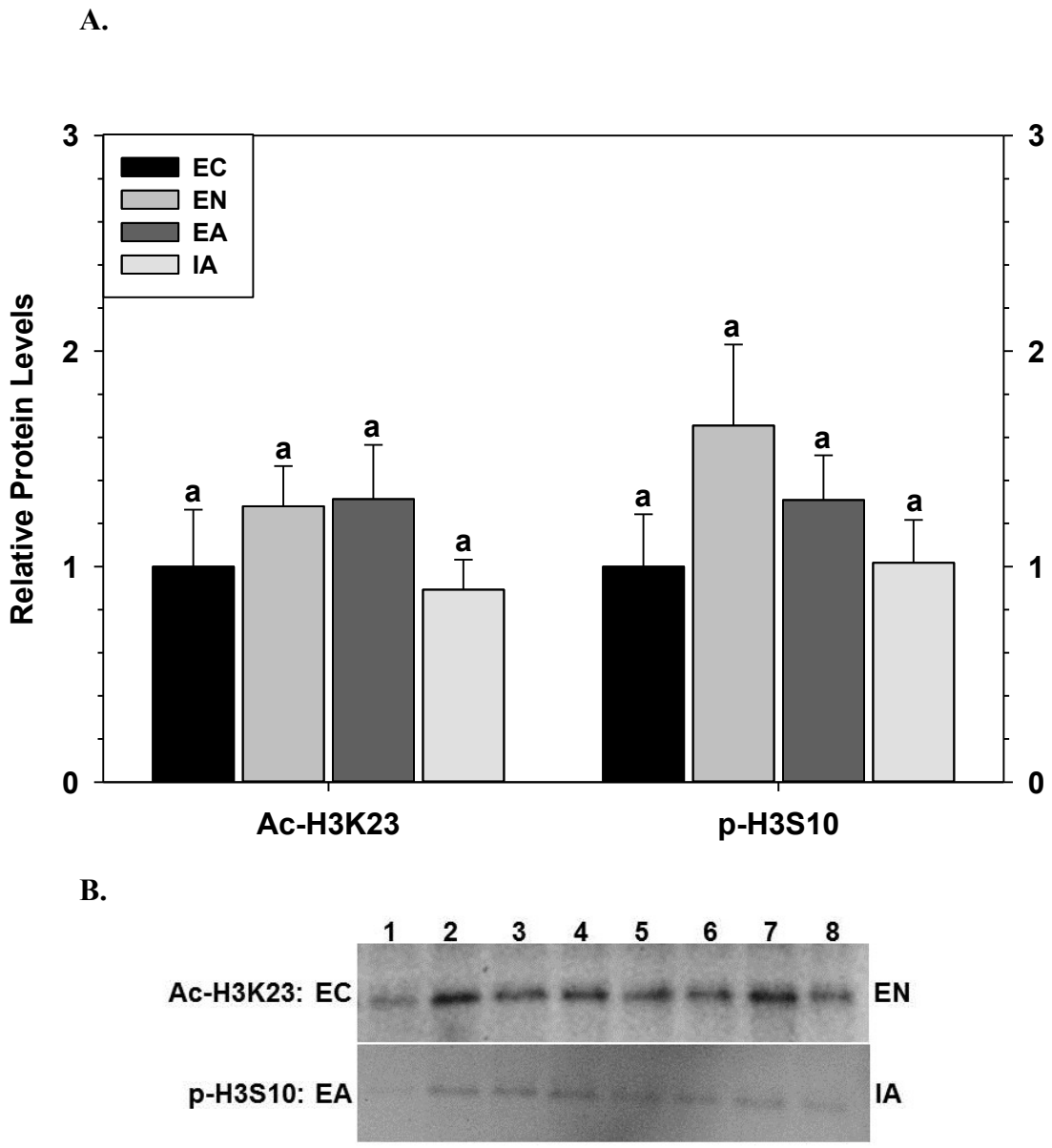

Figure 2.2: Relative changes in histone H3 protein acetylated at lysine 23 (Ac-H3K23) or phosphorylated at serine 10 (p-H3S10) in skeletal muscle from thirteen-lined ground squirrels over the torpor-arousal cycle. A. Histograms show mean relative expression levels (± S.E.M., n=4 independent proteins isolations) for four sampling points. B. Representative Western blots are shown for Ac-H3K23 and p-H3S10. The protein of interest and selected experimental conditions are labeled to the left and right while sample numbers (lanes) are labeled along the top indicating 4 samples of one type (e.g., EN lanes 1, 2, 3, 4) and 4 samples of another (e.g. LT lanes 5, 6, 7, 8). Other information as in Figure 2.1.

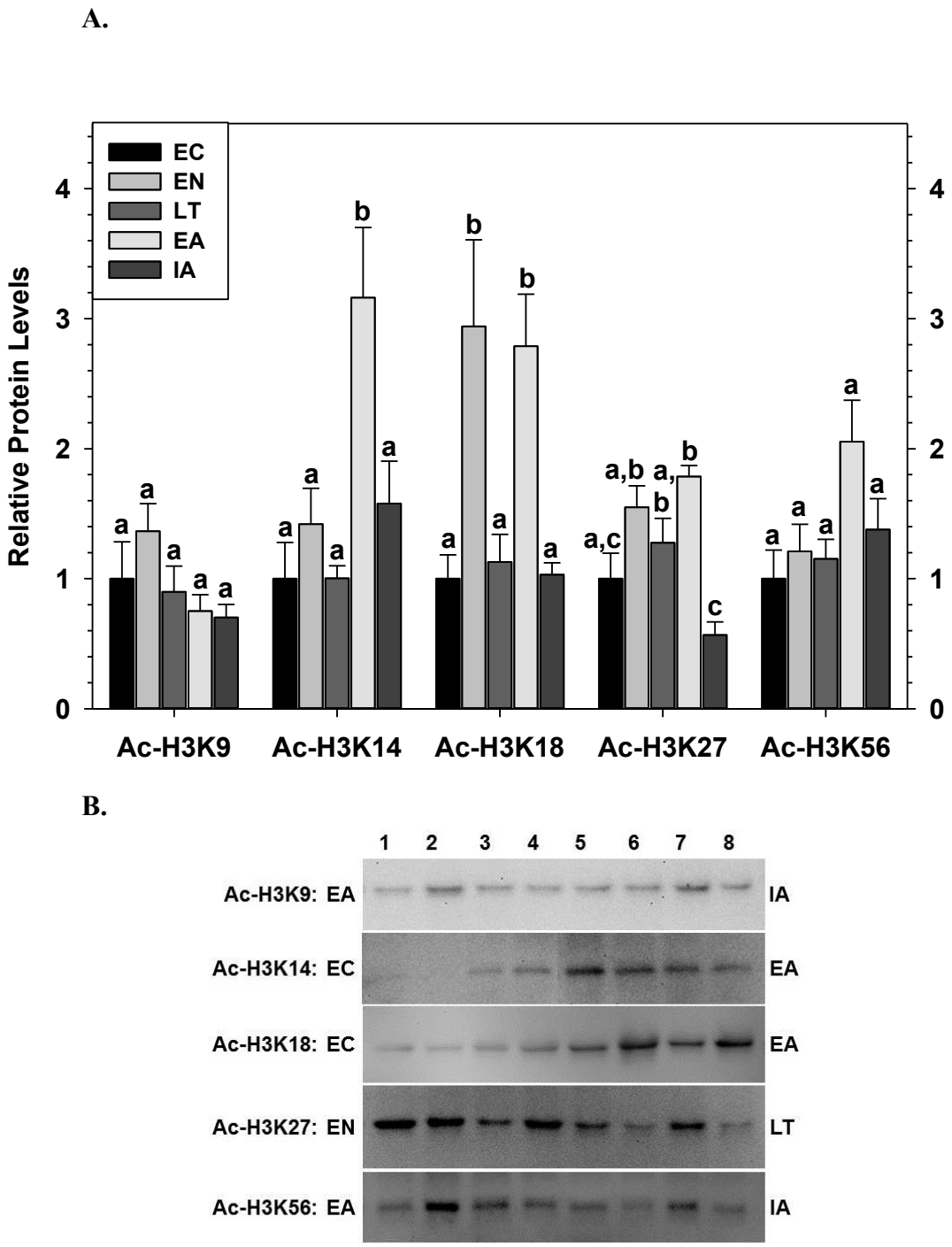

Figure 2.3: Relative changes in histone H3 protein acetylated at lysine 9, 14, 18, 27, or 56 in skeletal muscle from thirteen-lined ground squirrels over the torpor-arousal cycle. A. Histograms show mean relative expression levels (± S.E.M., n=4 independent protein isolations) for five sampling points. B. Representative Western blots are shown for Ac-H3K9, Ac-H3K14, Ac-H3K18, Ac-H3K27, Ac-H3K56. The protein of interest and selected experimental conditions are labeled to the left and right while sample numbers (lanes) are labeled along the top indicating 4 samples of one type (e.g., EA lanes 1, 2, 3, 4) and 4 samples of another (e.g. IA lanes 5, 6, 7, 8). Other information as in Figure 2.1.

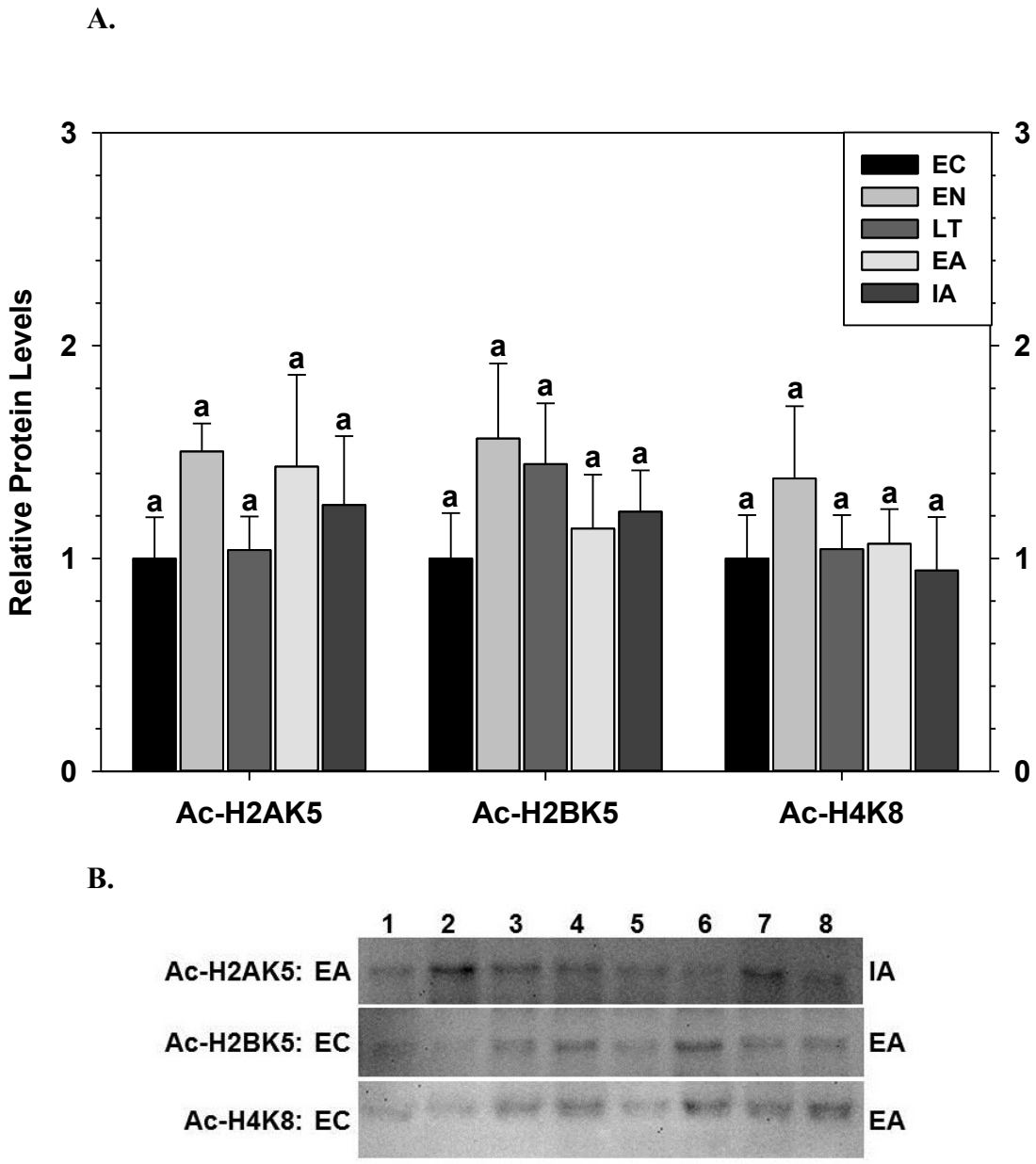

Figure 2.4: Relative changes in histone H2A and H2B proteins acetylated at lysine 5 and histone H4 acetylated at lysine 8 from thirteen-lined from skeletal muscle of ground squirrels over the torpor-arousal cycle. A. Histograms show mean relative expression levels (± S.E.M., n=4 independent proteins isolations) for five sampling points. B. Representative Western blots are shown for Ac-H2AK5, Ac-H2BK5, and Ac-H4K8. The protein of interest and select experimental conditions are labeled to the left and right while sample numbers (lanes) are labeled along the top indicating 4 samples of one type (e.g., EA lanes 1, 2, 3, 4) and 4 samples of another (e.g. IA lanes 5, 6, 7, 8). Other information as in Figure 2.1.

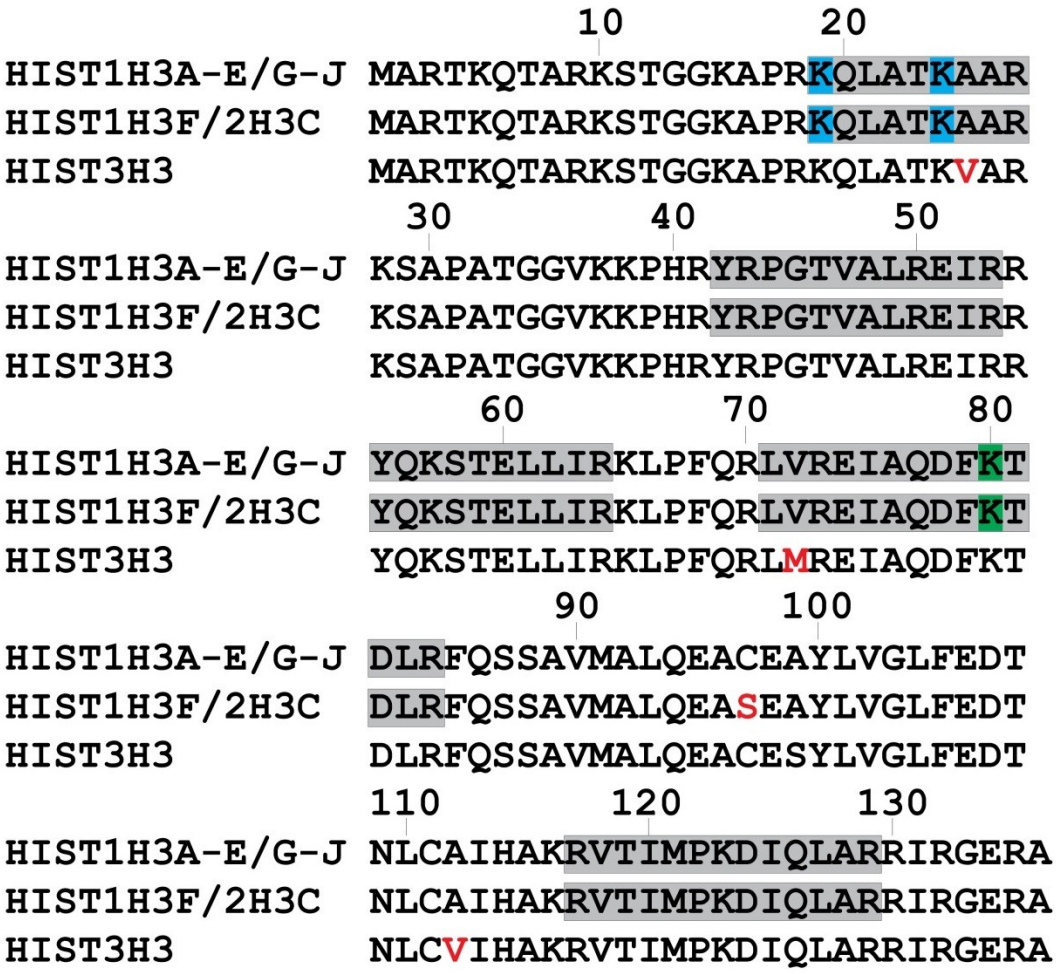

Figure 2.5: Full amino acid sequence alignment of human Histone H3 variants including HIST1H3A (NP_003520.1), HIST1H3F (NP_066298.1), HIST3H3 (NP_003484.1). Histone H3 was purified from the skeletal muscle of thirteen-lined ground squirrels and peptides were sequenced by mass spectrometry; the peptides retrieved are shown as gray boxes and were identical with those of the human sequences. Proteins that contained similar peptides and could not be differentiated based on MS/MS analysis alone were grouped to satisfy the principles of parsimony. Variable modifications were assessed including methylation of lysine (shown as green boxes) and acetylation of lysine (shown as blue boxes), or a lysine residue which contained either a methylation or acetylation (shown as red box). Dashed lines are inserted when residues are not present in all sequences, black letters are identical comparing the human H3 variants, and red letters represent substitutions.

Figure 2.6: Full amino acid sequence alignment of human Histone H2A variants including HIST1H2A (NP_003520.1), HIST1H2AA (NP_734466.1), HIST1H2AB (NP_003504.2), and HIST1H2AC (NP_003503.1). Histone H2A was purified from the skeletal muscle of thirteen-lined ground squirrels and peptides were sequenced by mass spectrometry (shown as gray boxes). Other information as in Fig. 2.5.

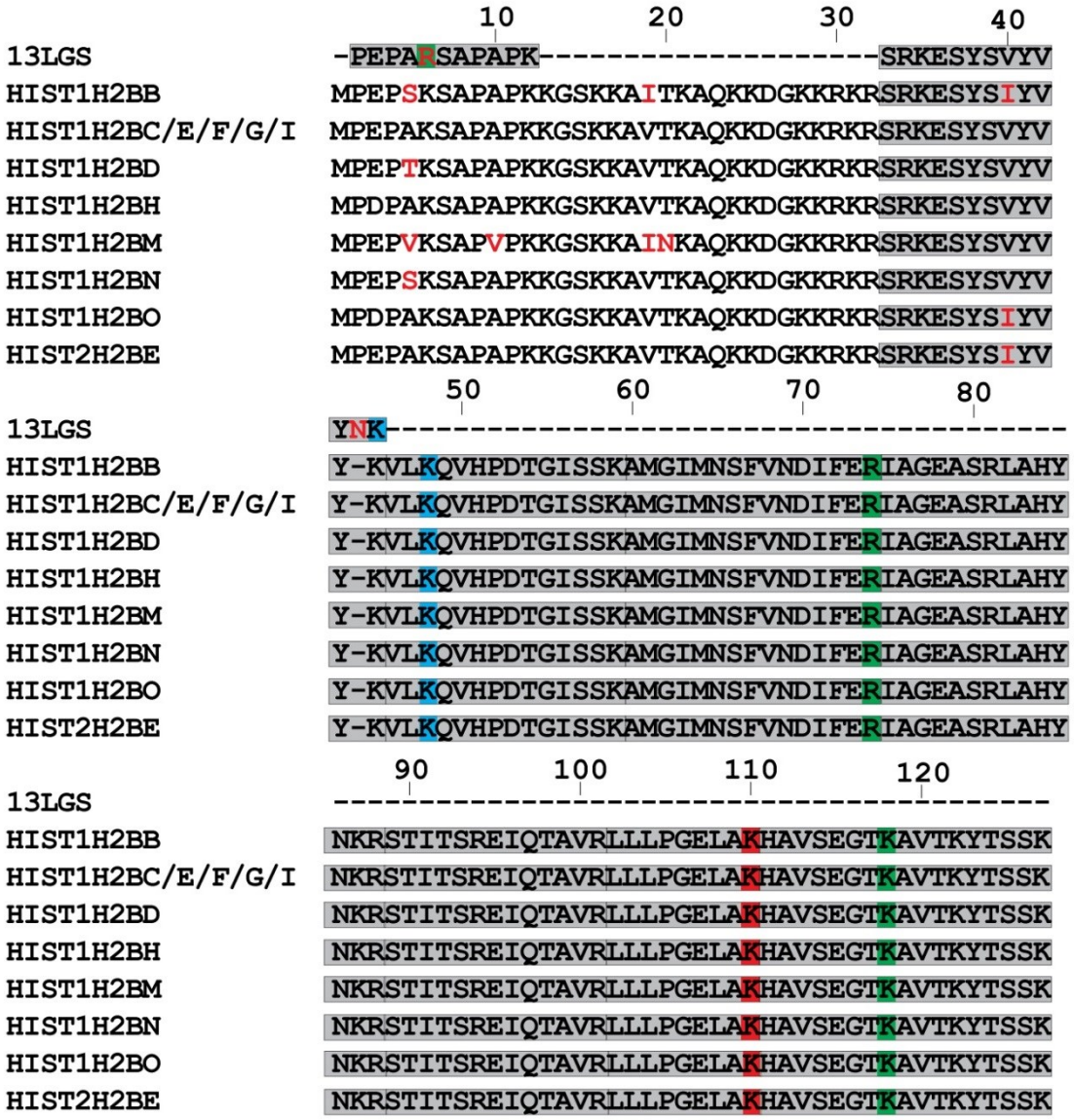

Figure 2.7: Full amino acid sequence alignment of human Histone H2B variants including HIST1H2BB (NP_066406.1), HIST1H2BC (NP_003517.2), HIST1H2BD (NP_066407.1), HIST1H2BH (NP_003515.1), HIST1H2BM (NP_003512.1), HIST1H2BN (NP_003511.1), HIST1H2BO (NP_003518.2), and HIST1H2BE (NP_003514.2). Histone H2B was purified from the skeletal muscle of thirteen-lined ground squirrel and peptides were sequenced by mass spectrometry (shown as gray boxes). Lysine residues that contained either a methylation or acetylation are shown as red boxes; other information as in Fig. 2.5.

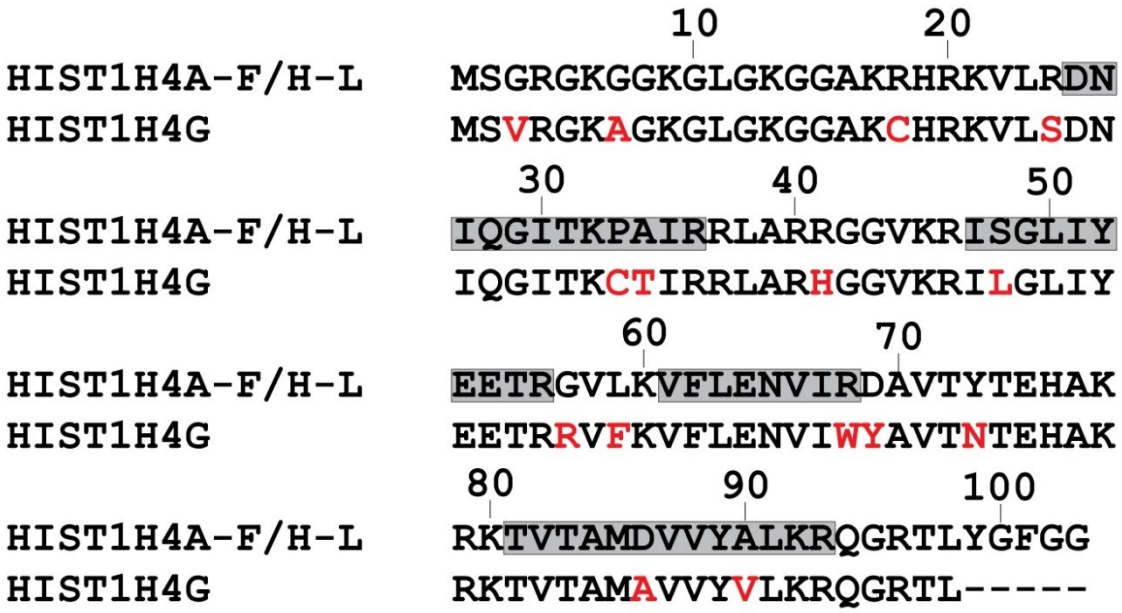

Figure 2.8: Full amino acid sequence alignment of human Histone H4 variants including HIST1H4A (NP_003529.1) and HIST1H4G (NP_003538.1). Histone H4 was purified from the skeletal muscle of thirteen-lined ground squirrels and peptides were sequenced by mass spectrometry. The peptides retrieved are shown as gray boxes and were identical with those of the human sequences (shown as gray boxes). Other information as in Fig. 2.5.

Histone	Peptide and modified residue (denoted by *)	13 LGS residue; modification(s)	Human residue from literature (and UnitProt); modification(s)
H3(Ref: P68431)	K*QLATKAAR	lysine 19; acetylation	lysine 18 (K19); acetylated, methylated (mono), ubiquitination
	KQLATK*AAR	lysine 24; acetylation	lysine 23 (K24): acetylated, methylated (mono, tri), ubiquitination, sumoylated
	LVREIAQDFK*TDLR	lysine 80; methylation	lysine 80 (K80); acetylated, methylated (mono, di, tri), ubiquitination
H2B (Ref: P33778)	PEPAR*SAPAPK	arginine 6; methylation	lysine 5 (K6); acetylation, ubiquitination
	SRKESYSVYVYNK*	lysine 45; acetylation	lysine 44 (K44); acetylation, ubiquitination
	VLK*QVHPDTGISSK	lysine 48; acetylation	lysine 47 (K47); acetylation, methylation (mono, di), ubiquitination
	AMGIMNSFVNDIFER*	arginine 77; methylation	no known modifications
	LLLPGELAK*	lysine 110; acetylation or methylation	lysine 109 (K109); acetylation, methylation (mono, di), ubiquitination
	HAVSEGTK*AVTKYTSSK	lysine 118; methylation	lysine 117 (K117); acetylation, ubiquitin

Table 2.1: Summary of peptides and posttranslational modifications obtained by mass spectrometry of thirteen-lined ground squirrel histone proteins purified from skeletal muscle. Peptides are indicated along with the specific modified residue (denoted by an asterisk) and amino acid substitutions (relative to the human sequence) are indicated by a red letter. The residue number is assigned based on the associated amino acid in each figure (for the 13LGS residue) and according to specific assignments in the literature and PhosphoSitePlus (for the human sequence).

Discussion

The present chapter aimed at deepening our understanding of epigenetic factors including DNA methylation and the involvement of posttranslational modifications on histones during hibernation in the thirteen-lined ground squirrel. DNA methylation is believed to play a crucial role in repressing gene expression, perhaps by blocking the promoters at which activating transcription factors bind. Furthermore, DNA methylation has been shown to play a vital role in numerous cellular processes, and abnormal patterns of methylation have been linked to several human diseases. DNA is packaged into nucleosomes by histone proteins that contain a high proportion of positively charged basic side chains that are attracted to the negatively charged DNA backbone. One general mechanism to overcome this repressive effect is to add an acetyl functional group to the histone, neutralizing the positive charge and transforming condensed chromatin to a more relaxed structure [Shahbazian and Grunstein 2007]. While other histone modifications have also been shown to play important roles, their biological function is more site-specific [Kouzarides 2007]. Since a common biochemical theme among organisms entering hypometabolic states is global controls on gene suppression [Morin and Storey, 2006; Krivoruchko and Storey, 2010], it was of interest to expand current knowledge in this area in order to discern the importance of epigenetic regulatory mechanisms in achieving this response.

While seasonal increases in 5-mC were hypothesized to occur in ground squirrel skeletal muscle during the winter, as compared to summer conditions, Figure 2.1 shows that there were no relative increases in any of the three DNA methylation modifications presently studied. Hence, these data suggest that changes in 5-mC may not provide a

global platform for decreased transcription in the skeletal muscle of hibernating ground squirrels. However, since only global changes were considered it remains a possibility that individual gene promoter regions are regulated in this way. Furthermore, since tissue-specific differences are known to occur during hibernation, global changes in DNA methylation may nonetheless remain a plausible hypothesis in other tissues. While there were no significant increases in DNA methylation modifications, 5-caC did show a significant decrease during IA, as compared to LT but not summer conditions.

The ten-eleven translocation (TET) family enzymes oxidize 5-mC into 5-hmC and further into 5-fC and 5-caC [Kohli and Zhang 2013]. While the functional effects of 5caC in the genome are unclear, one study reported a significant reduction of RNA Polymerase II nucleotide incorporation and elongation efficiency on a template containing 5caC relative to those for the C template [Kellinger et al. 2012]. It is known that the activity of RNA Pol II from the muscle of torpid squirrels was only 57% of the euthermic value [Morin and Storey 2006] and significant decreases in 5-caC during interbout arousal may reflect a rebound of RNA Pol II activity during this experimental condition. Alternatively, different DNA modifications could be specifically recognized by different DNA-binding proteins. Although there is very limited data which describe changes in DNA-protein interactions for the newly discovered 5-caC, many methyl-CpG-binding domain proteins do not bind 5-hmC [Jing et al. 2010], suggesting these principles may extend to other DNA modifications.

While only very small changes were observed in DNA modifications, the more transient and reversible posttranslational modifications on histone proteins showed fluctuations over the torpor-arousal cycle (Fig. 2.2-2.4). In general, the PTMs measured

in the present chapter including acetylation of lysine 9, 14, 18, 23, 27, and 56 and phosphorylation of serine 10 on histone H3, acetylation of lysine 5 on H2A and H2B, and acetylation of lysine 8 on H4 are generally associated with transcriptional activation. Previous studies have assessed the role of histone H3 as an epigenetic mechanism to achieve reduced transcriptional states during hibernation in ground squirrels; relative phosphorylation of Ser 10 and acetylation of Lys 23 on histone H3 were significantly reduced by 38-39% in muscle during hibernation [Morin and Storey 2006]. The present studies expanded these measurements to include additional time points across the torpor-arousal cycle. Figure 2.2 illustrates that reversible modifications of H3 phosphorylated at serine 10 or acetylated at lysine 23 were strictly correlated with late torpor since no changes were observed at other time points. Histone H3 acetylations at lysine 9, 14, 18, 27, and 56 were also measured over the torpor-arousal cycle in skeletal muscle (Fig.2.3). The data showed a unique expression pattern as compared to the response seen for Ac-H3K23. While there was no change in relative acetylation over torpor-arousal for Ac-H3K9 or Ac-H3K56, the content of Ac-H3K14, Ac-H3K18 and Ac-H3K27 was significantly increased during early arousal, as compared to EC values. Curiously, the relative acetylation of lysine 18 was also enhanced during entrance; however, acetylation of H2A at lysine 5, H2B at lysine 5, and H4 at lysine 8 were unaffected over torpor-arousal in skeletal muscle (Fig. 2.4). While the biological significance of this is incompletely understood, this response suggests that changes in the properties of nucleosomes are particularly relevant in mediating transitions into and out of torpor.

The lack of a common trend amongst relative changes in lysine acetylation across histone proteins over the torpor-arousal cycle suggests that modifications on histone

proteins are likely quite complex during hibernation and additional data will surely be required in order to fully comprehend their functional consequences. Nonetheless, it may be suggested that Ac-H3K23 remains an essential modification which is correlated with deep torpor [Morin and Storey 2006]. Furthermore, relative increases in acetylation of H3K14, H3K18, and H3K27 may aid in reversing a torpor-induced condensed state of chromatin during the arousal process. Since skeletal muscle plays a critical role in supporting arousal by generating heat via shivering thermogenesis such a chromatin relaxation to allow renewed gene transcription may be vital to this response. Alternatively, while regulation of transcription is thought to be the primary function of reversible histone modifications, acetylation of K14, 18, and 23 on H3 and K8 on H4 may also play a secondarily role in DNA repair, as evidenced by the interaction of DNA repair proteins at these acetylated sites [Peterson and Laniel 2004]. These discrepancies may be resolved by considering several such modifications in combination. For example, H4K8 and H3K14 acetylation together with H3S10 phosphorylation is thought to be a signature that is more closely associated with transcriptional regulation than with DNA repair [Peterson and Laniel 2004]. Future studies which identify combinations of histone modifications may bring more clarity on the subject.

With an appreciation of the complexity of histone acetylation during hibernation, I aimed to identify specific PTMs on histones via mass spectrometry, especially since limited sites are available for measurement via western blotting. It should be noted, however, that mass spectrometry of acetylated versus tri-methylated lysines may require further validation (e.g. via antibody recognition). To my knowledge these studies are the first to identify novel peptides and PTMs in hibernating ground squirrels (summarized in

Table 2.1). Mass spectrometry identified common PTM sites which were also assessed by western blotting in the present chapter including lysine 18 and 23 acetylation on histone H3. Located in the histone H3 tail, these sites may represent critical regulatory loci during hibernation since both were responsive to torpor-arousal cycles. Additionally, lysine methylation was also shown to occur at lysine 80 in thirteen-lined ground squirrel (Fig. 2.5). Lysine methylation at this site also occurs in humans (UnitProt Ref#P68431) and mice (UnitProt Ref#P68433) and this site is also subject to acetylation and ubiquitination in both speciess. Since this H3K80 (also H3K79) methylation site is one of three implicated in the activation of transcription (also includes H3K4, H3K36) [Kouzarides 2007], this may represent a future site of interest for further investigation in thirteen-lined ground squirrels during hibernation. Conversely, three lysine methylation sites are connected to transcriptional repression including H3K9, H3K27, H4K20 [Kouzarides 2007] and may also be interesting as future directions.

Multiple modifications on H2B were also detected including two particularly interesting modifications which occurred on peptides that are also found in the naked mole rat [Kim et al. 2011], but not in the human sequence. Naked mole rats are of interest to researchers because they have recorded lifespans approximately nine times greater than predicated for their body size [O'Connor et al. 2002] and are remarkably tolerant to stresses (e.g. brain slices are significantly more tolerant of oxygen and nutrient deprivation) [Nathaniel et al. 2009; Buffenstein 2008]. Additionally, naked mole rats are remarkable among mammals because they display a weak capacity to maintain body temperatures above ambient and a relatively low metabolic rate [Goldman et al. 1999]. Consequently, a comparison between naked mole rats and mammalian hibernators is

particularly interesting since, although naked mole rats are not hibernators, they do display parallel features and, by extension, common molecular/biochemical themes may also be observed. For example, naked mole rats have mechanisms in place to protect against stressors, especially oxidative damage including a role for Nrf2 transcription factors [Lewis et al, 2012] which are also responsive to hibernation in thirteen-lined ground squirrels (see Chapter 4). Naked mole rats and mammalian hibernators also display commonalities in fuel utilization during metabolic rate depression; glycolytic pathways seem to be of lesser importance in mole rats (in comparison to mice), as evidenced by the differential regulation of pyruvate kinase [Gesser et al. 1977]. Similarly, data obtained from hibernating golden-mantled ground squirrels (*Spermophilus lateralis*) also showed coordinated reduction in glycolytic rate [Brooks and Storey 1992].

The peptides which were found to be conserved between thirteen-lined ground squirrels and naked mole rats included PEPAR*SAPAPK and SRKESYSVYVYNK* which contained a methylation on arginine 6 and an acetylation on lysine 45, respectively. These sites correspond/align with lysines at residues 5 and 44 in the human sequence. As mentioned above, lysine 5 on histone H2B plays a role in transcriptional regulation [Cheung et al. 2000] and, as a result, an amino acid substitution in such a location may have substantial cellular consequences. Additionally, an amino acid insertion was found in the -1 position to the lysine 45 acetylation site in thirteen-lined ground squirrel. Since lysine acetylation (corresponding to lysine 44 in the human sequence) was nonetheless present in this particular thirteen-lined ground squirrel sequence, it is clear that this amino acid substitution does not abolish the lysine modification but may have an influence on the effect of lysine 45 acetylation. For

example, this amino acid substitution may modify the recognition sequence that is the target for the acetyltransferase or deacetylase enzymes (or both) that modify this residue, and thereby exert an influence on histone-histone or histone-DNA interactions. Moreover, conserved peptides with known modifications, as compared to the human sequence, were also detected in histone H2B including an acetylation corresponding to lysine 48, 110, and 118. Although these residues are known to be present in the human sequence, there is very little data describing their functional role. Finally, arginine 74 methylation was detected in thirteen-lined ground squirrel which, to my knowledge, has not been identified in any other animal.

In summary, the present data elucidates the involvement of DNA methylation and demethylation pathways as well as histone protein modifications as a mechanism of achieving global controls on skeletal muscle gene expression over cycles of torpor-arousal. While the DNA methylation patterns did not change between summer and winter animals, 5-caC levels decreased significantly during interbout arousal compared with late torpor, possibly with consequences for RNA Pol II activtity. PTMs on histone proteins were differentially regulated during deep torpor (Ac-H3K23) and early arousal (Ac-H3K14, 18, 27), possibly playing roles in nucleosome dynamics during hibernation. Finally, a host of peptide sequences and PTMs were identified in thirteen-lined ground squirrels, especially in histone H3 and H2B. These sequences and PTMs have been confirmed in other species (e.g. human and naked mole rat), while novel modifications were also identified in thirteen-lined ground squirrel peptides. Further studies will be required in order to fully elucidate the functional roles for these sites.

Chapter 3

Linking signaling pathways to gene expression and the stress response during mammalian hibernation.

Introduction

Of particular interest in this chapter are the signal transduction pathways which convert information received at the cell-surface to regulatory targets within cells that promote changes in gene/protein expression programs as well as mitigate stress. Mammalian hibernators undergo profound behavioural, physiological and biochemical changes in order to cope with hypothermia, ischemia-reperfusion, and finite fuel reserves over weeks of continuous torpor [Storey, 2010]. Against a backdrop of global reductions in energy-expensive processes such as transcription and translation, a subset of genes/proteins are strategically up-regulated in order meet challenges associated with hibernation [Van Breukelen et al. 2004; Morin and Storey 2009; Storey 2014]. Consequently, hibernation provides a phenomenon with which to understand how a set of common genes/proteins can be differentially regulated in order to enhance stress tolerance beyond that which is possible for nonhibernators.

Conserved from yeast to humans, the family of mitogen-activated protein kinases (MAPK) are now known to be master regulators of gene expression and the stress response (Fig. 3.1). MAPKs utilize a three-tiered signal relay in which an activated MAPK kinase kinase (MAPKKK or MEKK) activates a MAPK kinase (MAPKK or MEK), which then activates a MAPK in one of three MAPK subfamilies: extracellular-signal-regulated kinases (ERKs); c-Jun N-terminal kinases (JNKs); and p38 kinases [Cowan and Storey 2003; MacDonald, 2004]. The ERK module responds primarily to growth factors and mitogens [Ramos 2001], whereas JNK and p38 are collectively called stress-activated MAPK (SAPKs) since they are activated by stress signals including heat shock, osmotic stress, oxidative stress, inflammatory cytokines, ischemia and UV

exposure [Kyriakis and Avruch, 2001]. While there is a large degree of specificity in different MAPK cascades, there is also significant overlap in the initiating signals observed among them. The 3-tiered MAPK cascade can provide a huge amplification of signal and, since both upstream activators and downstream targets can be shared between different subfamilies, there is also an enormous potential for cross-talk and feedback in signaling [MacDonald, 2004; Qi and Elion 2005; Turjanski et al. 2007].

A distinguishing feature of MAPK activation involves a dual phosphorylation event in the regulatory loop of the kinase, effectively acting as a "on" and "off" molecular switch to regulate kinase activity [Canagarajah et al. 1997]. This feature provides a convenient signature for the activation of MAPK pathways whereby phosphorylation sites are indicative of their activation profile. MAPKs have diverse downstream substrates which may be present in both the cytoplasm and the nucleus [MacDonald and Storey, 2005]. One group of downstream targets are transcription factors, making MAPKs major players in transcriptional programing with influences on all aspects of cell survival and physiological adaptation as well as pathological manifestations [Yang et al. 2003]. MAPKs phosphorylate many transcription factors in their transactivation domain (TAD) thereby enhancing their transcriptional activity [Turjanski et al. 2007]. Additionally, MAPKs can also activate a variety of kinases (e.g. MAPKAP kinases) and heat shock proteins (e.g. HSP27) which play central roles in the stress response [Nadeau and Landry 2007].

I hypothesized, therefore, that MAPKs would play an essential role in signal transduction pathways which modulate gene transcription in skeletal and cardiac muscle of the thirteen-lined ground squirrel (*Ictidomys tridecemlineatus*) over the torpor-arousal

cycles of hibernation. Additionally, I hypothesized that another central pathway of MAPK regulation would involve heat shock proteins which play an established role in multiple forms of hypometabolism [Storey and Storey, 2011]. Taken together, these regulatory mechanisms should mitigate stresses associated with cycles of torpor-arousal. The relative protein expression levels of multiple phosphorylated MAPK signaling pathway members including p-MEK1 Ser222, p-ERK1/2 Thr185/Tyr187, p-JNK Thr183/Tyr185, p-p38 Thr180/Tyr182, and effector substrates including p-MSK1 Ser212, p-CREB1 Ser133, p-ELK1 Ser383, p-c-Jun Ser73, p-ATF2 Thr71, p-p53 Ser15, as well as heat shock proteins HSP27, p-HSP27 Ser78, p-HSP27 Ser78/Ser82, HSP60, HSP70 (HSP72) and HSP90α were assessed by Luminex® Assays and western blotting. In muscle, p-JNK was differentially regulated with a particular role for p-JNK2/3 during early arousal. By contrast, all MAPKs analyzed were responsive to torpor-arousal in cardiac muscle with peak responses during early arousal. While the majority of transcription factors and HSPs were not responsive to hibernation, the relative expression of p-ELK1 and HSP60 were significantly enhanced in skeletal muscle during interbout arousal and late torpor as compared to euthermic controls, respectively.

Material and Methods

Animals

Thirteen-lined ground squirrels (*Ictidomys tridecemlineatus*) were captured, treated, and organs harvested following the same protocol as previously described in Chapter 2 [McMullen and Hallenbeck 2010]. The skeletal muscle used was sampled from hind limb muscles while cardiac muscle was a mixture of atrial and ventricular tissue.

Total Protein Extraction and Immunoblotting

Samples of frozen skeletal and cardiac muscle (~100 mg) were homogenized and prepared for Western blotting as previously described in Chapter 2. Total protein extracts to be used for Luminex® assays were extracted following a different protocol outlined below.

Western Blotting

Western blotting was performed as described in Chapter 2. Equal amounts of protein from each sample were loaded onto 10% polyacrylamide gels and run at 180 V for 45 minutes. To evaluate relative protein levels of p-JNK2/3 p54, p-JNK1 p46, p-CREB1 or p-ELK1, aliquots of 20 µg of protein were loaded into each well. PVDF membranes were blocked using 2.5% skimmed milk in TBST for 30 min, and were probed with specific primary antibodies for mammalian p-JNK Thr183/Tyr185 (Cell Signaling Technology, 9251), p-CREB1 Ser133 (Santa Cruz Biotechnology Inc., sc-7978), or ELK1 Ser383 (Cell Signaling Technology, 9181). Antibodies for JNK cross-created with two bands on immunoblots at the expected molecular masses of 54 and 46 kDa for the mammalian JNK2/3 and JNK1, respectively, whereas p-CREB1 cross-reacted with a single band at 43 kDa and p-ELK1 at 47 kDa. Antibodies were all used at 1:1000 v/v dilution in TBST and incubated overnight at 4^{o}C. Membranes were then probed with HRP-linked anti-rabbit IgG secondary antibody (~1:4000 v:v dilution). All membranes were washed three times between incubation periods in TBST for approximately 5 minutes/wash. Bands were visualized by enhanced chemiluminescence (H_2O_2 and

Luminol) and then blots were restained using Coomassie blue (0.25% w/v Coomassie brilliant blue, 7.5% v/v acetic acid, 50% methanol) to visualize all protein bands.

Protein Extraction for Luminex® Assays

Samples of frozen skeletal and cardiac muscle (50 mg) from n=4 individuals from each of five time points in the torpor-arousal cycle (EC, EN, LT, EA, IA) were separately extracted as per manufacturer's instructions (EMD Millipore; Cat #48-660 and 48-615MAG). Briefly, tissue samples were Dounce homogenized 1:4 w:v in ice cold lysis buffer (Millipore; Cat#43-040) containing phosphatase (1 mM Na_3VO_4, 10 mM ß-glycerophosphate) and protease (BioShop Cat# PIC001) inhibitors. After 30 min incubation on ice with occasional vortexing, samples were centrifuged (12,000 ×g, 20 min, 4°C) and the supernatants collected as total soluble protein lysates. Protein concentration of the lysates was determined using the Bradford assay (Bio-Rad; Cat# 500-0005), standardized to 5 µg/µl, and tissue extracts were stored at -80°C until further use. Aliquots were either combined with Milliplex MAP Assay Buffer 2 (Cat# 43-041) or Milliplex MAP Assay Buffer 1 (Cat# 43-010) for the MAPK and Heat Shock Protein panels, respectively. A final working concentration of 0.7 µg/µl for the MAPK/SAPK Signaling Panel (17.5 µg total protein/well) and 5.2 ng/µl for the Heat Shock Protein Panel (130 ng total protein/well) was prepared by diluting lysates at least 1:1 in their corresponding Assay Buffer.

Positive and negative controls were also prepared from human cell lines for each multiplex panel. For the Heat Shock Protein panel these consisted of cell lysates prepared from unstimulated HeLa cells (Millipore Cat# 47-205) versus heat shocked HeLa cells

(42°C for 30 min), grown for 16 h at 37°C, and treated with arsenite (400 μM for 30 min). For the MAPK/SAPK Signaling panel the controls consisted of unstimulated HeLa cell lysates (Cat#47-205), HeLa cell lysates treated with arsenite and heat shocked (Cat#47-211), A431 cell lysates stimulated with epidermal growth factor (Cat#47-210), and NIH/3T3 cell lysates treated with anisomycin (Cat#47-219). Lyophilized cell lysates were reconstituted in 100 μl ultrapure water, gently vortexed, and incubated at room temperature for 5 min. The reconstituted lysates were prepared for use by the addition of an appropriate amount of assay buffer, as specified by manufacturer instructions for each kit.

Luminex® Assays

Luminex® assay panels were purchased from EMD Millipore and were used according to the manufacturer's instructions. The assays employed in this study were used to measure MAP Kinase/SAP Kinase phosphoproteins (10-Plex MAPK/SAPK Signaling Panel – Phosphoprotein, Cat#48-660) and heat shock proteins (5-Plex Heat Shock Protein Magnetic Bead Panel, Cat#48-615MAG) in both skeletal and cardiac muscle of *I. tridecemlineatus* at each of five stages of the torpor-arousal cycle (as above). The protocol for multiplex analysis followed manufacturer's directions. Briefly, premixed antibody capture beads were sonicated, vortexed, and diluted as required. After incubation with assay buffer, sample or control lysates were individually combined with the premixed beads in a 96-well microplate. The assay wells were then incubated overnight at 4^{o}C on a plate shaker (600-800 rpm) while protected from light. Using a Handheld Magnetic Separator Block (Cat#40-285) to retain the magnetic beads, the assay

mixture was subsequently removed, and the wells were then washed three times each with assay buffer. Biotin-labeled detection antibodies were vortexed and diluted as required, and then added to wells containing the magnetic capture beads. After incubation for 1 h at room temperature on a plate shaker protected from light, the wells were decanted, washed, and incubated with appropriately prepared Streptavidin-Phycoerythrin for 15-30 min at room temperature on a plate shaker protected from light. After this incubation, amplification buffer was added to each well (15 min incubation at room temperature on a plate shaker) before decanting and resuspension in Sheath Fluid. Measurements were taken immediately after the assay was finished using either a Luminex 100® (MAPK/SAPK Panel) or a MAGPIX® (Heat Shock Protein Panel) instrument with xPonent software (Luminex® Corporation).

Quantification and Statistical Analysis

Bead-based assays used the net Median Fluorescence Intensity (MFI) of a population of measurements (with a minimum bead count of 50) in order to determine relative protein levels. Band densities on chemiluminescent immunoblots were visualized using a Chemi-Genius BioImaging system (Syngene, Frederick, MD) and quantified using the associated Gene Tools software. Immunoblot band density in each lane was normalized against the summed intensity of a group of Coomassie stained protein bands in the same lane. Data are expressed as means ± SEM, n = 3-4 independent samples from different animals. Statistical testing of normalized band intensities used one-way ANOVA and a post-hoc Tukey test ($p<0.05$).

Results

Regulation of MAPK signaling cascades in skeletal and cardiac muscle during hibernation

Phosphorylated protein levels of several members of the MAPK signaling pathway fluctuated significantly in both skeletal and cardiac muscle during hibernation (Fig. 3.2-3.4). In skeletal muscle, p-JNK Thr183/Tyr185 was the only MAPK that increased significantly as compared to EC values; relative expression levels during EA were 3.7 fold higher (Fig. 3.2). Furthermore, while p-JNK values in LT were not enhanced as compared to EC values, a statistical significant difference was observed when comparing EN and LT values (LT was 3.4 fold higher than EN). The relative expression of p-ERK1/2 Thr185/Tyr187 was significantly reduced during EN and IA; values decreased to 63% and 65% of EC values, respectively.

JNK is coded by three genes – JNK1 (p46), JNK2 (p54), and JNK3 (p54) – which display a high degree of homology (e.g. JNK1 and JNK2 exhibit 83% identity) as well as similarities in their regulatory mechanisms [Kallunki et al. 1994]. Since JNK was the only MAPK to increase over the torpor-arousal cycle in skeletal muscle and the 46 and 55 kDa protein kinases could be separated by western blotting, further experiments were carried out to determine which p-JNK isoform was significantly elevated. As evidenced in Figure 3.3, the relative expression of JNK1 p46 did not change during hibernation; however, JNK2/3 p54 increased significantly during EA as compared to EC values (EA was 4.5 fold higher than EC).

In cardiac muscle, levels of p-ERK1/2 were significantly elevated during EA as compared to EC (3.7 fold) and all other hibernation stages whereas the levels of p-MEK1

did not change significantly (Fig. 3.4). Levels of p-JNK were not significantly elevated over EC values, although statistically significant increases were observed when EA values were compared to values obtained from EN (3.2 fold), LT (2.3 fold), and IA (2.4 fold). Finally, the levels of p-p38 Thr180/Tyr182 rose during LT (3 fold) and peaked during EA (8.5 fold), as compared to EC values.

Regulation of MAPK effector kinases and transcription factors in skeletal and cardiac muscle during hibernation

Transcriptional activity is regulated by posttranslational modifications such as protein phosphorylation at several distinct sites on transcription factors. MAPKs are one class of kinases which phosphorylate transcription factors (e.g. p-CREB-1 Ser133, p-ELK1 Ser383, p-c-Jun Ser73, p-ATF2 Thr71, p-p53 Ser15) either directly or via the activation of intermediate kinases (e.g. p-MSK1 Ser212) thereby playing a critical role in gene expression programs. As such, phosphorylated protein levels of several stress-activated transcription factors were measured in both skeletal and cardiac muscle over the course of hibernation (Fig. 3.5-3.6). In skeletal muscle, the only target that was differentially regulation was p-ELK1 Ser383 whereby relative phosphorylation of the protein showed a rising trend during LT and EN and was significantly higher than the EC value during IA (by 2.1 fold) (Fig. 3.5).

Similarly, p-ELK1 was the only target that was differentially regulated during hibernation in cardiac muscle. In this case, however, statistically significant decreases were observed during IA; values were just 23% of EC values and 18% of LT and EA values.

Expression of Heat Shock Proteins in skeletal and cardiac muscle during hibernation

MAPKs also phosphorylate heat shock proteins which are pivotal to the stress response. Consequently, HSP27 which is regulated by MAPK phosphorylation on Ser78 was analyzed along with a panel of other HSPs with possible roles in aiding skeletal and cardiac muscle responses to hibernation. In skeletal muscle, the majority of heat shock proteins were not responsive to the torpor-arousal cycle and no changes in the phosphorylation state of HSP27 or HSP70 were observed. However, HSP60 increased significantly during LT, as compared to EC (3 fold), EN (2.7 fold), EA (3.6 fold), and IA (5.5 fold) (Fig. 3.7).

In cardiac muscle, none of the HSPs analyzed showed differential regulation over the torpor-arousal cycle as compared to EC values (Fig. 3.8). However, HSP27 levels decreased significantly during LT as compared to EN (by 50% of EC) and p-HSP27 Ser78 levels decreased during EN by 49% as compared to LT and IA values.

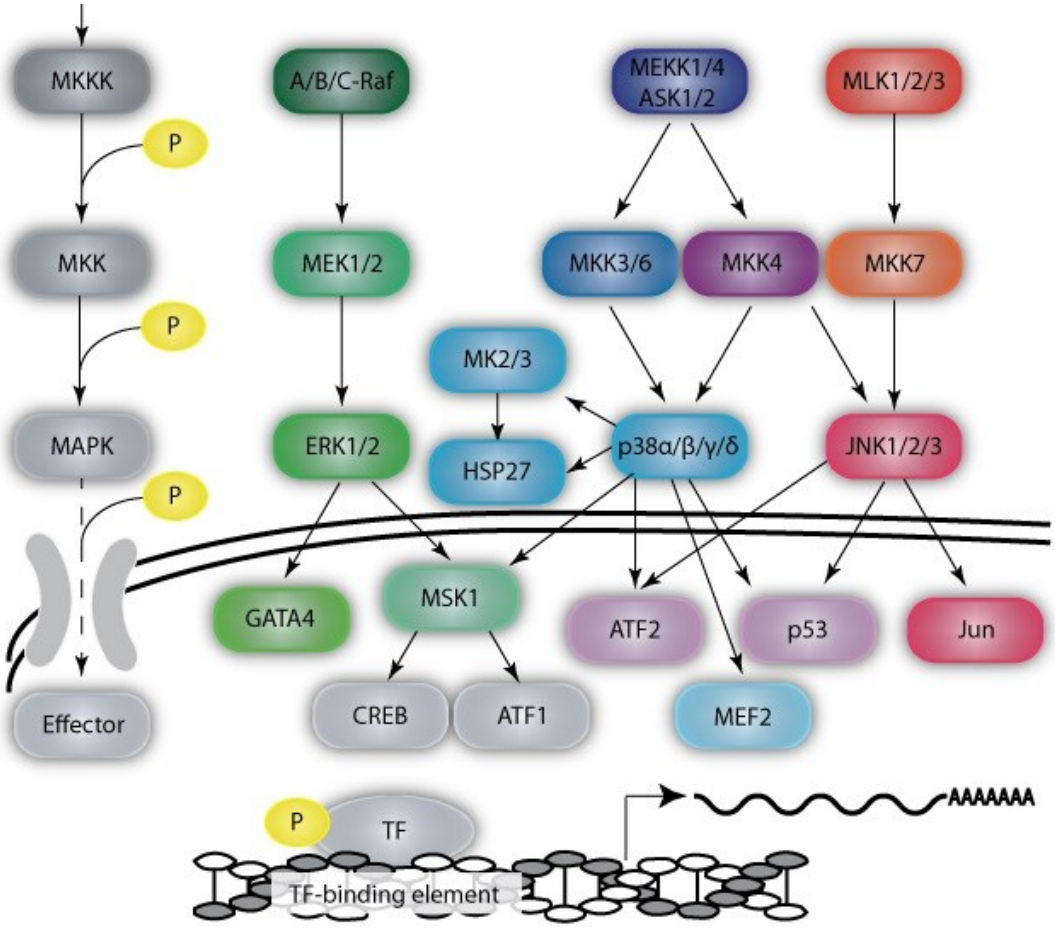

Figure 3.1: Mitogen-activated protein kinase (MAPK) signaling. MAPK pathways are characterized by three-tiered protein kinase cascades in which an external stimulus serves to activate a MAPK kinase kinase (MAPKKK, e.g. A/B/C-Raf, MEKK1/4, MLK1/2/3), which then activates a MAPK kinase (MAPKK, e.g. MEK1/2, MKK3/6, MKK4, MKK7), which subsequently activates a terminal MAPK. The extracellular-signal regulated kinases (ERK1/2; indicated in green), the p38 (indicated in blue), and the c-Jun amino-terminal kinases (JNK; indicated in red) represent three major MAPK pathways. MAPKs then proceed to phosphorylate downstream effector molecules such as transcription factors (e.g. GATA4, CREB-1, ATF1, ATF2, MEF2, p53, Jun), heat shock proteins (HSPs), and others, either directly or via the activation of intermediate kinases (e.g. MSK1, MK2/3). P and TF denote a phosphate group and transcription factor, respectively.

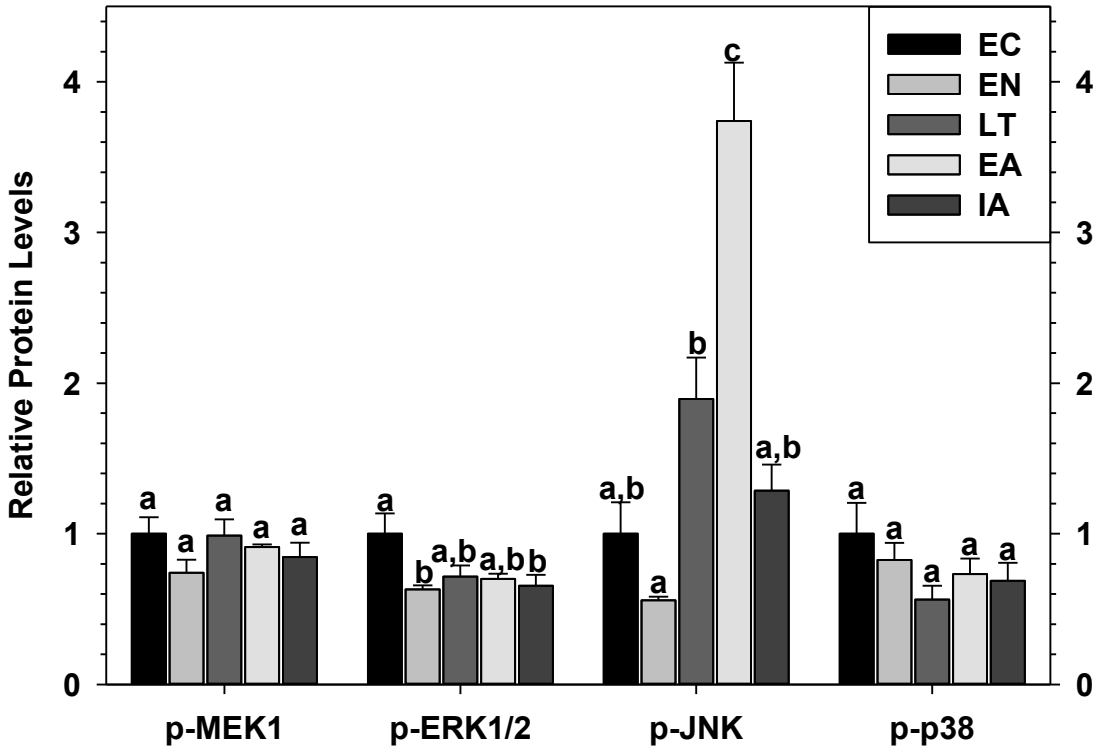

Figure 3.2: Relative phosphorylation status of the MAPK signaling pathway kinases MEK1 Ser222, ERK1/2 Thr185/Tyr187, JNK Thr183/Tyr185, and p38 Thr180/Tyr182 in skeletal muscle of *I. tridecemlineatus* over the torpor-arousal cycle. Histograms showing relative protein levels for bead-based assays were determined using the net MFI as measured by Luminex®. Data are means ± S.E.M. (N=3-4 independent protein isolations from different animals). Data were analyzed using analysis of variance with a post hoc Tukey test ($p<0.05$); values that share the same letter notation are not significantly different from one another.

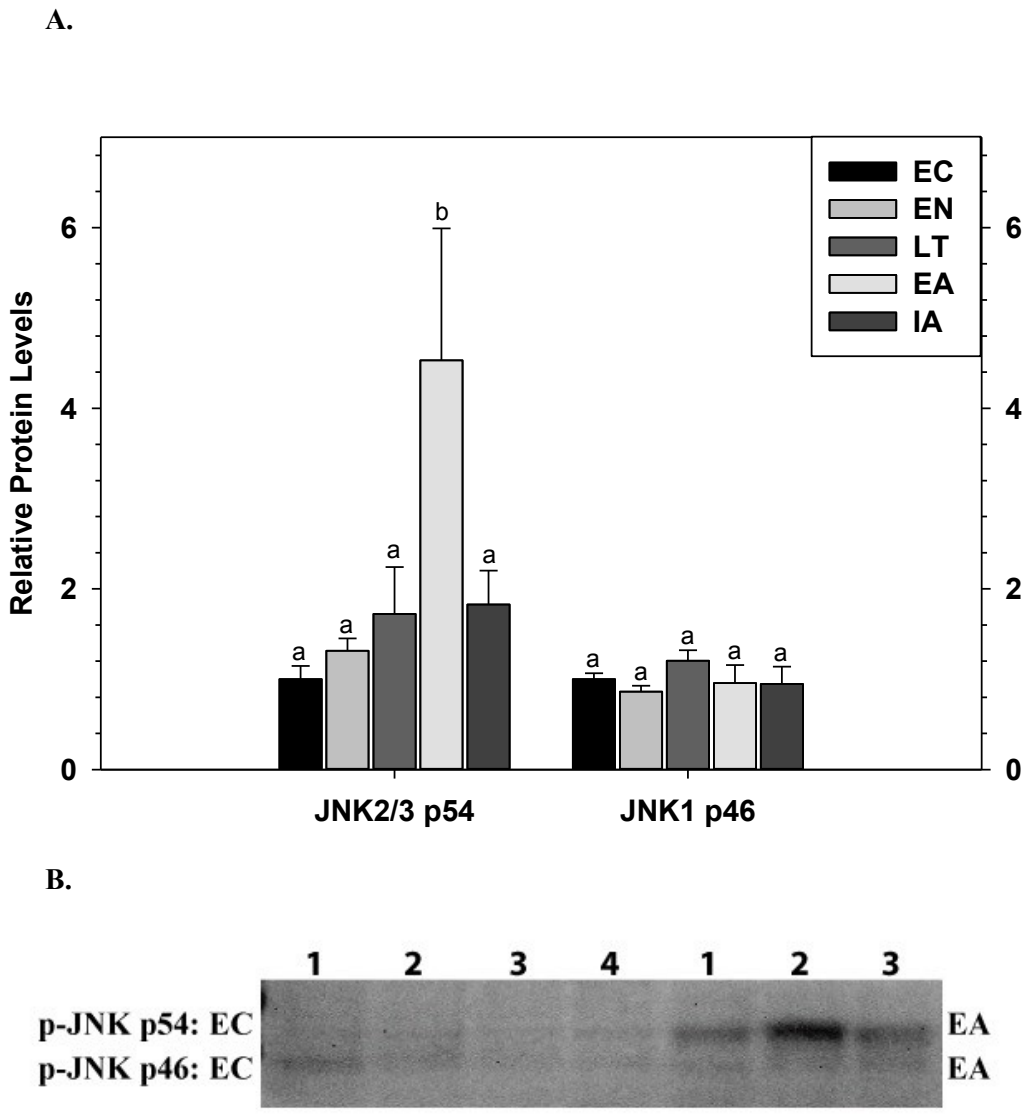

Figure 3.3: Relative phosphorylation status of the MAPK signaling pathway kinases, JNK2/3 p54 Thr183/Tyr185 and JNK1 p46 Thr183/Tyr185, in skeletal muscle of *I. tridecemlineatus* over the torpor-arousal cycle. A. Histograms showing relative protein levels were determined using band densities from immunoblotting. Data are means ± S.E.M. (N=3-4 independent protein isolations from different animals). B. Representative immunoblots are shown for selected experimental conditions. The protein of interest and select experimental conditions are labeled to the left and right while sample numbers (lanes) are labeled along the top indicating 4 samples of one type (e.g., EC lanes 1, 2, 3, 4) and 3 samples of another (e.g. EA lanes 1, 2, 3). Other information as in Figure 3.2.

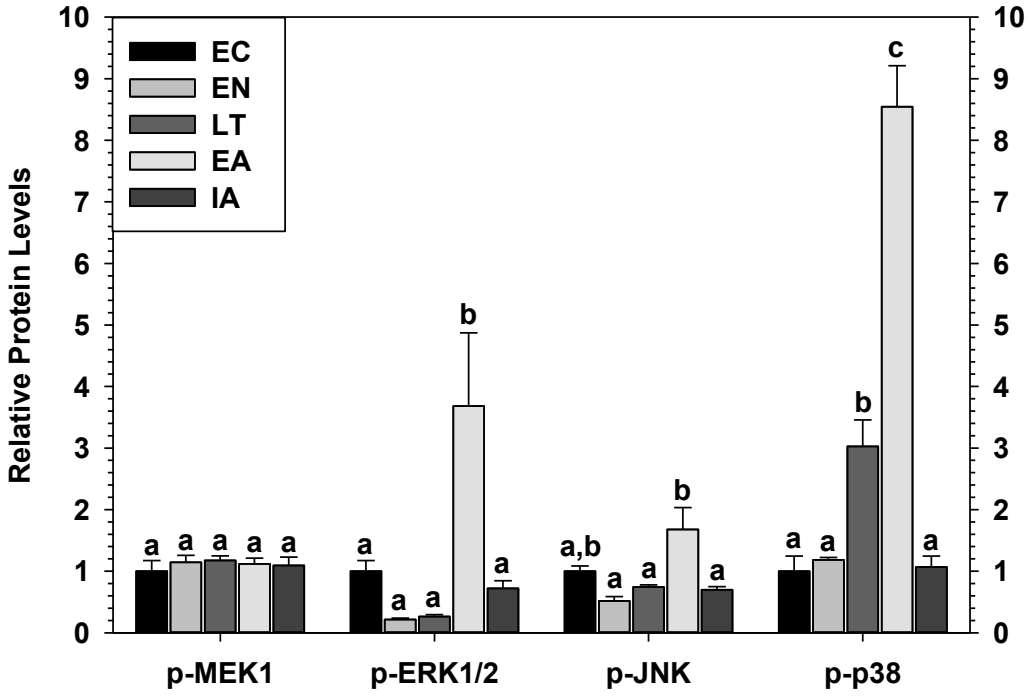

Figure 3.4: Relative phosphorylation status of the MAPK signaling pathway kinases MEK1 Ser222, ERK1/2 Thr185/Tyr187, JNK Thr183/Tyr185, and p38 Thr180/Tyr182 in cardiac muscle of *I. tridecemlineatus* over the torpor-arousal cycle. Histograms showing relative protein levels for bead-based assays were determined using the net MFI as measured by Luminex®. Data are means ± S.E.M. (N=3-4 independent protein isolations from different animals). Other information as in Figure 3.2.

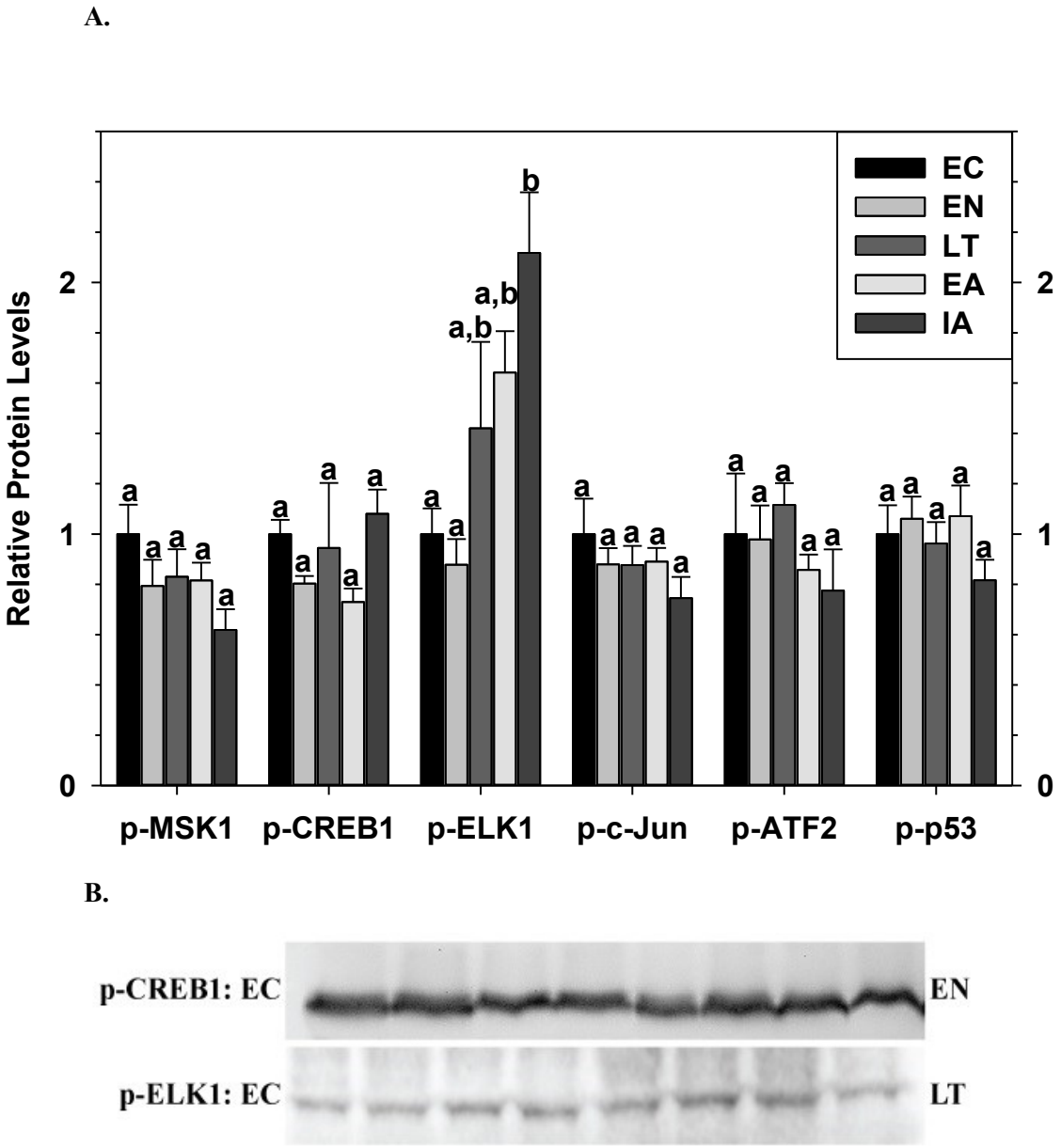

Figure 3.5: Relative phosphorylation status of the effector kinase p-MSK1 Ser212 and transcription factors p-CREB1 Ser133, p-ELK1 Ser383, p-c-Jun Ser73, p-ATF2 Thr71, p-p53 Ser15 in skeletal muscle of *I. tridecemlineatus* over the torpor-arousal cycle. A. Histograms showing relative protein levels were determined using the net MFI for bead-based assays (p-c-Jun Ser73, p-ATF2 Thr71, p-p53 Ser15) or band densities for immunoblotting (p-CREB1 Ser133, p-ELK1 Ser383). Data are means ± S.E.M. (N=3-4 independent protein isolations from different animals). B. Representative immunoblots are shown for selected experimental conditions. The protein of interest and select experimental conditions are labeled to the left and right while sample numbers (lanes) are labeled along the top indicating 4 samples of one type (e.g., EC lanes 1, 2, 3, 4) and 4 samples of another (e.g. EN/LT lanes 1, 2, 3, 4). Other information as in Figure 3.2.

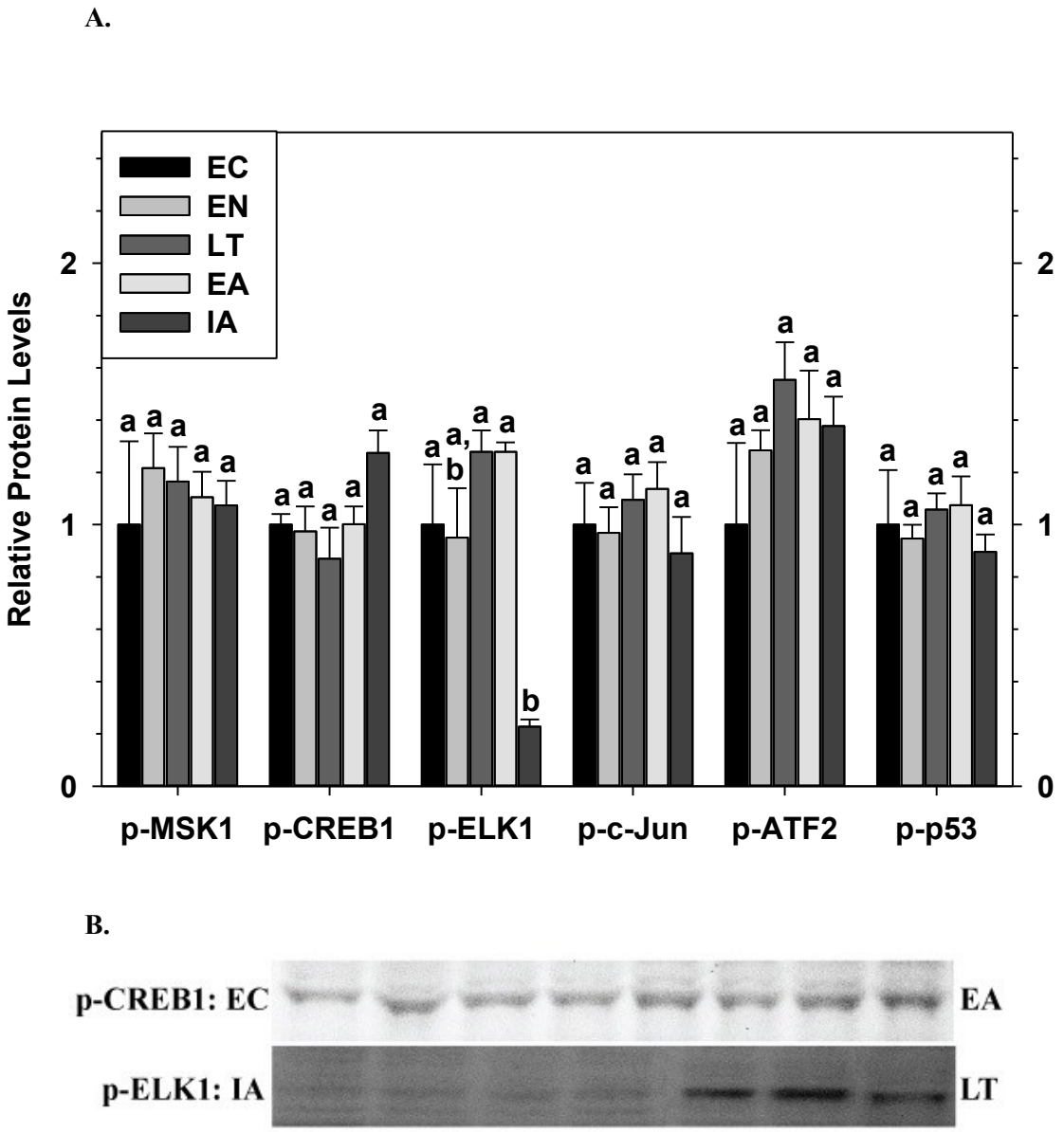

Figure 3.6: Relative phosphorylation status of the effector kinase p-MSK1 Ser212 and transcription factors p-CREB1 Ser133, p-ELK1 Ser383, p-c-Jun Ser73, p-ATF2 Thr71, p-p53 Ser15 in cardiac muscle of *I. tridecemlineatus* over the torpor-arousal cycle. A. Histograms showing relative protein levels were determined using the net MFI for bead-based assays (p-c-Jun Ser73, p-ATF2 Thr71, p-p53 Ser15) or band densities for immunoblotting (p-CREB1 Ser133, p-ELK1 Ser383). Data are means ± S.E.M. (N=3-4 independent protein isolations from different animals). B. Representative immunoblots are shown for selected experimental conditions. The protein of interest and select experimental conditions are labeled to the left and right while sample numbers (lanes) are labeled along the top indicating 4 samples of one type (e.g., EC/EA lanes 1, 2, 3, 4) and 3/4 samples of another (e.g. EA/IA lanes 1, 2, 3, 4). Other information as in Figure 3.2.

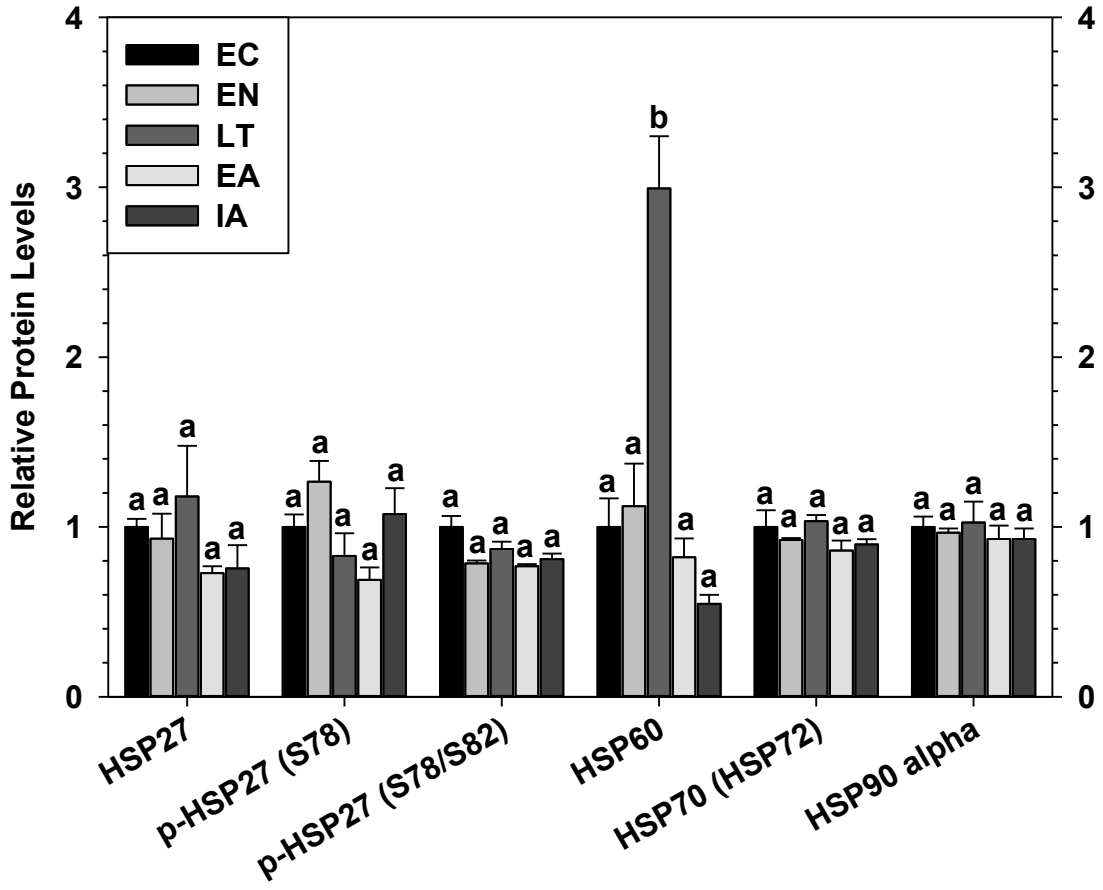

Figure 3.7: Relative protein expression of selected heat shock proteins and their phosphorylated forms in skeletal muscle of *I. tridecemlineatus* over the torpor-arousal cycle: HSP27, p-HSP27 Ser78, p-HSP27 Ser78/Ser82, HSP60, HSP70 (HSP72) and HSP90α. Histograms showing relative protein levels for bead-based assays were determined using the net MFI as measured by Luminex®. Data are means ± S.E.M. (N=3-4 independent protein isolations from different animals). All other information as in Fig. 3.2.

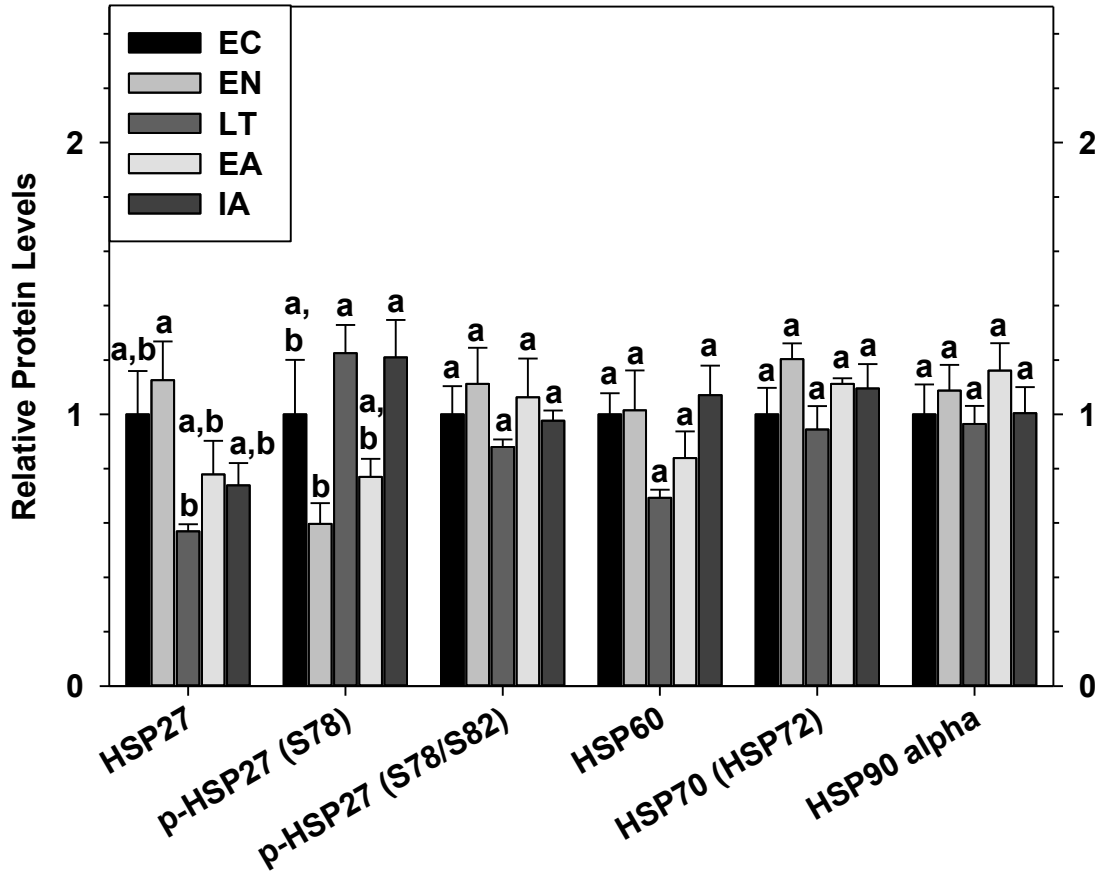

Figure 3.8: Relative protein expression of selected heat shock proteins and their phosphorylated forms in cardiac muscle of *I. tridecemlineatus* over the torpor-arousal cycle: HSP27, p-HSP27 Ser78, p-HSP27 Ser78/Ser82, HSP60, HSP70 (HSP72) and HSP90α. Histograms showing relative protein levels for bead-based assays were determined using the net MFI as measured by Luminex®. Data are means ± S.E.M. (N=3-4 independent protein isolations from different animals). All other information as in Fig. 3.2.

Discussion

Signal transduction pathways and their regulatory effects on gene expression have been shown to be pivotal in meeting challenges associated with hibernation in ground squirrels and bats. MAP kinases are differentially regulated in selected tissues of Richardson's ground squirrels (*Spermophilus richardsonii*) [MacDonald and Storey, 2005; Abnous et al. 2012], arctic ground squirrels (*Spermophilus parryii*) [Zhu et al. 2005], little brown bats (*Myotis lucifugus*) [Eddy and Storey 2005], and greater horseshoe bats (*Rhinolopus ferrumequinum*) [Lee et al. 2002]. Most recently, responses of MAPKs during hibernation in the white and brown adipose tissue of thirteen-lined ground squirrels has also been shown [Rouble et al. 2014]. Therefore, the present chapter aimed at comparing and contrasting MAPK regulation in skeletal and cardiac muscle of the thirteen-lined ground squirrel (*Ictidomys tridecemlineatus*) during hibernation. Furthermore, given the breadth of MAPK regulation, multiple downstream effector proteins were surveyed in order to glean information about the cellular consequences of differential MAPK regulation. Transcription factors are one class of particularly relevant downstream effector targets since they represent the bridge between sensing external cues and directing the transcription of genes which allow a cell to survive adverse conditions. Furthermore, HSP27 is also regulated by select MAPKs in response to stress [Armstrong et al. 1999]. Since HSPs are a conserved feature of hypometabolism [Storey and Storey 2011], the phosphorylation status of HSP27 during hibernation was also evaluated along with other important HSP targets.

While a host of transcription factors under MAPK regulation have already been shown to be differentially regulated during hibernation [Mamady and Storey 2008; Eddy

et al. 2005; Tessier and Storey, 2010; Tessier and Storey 2012], additional hibernation-responsive transcription factors which are well known nuclear targets of MAP-kinase family members were identified by the current research. AP-1 transcription factors are bZIP DNA binding proteins which belong to the Jun and Fos families and are responsive to growth factors, cytokines, and cellular stress [Whitmarsh and Davis 1996]. Jun and Fos associate in various combinations with other transcription factors and the resulting dimeric complexes are thought to be essential to their cellular function [Kayahar et al. 2005]. For example, when c-Jun is complexed with c-Fos the dimer is targeted to the tetradecanoyl-phorbol ester response element (TRE), while interactions of c-Jun with ATF2 target the complex to the cAMP response element (CRE) [Whitmarsh and Davis 1996]. ELK1 is an ETS-domain transcription factor which has been shown to regulate the core gene regulation machinery including basal transcription complex components, spliceosome subunits, and ribosomal proteins [Boros et al. 2009]. The p53 transcription factor is a crucial stress-responsive transcription factor which regulates cell cycle, DNA repair, and apoptosis [Wu 2004]. Finally, HSP family members are chaperone proteins that prevent the aggregation of unfolded proteins as well as facilitate the folding of newly synthesized and malfolded proteins [Gething and Sambrook 1992].

Diverse stress signals activate JNK and p38 whereas the ERK family is primarily regulated by mitogenic stimuli [Cowan and Storey 2003]. As a result, it is no surprise that there was only minimal correlation in the activation profiles of individual MAPKs assessed in ground squirrel skeletal muscle (Fig. 3.2). This trend was also observed in other hibernators whereby changes in the activation patterns of individual MAPKs within a given tissue appeared to be independent [Lee et al. 2002; MacDonald and Storey 2005].

In contrast, cardiac muscle showed a much more concerted response with the phosphorylation of all MAPKs presently measured increasing during early arousal (Fig 3.4). Indeed, other studies in thirteen-lined ground squirrels have also suggested a more unified MAPK response during arousal; p-ERK, p-JNK, and p-p38 were all generally enhanced in brown adipose tissue, while all MAPKs were generally decreased in white adipose tissue [Rouble et al. 2014]. Furthermore, one particular striking theme in the present study, but also extending to data obtained in white and brown adipose tissue [Rouble et al. 2014], is the observation that all MAPKs which were responsive to hibernation were activated during either early or interbout arousal in striated muscle cells or adipocytes, respectively. While tissue-specific differences are expected since each tissue faces unique stresses during hibernation, these data nonetheless suggest that regulatory factors under the control of MAP-kinases are particularly important in achieving transitions back to euthermic body temperatures following deep torpor. A connection between MAPK regulation and modifications on histone proteins may be hypothesized in light of concerted increases in these two pathways during arousal (see Chapter 2). Although further studies are required, MAPKs interact with the epigenetic machinery with capacity to influence post-translational modifications on histone proteins.

Although commonalities in the regulation of MAPKs are evident when comparing responses within a given species, there seems to be very little consistency when comparing data collected across species [Lee et al. 2002; Eddy and Storey 2005; MacDonald and Storey 2005; Zhu et al. 2005; Rouble et al. 2014]. As the closest comparison to the present study, MacDonald and Storey (2005) surveyed five organs of Richardson's ground squirrels; the activity of p-ERK1/2, p-JNK, and p-38 all increased in

skeletal muscle during torpor as compared to controls whereas p-JNK and p-38 were the only MAPKs to change in the heart. These differences may be attributed to differences in the experimental conditions whereby deep torpor in Richardson's ground squirrels is defined as animals in continuous cold torpor for 2 days, rather than 5 days in thirteen-lined ground squirrels. Alternatively, species-specific differences may be particularly relevant as it pertains to MAPK signal transduction.

Despite the diversity of signals which regulate select MAPK, one particularly specific response was observed in the skeletal muscle of thirteen-lined ground squirrels. As compared to euthermic controls, the relative expression of JNK2/3 was significantly elevated during early arousal from torpor while JNK1 relative expression remained constant in muscle (Fig. 3.3). JNK isoforms display a high degree of homology as well as similarities in their regulatory mechanisms [Kallunki et al. 1994]; however, they have been shown to display preferences for specific substrates thereby influencing cellular outcome [Chen et al. 2002]. For example, c-Jun binds to JNK2 twenty-five times more efficiently than JNK1 [Kallunki et al. 1994]. While JNK2/3 levels were enhanced during early arousal, concomitant changes in c-Jun or other transcription factors regulated by JNK (e.g. p-ATF2, p-53) were not observed in the present study (Fig. 3.5), suggesting that JNK2/3 must serve a different role during hibernation. While further evidence is required in order to fully delineate the cellular effects of JNK2/3 activation, another possible substrate may be the redox-sensitive transcription factor Nrf2 which is further described in Chapter 4. JNK has been shown to regulate Nrf2 *in vivo* through direct phosphorylation [Sun et al. 2009b]. In this capacity, five residues were identified as putative phosphorylation sites and, when mutated to alanine, showed significantly

decreased phosphorylation levels compared to wild-type Nrf2 in the presence of overexpressed JNK2 [Sun et al. 2009b]. Taken together, JNK2 may play a role in the phosphorylation of Nrf2 in the skeletal muscle of thirteen-lined ground squirrels during early arousal.

In the present study, ELK1 was the only transcription factor in muscle which showed a mounting response over the torpor-arousal cycle with statistically significant increases only observed in interbout arousal, as compared to controls (Fig. 3.5). Since interbout arousal is generally characterized as a period of renewal and ELK1 regulates components of the core gene regulation machinery, these data suggest that ELK-1 may be vital to achieving this response. This response may be particular relevant to skeletal muscle which must be resistance to extended periods of disuse [Lee et al. 2008; Choi et al. 2009] and, by extension, the arousal phase may represent an essential phase in the maintenance of muscle mass. ELK1 is one of the best studied targets of the ERK cascade, although it is also a p38, JNK, and Akt/PKB substrate [Whitmarsh et al. 1995; Yang et al. 1998; Figueroa and Vojtek 2003]. The activation profile of ELK1 did not correlate with ERK1/2 or p38 and was slightly delayed in comparison to JNK, suggesting ELK1 may be primarily regulated by other kinases such as Akt/PKB during hibernation. Finally, the activation profile of muscle-specific ERK1/2 and p38 matched those of MSK1 and CREB-1 phosphorylation, suggesting this pathway is not activated during hibernation.

In cardiac muscle, the phosphorylated form of ERK1/2 was significantly enhanced during early arousal as compared to all other experimental conditions, p-JNK was significantly enhanced during early arousal as compared to EN, LT, and IA, and p-p38 was elevated during LT with peak values in EA as compared to all other

experimental conditions. These data suggest that the response of MAPKs in the hibernator heart is quite substantial and most important during early arousal from torpor. Despite this unified activation pattern, the phosphorylation status of the downstream transcription factors presently measured were not similarly enhanced, attesting to the capacity for MAPKs to propagate highly specific responses despite a vast range of downstream substrates. Other possible substrates for cardiac-specific MAPK regulation may include MEF2 (regulated by p38 and ERK5) and GATA4 (regulated by ERK1/2) transcription factors which have previously been shown to play an important role in the heart of thirteen-lined ground squirrels during torpor[Tessier and Storey, 2012; Luu et al. 2014]. In these studies, GATA4 phosphorylation increased significantly during early arousal from torpor, suggesting that GATA4 may be regulated by ERK1/2 at this hibernation stage. In contrast, MEF2A/C activation did not correlate with p38 activity, leaving open the possibility that ERK5 is the preferential regulator of MEF2 in hibernator hearts. Indeed, other possibilities for p38 activity in cardiac muscle may include the regulation of the translation initiation factor eIF4E (via MNK1) since phosphorylation of this target is a central signal leading to decreased translational competence [Shveygert et al. 2010]. Of course, it is well established that the regulation of initiation and elongation translation factors is employed as a necessary means to achieve global reductions in translation during hibernation [Van Breukelen et al. 2004]. GADD153 is another plausible p38 target which may be targeted during hibernation. Although it is not known if the phosphorylation of GADD153 is increased during hibernation, Mamady and Storey (2008) demonstrated significant increases in the relative amount of of GADD153 protein suggesting that its activity may also increase. Nonetheless, further evidence will surely

unravel targets under the control of MAPK regulation during deep torpor and early arousal in the heart.

A second class of downstream effector molecules considered in the present study were heat shock proteins, in particular HSP27 which is a chaperone protein that also plays an established role in the regulation of translation and controlling stress-induced apoptosis [Cuesta et al. 2000; Zheng et al. 2006]. The p38 MAPK has been shown to phosphorylate HSP27 either directly or indirectly via MAPKAPK2/3 (MK2/3) [Zheng et al. 2006]. However, as evidenced in Fig. 3.7 and 3.8, the relative levels of HSP27 phosphorylation were not responsive to the torpor-arousal cycle in either skeletal or cardiac muscle. Extending these measurements to additional HSP targets allowed a broader assessment of HSP roles in stress resistance during hibernation. Only one HSP was significantly enhanced in muscle over the torpor-arousal cycle whereby HSP60 was elevated in LT as compared to all other experimental conditions. HSP60 proteins are the chaperones of the mitochondrial compartment [Storey and Storey 2011], suggesting that HSP60 may play an important role in the stabilization of mitochondrial proteins at times when metabolic rate (ie. mitochondrial ATP production) is severely reduced. Similarly, this response was also hypothesized to be important in liver of thirteen-lined ground squirrels during deep torpor [Epperson et al. 2010] and in white adipose tissue when ground squirrels transition to lower body temperatures during the EN phase [Rouble et al. 2014].

In summary, the present study examines the regulation of MAPKs and various downstream effector targets such as transcription factors and HSPs in skeletal and cardiac muscle during ground squirrel hibernation. The only MAPK activated in skeletal muscle

was JNK2/3 whereas a unified response of all three MAPKs was observed in cardiac muscle. All MAPKs which were responsive to hibernation were activated during early arousal, suggesting that regulatory mechanisms under the control of MAP-kinases are particularly important during the transition from cold to warm body temperatures. Furthermore, ELK1 may also play an important role during arousal from torpor in muscle and HSP60 is probably more important during deep torpor.

Chapter 4

Modulating Nrf2 transcription factor activity: revealing the regulatory mechanisms of antioxidant defenses during hibernation.

Introduction

Of particular interest in this chapter are the molecular mechanisms which counter conditions known to cause oxidative stress in nonhibernating mammals. During deep torpor, thirteen-lined ground squirrels experience conditions that would be considered ischemic in nonhibernators including reductions in heart rate (1% of normal), respiration rate (3% of normal), and cerebral blood flow (10% of normal) [Zatzman 1984; McArthur and Milsom 1991; Martin et al. 1999; Geiser 2004; Heldmaier et al. 2004; Chung et al. 2011; Dave et al. 2012]. Following prolonged periods of torpor, intermittent arousals are fueled by a 10–20-fold surge in oxygen consumption occurring within minutes as the animal rewarms thereby causing the production of damaging reactive oxygen species (ROS) [Storey 1996]. Since attack by ROS is a major cause of damage to cellular macromolecules (e.g. DNA, protein, lipids), most organisms that use hypometabolism possess enhanced antioxidant defenses, which protect macromolecules from damage by ROS both over extended periods of torpor and during the arousal process [Morin and Storey 2007; Allan and Storey 2012; Vucetic et al. 2013].

Critical intracellular antioxidant enzymes, such as superoxide dismutase (SOD), catalase, heme oxygenase-1 (HO-1), and glutathione peroxidase (GPox) are responsible for the main antioxidant defense system of mammals. Nrf2 [Nuclear factor (erythroid-derived 2)-like 2, also known as NFE2L2] is a basic leucine zipper transcription factor responsible for regulating a variety of antioxidant and detoxification [e.g., glutathione S-transferase (GST)] enzymes [Giudice and Montella 2006]. Studies with Nrf2 knockout mice showed that expression levels of important antioxidant and detoxifying enzymes such as SOD, catalase, HO-1, GST, and others, were strongly reduced thereby implicating Nrf2 as a central regulator of the antioxidant defense system in mammals

[Chan and Kan 1999]. Nrf2 is maintained in an inactive form by interaction the repressor KEAP1 (Kelch-like ECH-associated protein 1) a component of the Cul3-Keap1 ubiquitin ligase complex (Figure 4.1) [Taguchi et al. 2011]. The high affinity of Nrf2 for Keap1 under normal conditions means that Nrf2 is relatively short-lived because it is readily polyubiquitinated and subsequently degraded by the proteasome [Taguchi et al. 2011]. Nrf2 also interacts with actin, a building block of microfilaments, and this interaction has been hypothesized to participate in nuclear localization of Nrf2 [Kang et al. 2002]. Binding of Nrf2 in the actin complex has been shown to have a covalent component since the denaturing conditions of SDS-PAGE, which are typically known to disrupt protein-protein interactions, do not disrupt the Nrf2-actin pair [Kang et al. 2002; Ni and Storey 2010]. As a result, Nrf2 immunoblots cross-react with a ~60 kDa band at the expected molecular mass for Nrf2 as well as an additional 100 kDa band which represents the Nrf2-actin complex [Kang et al. 2002].

Under conditions of oxidative stress Nrf2 is phosphorylated by protein kinase C (PKC) at S40 thereby releasing Nrf2 from its negative regulator KEAP1 and mediating its movement into the nucleus [Huang et al. 2000]. Whereas PKC phosphorylation is of central importance to Nrf2 activity, other protein kinases have also been shown to phosphorylate Nrf2 including phosphoinositide 3-kinase (PI3K) [Kang et al. 2002], mitogen-activated protein kinases (MAPKs) [Yu et al. 2000], protein kinase RNA-like endoplasmic reticulum kinase (PERK) [Cullinan and Diehl 2004], and protein kinase casein kinase II (CK2) [Pi et al. 2007]. Once released from Keap1, Nrf2 may dimerize with other basic leucine zipper proteins such as small Mafs (sMafF, sMafG, sMafK; small musculoaponeurotic fibrosarcoma), JunD, ATF4 (activating transcription factor-4),

and polyamine-modulated factor-1 protein (PMF-1) [Giudice and Montella 2006]. These interactions lead to the binding of Nrf2 to the antioxidant response element (ARE) that is present in the promoter region of many genes that respond to oxidative stress [Giudice and Montella 2006]. In addition, post-translational modifications such as acetylation by CREB-binding proteins (CBP) increases Nrf2 transcriptional activity while sirtuin 1 (SIRT1) antagonizes this interaction by deacetylating Nrf2 [Katoh et al. 2001; Kawai et al. 2011]. Furthermore, a recent study demonstrated that in the presence of a SUMO-specific protease, Nrf2-induced transcription was greatly enhanced, suggesting that sumoylation inhibits Nrf2-induced gene transcription [Theodore et al. 2010]. While there is a consensus SUMO site located in the ZIP domain of Nrf2, further work will be required to determine whether this site can be sumoylated *in vivo*.

I hypothesized, therefore, that natural cellular preservation strategies which regulate the synthesis of key enzymes responsible for cellular antioxidant defense and detoxification, such as Nrf2, may be of central importance to skeletal muscle of the hibernating thirteen-lined ground squirrel (*Ictidomys tridecemlineatus*). To test this, the relative protein expression levels of Nrf2, its binding partner KEAP1 and the downstream target catalase were assessed by western blotting and showed no significant differences in relative protein expression over the torpor-arousal cycle. However, Nrf2-KEAP1 protein-protein interactions and posttranslational modifications (PTMs) on Nrf2 including serine phosphorylation and lysine acetylation were responsive to cycles of torpor-arousal with peak responses occurring during early arousal. These regulatory mechanisms (i.e. protein-protein interactions and PTMs) are crucial during hibernation since they provide mechanisms to mitigate stresses by modifying Nrf2 activity/action in a manner that does

not require the large inputs of energy that would otherwise be needed to regulate Nrf2 via de novo synthesis of the protein.

Materials and Methods

Animals

Thirteen-lined ground squirrels (*Ictidomys tridecemlineatus*) were captured, treated, and organs harvested following the same protocol as previously described in Chapter 2 [McMullen and Hallenbeck 2010]. The skeletal muscle used was sampled from hind limb muscles.

Computational analysis

The full sequence for ground squirrel Nrf2 was deduced using whole genome shotgun (wgs) reads. A wgs BLAST (NCBI) search using the human coding sequence allowed overlapping contigs to be assembled into the full coding sequences for the ground squirrel. Human sequences used for Nrf2 wgs BLAST (NCBI) searches had the accession number NM_006164.4. A minimum of two overlapping contigs were used to construct the full ground squirrel sequence. Additionally, the partial ground squirrel sequence, as obtained previously by Morin et al. (2008), was obtained from GenBank (DQ328859) and aligned with the predicted ground squirrel sequence from Ensemble (ENSSTOG00000000313) in order to create the predicted sequence. The predicted ground squirrel mRNA coding sequence was translated into amino acids and aligned with human using Geneious (Biomatters Ltd) in order to determine percent homology.

Western Blotting

Western blotting was performed as described in Chapter 2. Equal amounts of protein from each sample were loaded onto 10% polyacrylamide gels and run at 180 V for 45 minutes. To evaluate relative protein levels of Nrf2 and KEAP1, 20 μg of protein was loaded into each well. PVDF membranes to be probed with antibodies specific for Nrf2 and KEAP1 were blocked with 2.5% w/v non-fat dried milk dissolved in TBST (0.05% Tween-20) for 30 min. Antibodies specific for mammalian Nrf2 (sc-722) and KEAP1 (sc-15246) were purchased from Santa Cruz Biotechnologies while catalase antibody was purchased from GenScript (A01187-40). Antibodies specific for posttranslational modifications were purchased from the following companies: Life Technologies (phospho-serine; 61-8100), Santa Cruz Biotechnologies (acetyl-lysine; sc-8663), and Abcam (ubiquitin-lysine; 19247). Antibodies for α-SUMO1-lysine and α-SUMO2/3-lysine were obtained from the laboratory of Dr. Hallenbeck at the NIH [Saitoh and Hinchey 2000; Azuma et al. 2003; Lee et al. 2007]. Antibodies for Nrf2 cross-reacted with two bands on the immunoblots at the expected molecular masses of 62 and 100 kDa for the mammalian proteins while KEAP1 and catalase cross-reacted with single bands at 70 and 60 kDa, respectively. Antibodies were all used at 1:1000 v/v dilution in TBST. Membranes were then probed with either HRP-linked anti-goat IgG secondary antibody (~1:8000 v:v dilution), HRP-linked anti-mouse IgG secondary antibody (~1:2000 v:v dilution) or HRP-linked anti-rabbit IgG secondary antibody (~1:4000 v:v dilution). All membranes were washed three times between incubation periods in TBST for approximately 5 minutes/wash. Bands were visualized by enhanced chemiluminescence and then blots were restained using Coomassie blue to visualize all protein bands.

Chemical cross-linking of primary antibody

When running a Co-IP on a denaturing SDS-PAGE gel the primary antibody heavy chain will run at approximately 55 kDa while the light chain will run at 25 kDa. In order to remove this interference, the primary antibody heavy and light chains were covalently cross-linked using dimethyl pimelimidate (DMP). The chemically cross-linked antibody and protein-A agarose beads were added as a unit after the pre-clear step (see *Co-immunoprecipitation* below). The desired volume of beads were extracted from the stock and centrifuged at 500 RPM for 1 min. After discarding the supernatant, an equal volume of 1X phosphate-buffered saline (PBS: 137 mM NaCl, 2.7 mM KCl, 10 mM Na_2HPO_4, 2 mM KH_2PO_4, pH 7.4) was added to the beads (end concentration should be 50% bead slurry) and rotated overnight on a rotisserie at 4°C. The following day, the bead slurry was centrifuged (500 RPM, 1 min) and the PBS supernatant was discarded. An equal volume of dilution buffer (1 mg/mL bovine serum albumin in 1X PBS) was added to the beads, rotated on a rotisserie for 10 min at 4°C, centrifuged (500 RPM, 1 min), and the supernatant discarded as before. During this incubation, the primary antibody was diluted in dilution buffer as per the manufacturer's instructions. Generally, 1-10 µl of antibody was used per 25-50 µl of bead slurry and this was combined with lysates containing 200-600 µg of total protein.

The diluted antibody was added at a 1:1 ratio to the beads, mixed gently, rotated on the rotisserie for 2 hours (4°C), centrifuged, and the supernatant discarded as before. The dilution buffer (without primary antibody) was then added to the beads at a 1:1 ratio, mixed gently, rotated for 5 min at 4°C, centrifuged and the supernatant discarded as before. This wash step with dilution buffer was repeated with 1X PBS before the addition

of the chemical cross-linker DMP. The DMP was prepared in wash buffer (0.2 M triethanolamine in 1X PBS) at a concentration of 6.5 mg/mL, pH 8.2. The DMP was added to the beads at a 1:1 ratio, mixed gently, and rotated on the rotisserie at room temperature for 30 min. After this incubation the sample was centrifuged, the supernatant discarded, and the beads were washed with wash buffer for 5 min at room temperature. The DMP crosslinking-wash cycle was repeated four-five times, resulting in a total cross-linking time of 2.5-3 hours. After the final wash, quench buffer (50 mM ethanolamine in 1X PBS) was added at a 1:1 ratio, mixed gently, rotated for 5 min at room temperature, centrifuged, and the supernatant discarded. The quenching step was repeated two more times followed by a wash in 1X PBS. To remove the excess (unlinked) antibody the sample was combined 1:1 with elution buffer (1 M glycine), mixed gently, rotated for 10 min at room temperature, centrifuged and the supernatant discarded. The removal of excess antibody was repeated three more times. Before addition to the homogenate, the cross-linked antibody and beads were equilibrated in wash buffer (50 mM Tris, 150 mM NaCl, 0.05% Triton X) by three rounds of washing (addition of wash buffer at 1:1 ratio, mix gently, 5 min rotation on rotisserie, centrifuge, and discard supernatant). Antibody-protein-A-agarose beads were directly added to lysates.

Lysate preparation for co-immunoprecipitation

Samples of frozen tissue from five time points in the torpor-arousal cycle (EC, EN, LT, EA, IA) were be separately extracted (N=4). Co-immunoprecipitation was performed on lysates containing total protein. Samples of skeletal muscle were quickly weighed, crushed into small pieces under liquid nitrogen, and then homogenized in lysis

buffer (1:2 w:v) using a Dounce homogenizer (~ 20 piston strokes). Lysates were prepared with a medium salt lysis buffer containing 23 mM Tris, 150 mM NaCl, 0.1% Triton X, 0.1 mM Na_3VO_4, 10 mM β-glycerophosphate, 10 µl/mL Sigma Protease Inhibitor cocktail (containing EDTA), pH 7.4. Following homogenization, total protein preparations were incubated on ice for 20 min, mixing gently every 5 minutes. The samples were then centrifuged at 12,000 RPM for 20 min (at 4°C) and the supernatant containing soluble proteins was transferred to a sterile Eppendorf tube.

While centrifugation was taking place, protein A-agarose beads for preclearing were prepared. Beads were equilibrated in wash buffer (50 mM Tris, 150 mM NaCl, 0.05% Triton X). Approximately 25 µl of bead slurry per 500 µl of sample lysate was removed from the stock and spun down for 2 min at 500 RPM. The supernatant was removed and the beads were re-suspended in wash buffer (1:1 bead:wash buffer ratio). This process was repeated at least three more times and beads were finally re-suspended in a 1:1 bead:wash buffer ratio. The equilibrated beads were then combined with the lysate supernatant for 2 hours at 4°C on a rotisserie machine. After the incubation the samples were centrifuged at 500 RPM for 5 minutes and supernatant transferred to a new tube. The protein content was then measured using the Bio-Rad assay and normalized to 2 µg/µl using lysis buffer.

Co-immunoprecipitation

Crosslinked antibody and beads (prepared as above) were then added to the precleared homogenates (~25-50 µl bead-antibody/slurry per 200-600 µg of protein). The crosslinked antibody/beads and lysates were incubated overnight at 4°C on a rotisserie.

After this incubation, the samples were centrifuged for 5 min at 500 RPM and the supernatant removed. The precipitated product was washed 4 times with lysis buffer and re-suspended in a final 1:1 ratio with lysis buffer. Equal volumes of 2X SDS buffer were added to the samples, boiled, briefly centrifuged, and the supernatant transferred to a clean Eppendorf tube. The samples were stored at -20°C until use. Samples were run and transferred as described in the western blotting procedure above. Approximately 10 µl of each sample was loaded per well. PVDF membranes were probed with antibodies specific for the purified protein of interest, possible binding partners, and the following antibodies; phospho-serine, acetyl-lysine, ubiquitin-lysine, and SUMO1/2/3-lysine.

Quantification and statistics.

Band densities on chemiluminescent immunoblots were visualized using a Chemi-Genius BioImaging system (Syngene, Frederick, MD) and quantified using the associated Gene Tools software. Immunoblot band density in each lane was normalized against the summed intensity of a group of Coomassie stained protein bands in the same lane. Data are expressed as means ± SEM, n = 4-5 independent samples from different animals. Statistical testing of normalized band intensities used one-way ANOVA and a post-hoc test (Tukey, $p<0.05$).

Results

Characterization of thirteen-lined ground squirrel Nrf2

The partial coding sequence for the thirteen-lined ground squirrel Nrf2 was obtained from GenBank with the accession number DQ328859 [Morin et al. 2008]. The human Nrf2 mRNA coding sequence was used in whole genome shotgun NCBI BLAST

analysis and, in combination with the Ensemble website (ENSSTOG00000000313), the amino acid sequence was deduced in order to derive the remainder of the ground squirrel Nrf2 sequence. Figure 4.2 shows the alignment of the amino acid sequence of ground squirrel Nrf2 and the human protein. The protein alignment scores revealed that the ground squirrel and human amino acid sequences were highly conserved (89.9%). The full Nrf2 sequence has 605 residues in human and the ground squirrel sequence is predicted to have 600 residues. Nrf2 transcriptional activity is regulated by posttranslational modifications such as protein phosphorylation, acetylation, ubiquitination, and sumoylation at several distinct sites. Figure 4.3 summarizes the possible posttranslational modifications mapped onto the Nrf2 sequence; numbers indicate amino acids corresponding to the ground squirrel residues followed by the human residues. All known amino acid residues which are predicted to undergo posttranslational modifications are conserved between the ground squirrel and human sequence.

Analysis of Nrf2, KEAP1, and Catalase protein levels

Nrf2 protein levels in skeletal muscle were analyzed by immunoblotting comparing muscle from euthermic control animals (EC) with four time points on the torpor–arousal cycle: EN, LT, EA, and IA (Fig. 4.4). The antibodies cross-reacted with two bands on the immunoblots at the expected molecular masses for Nrf2 of 62 kDa and 100 kDa, as was also confirmed in ground squirrels in previous studies from our lab [Ni and Storey 2010]. The unusually slow migration of Nrf2 100 kDa in SDS-PAGE has been hypothesized to be related to posttranslational modifications of Nrf2 such as phosphorylation [Pi et al. 2007] or ubiquitination [Li et al. 2005]. Additionally, covalent

binding of an actin monomer (43 kDa) [Kang et al. 2002] may be responsible for the slow mobility and previous studies in our lab have confirmed that the actin antibody also shows the same double band pattern [Ni and Storey 2010]. Nrf2 62 kDa protein levels did not change across the torpor-arousal cycle whereas protein levels of Nrf2 100 kDa increased significantly by 1.7 fold, as compared to EC values ($p<0.05$). While KEAP1 total protein levels did not change across the torpor-arousal cycle, catalase increased significantly by 1.6 fold during IA, as compared to EC values.

Analysis of Nrf2 posttranslational modifications

Transcriptional activity is generally enhanced when Nrf2 is phosphorylated and acetylated [Cullinan et al. 2003; Sun et al. 2009a; Sun et al. 2009b; Kawai et al. 2011] and reduced when Nrf2 is ubiquitinated and sumoylated [Zhang et al. 2004; Kim et al. 2011; Malloy et al. 2013]. Therefore, pan-specific antibodies that recognize these posttranslational modifications were used to monitor the activity state of Nrf2 purified by co-immuniprecipitation from five experimental conditions over the torpor-arousal cycle (Fig. 4.5 and 4.6). Relative phosphorylation of Nrf2 62 kDa increased significantly during LT (5-fold higher than EC), peaked in EA (10.3-fold higher than EC), and remained elevated in IA (2.3-fold higher than EC). Similarly, relative acetylation of Nrf2 62 kDa increased significantly during EA (2.1-fold higher than EC) and IA (2.4-fold higher than EC). Relative ubiquitination of Nrf2 62 kDa remained constant throughout the torpor-arousal cycle showing very low levels from EC to EA stages and showing an increase during IA (2-fold higher than EC). Finally, the relative Nrf2 62 kDa SUMO1 and SUMO2/3 levels did not fluctuate over the torpor-arousal cycle, except for an increase in SUMO1 during EA (1.4-fold) as compared to EC.

Changes in the posttranslational modifications of Nrf2 100 kDa were also observed over the torpor-arousal cycle (Fig. 4.6). Relative phosphorylation of Nrf2 100 kDa increased significantly during LT (1.6-fold higher than EC), peaked in EA (2.2-fold higher than EC), and returned to control levels during IA. Relative acetylation levels increased modestly during EA (1.4-fold higher than EC) whereas ubiquitination showed the opposite response whereby relative levels were lowest during EA (38% of the EC levels). Relative Nrf2 100 kDa SUMO1 levels decreased during LT (32% of the EC levels) before returning back to values that were not statistically significant from EC values; however, SUMO2/3 levels were not responsive to the torpor-arousal cycle.

Analysis of Nrf2 protein-protein interactions

KEAP1 (Kelch-like ECH-associated protein 1) sequesters Nrf2 in the cytoplasm, thereby facilitating Nrf2 inhibition and ubiquitination. Consequently, the physical interaction between KEAP1 and Nrf2 was assessed across the torpor-arousal cycle (Fig. 4.7). The total protein levels of KEAP1 did not change over torpor-arousal when assessed via immunoblotting of total soluble protein extracts. However, the amount of KEAP1 that co-purified with Nrf2 changed across the torpor-arousal cycle. As compared to EC, levels of KEAP1 associated with Nrf2 in LT, EA, and IA decreased significantly to 56%, 44%, 18%, respectively, demonstrating a consistent decrease in the amount of KEAP1 that co-purified with Nrf2 throughout the torpor-arousal cycle. Furthermore, immunoblotting for PTMs only showed cross-reaction with the Nrf2 protein bands and not KEAP1. These data suggest that KEAP1 co-purified with Nrf2 is not phosphorylated, acetylated, ubiquitinated, or sumoylated, although it is not known if PTMs occur on KEAP1 that was not bound to Nrf2.

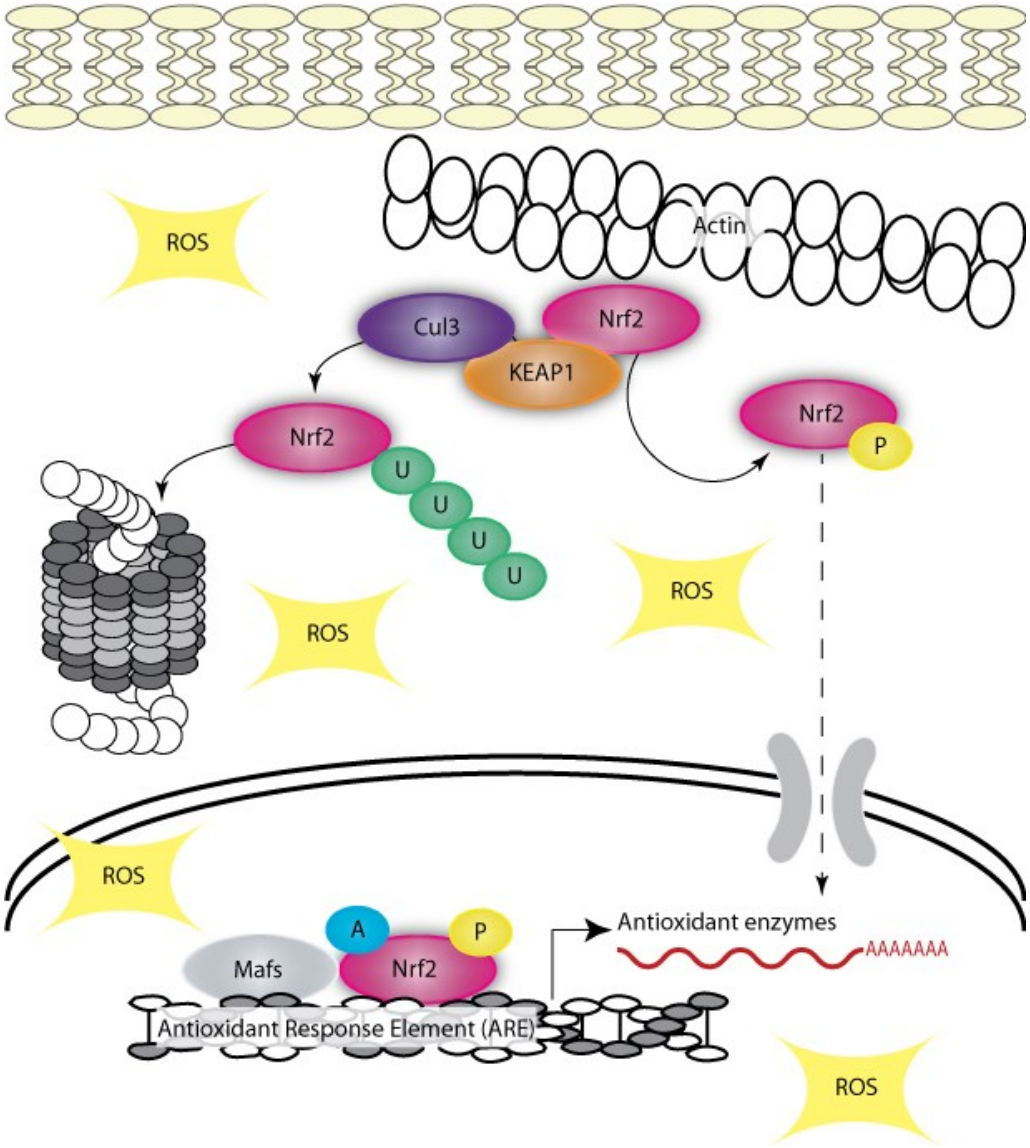

Figure 4.1: Proposed Nrf2-ARE signaling pathway. KEAP1 sequesters Nrf2 in the cytoplasm, thereby facilitating Nrf2 ubiquitination. In cells under stress, stabilization of Nrf2 is thought to be dependent on mechanisms which prevent or reduce access of KEAP1 to Nrf2. Mechanisms which mediate KEAP1–Nrf2 interactions include several redox sensitive cysteine residues in KEAP1 and phosphorylation events in Nrf2. Phosphorylated Nrf2 translocates to the nucleus where it forms heterodimers with small Maf-family proteins to activate the expression of antioxidant genes. U, P, A, and ROS denotes ubiquitination, phosphorylation, acetylation, and reactive oxygen species, respectively.

```
13LGS   1-MMDMELPPPGLPSQQDMDLIDILWRQDIDLGVSREVFDFSQRQKEYELEKQKKLEKERQEQLQKEQEKAF-70
HUMAN   1-MMDLELPPPGLPSQQDMDLIDILWRQDIDLGVSREVFDFSQRRKEYELEKQKKLEKERQEQLQKEQEKAF-70

13LGS  71-FAQLQLDEETGEFLPIQPAQHTQSETSGSANYSQVAHIPKPDALYFDDCMQLLAETFPFVDDNEVSSATF-140
HUMAN  71-FAQLQLDEETGEFLPIQPAQHIQSETSGSANYSQVAHIPKSDALYFDDCMQLLAQTFPFVDDNEVSSATF-140

13LGS 141-QSLVPDIPSHIESPVFNAPPQAQSPETSLDGAMA-DLNNIQQDIEQVWQELFSIPELQCLNIENDKLVET-209
HUMAN 141-QSLVPDIPGHIESPVFIATNQAQSPETSVAQVAPVDLDGMQQDIEQVWEELLSIPELQCLNIENDKLVET-210

13LGS 210-TTVPSPEAKLTEIDNNYFYPSIPSLEKEVGNCSPHFLNAFEDSFSSILSTEDPNQLTVNSLNSDATLNTD-279
HUMAN 211-TMVPSPEAKLTEVDNYHFYSSIPSMEKEVGNCSPHFLNAFEDSFSSILSTEDPNQLTVNSLNSDATVNTD-280

13LGS 280-FGDEFYSAFIAEPSTSNSMPSSATVSQSLSELLYG----SDLSLCKAFNQNHPESTAEFNDSDSGISLNT-345
HUMAN 281-FGDEFYSAFIAEPSISNSMPSPATLSHSLSELLNGPIDVSDLSLCKAFNQNHPESTAEFNDSDSGISLNT-350

13LGS 346-SPSMASPEHSVESSIYGDPPPGFSDSEMEELDNAPGSVKQNVPKTQPIHSGDTVQPLSPSQVHSAPVHDA-415
HUMAN 351-SPSVASPEHSVESSSYGDTLLGLSDSEVEELDSAPGSVKQNGPKTPVHSSGDMVQPLSPSQGQSTHVHDA-420

13LGS 416-YSENTPKKEMPLSPGHRKTPFTKDKHSSRLEAHLTRDELRAKALHIPFPVEKIINLPVDDFNEMMSKEQF-485
HUMAN 421-QCENTPEKELPVSPGHRKTPFTKDKHSSRLEAHLTRDELRAKALHIPFPVEKIINLPVVDFNEMMSKEQF-490

13LGS 486-NEAQLALIRDIRRRGKNKVAAQNCRKRKLENIVELEQDLGHLKDEKEKLLKEKGENDKSLHLLKKQLSTL-555
HUMAN 491-NEAQLALIRDIRRRGKNKVAAQNCRKRKLENIVELEQDLDHLKDEKEKLLKEKGENDKSLHLLKKQLSTL-560

13LGS 556-YLEVFSMLRDEDGKPYSPSEYSLQQTRDGNVFLVPKSKKPDVKKN-600
HUMAN 561-YLEVFSMLRDEDGKPYSPSEYSLQQTRDGNVFLVPKSKKPDVKKN-605
```

Figure 4.2: Predicted amino acid sequence of Nrf2 from 13-lined ground squirrels (13LGS; *I. tridecemlineatus*) compared to the Nrf2 sequence of human (NP_006155). The portion highlighted in yellow corresponds to the Genbank accession number for thirteen-lined ground squirrel Nrf2 (DQ328859) obtained from sequencing results in Morin et al. (2008). In combination with the Ensemble website (ENSSTOG00000000313), the human mRNA coding sequences was used in whole genome shotgun NCBI BLAST analysis to deduce the full length protein. The full length protein is 600 amino acids for 13LGS and 605 for human Nrf2. Dashed lines are inserted when residues are not present in all sequences, black letters are identical comparing the ground squirrel and human sequence, red letters represent substitutions.

A.

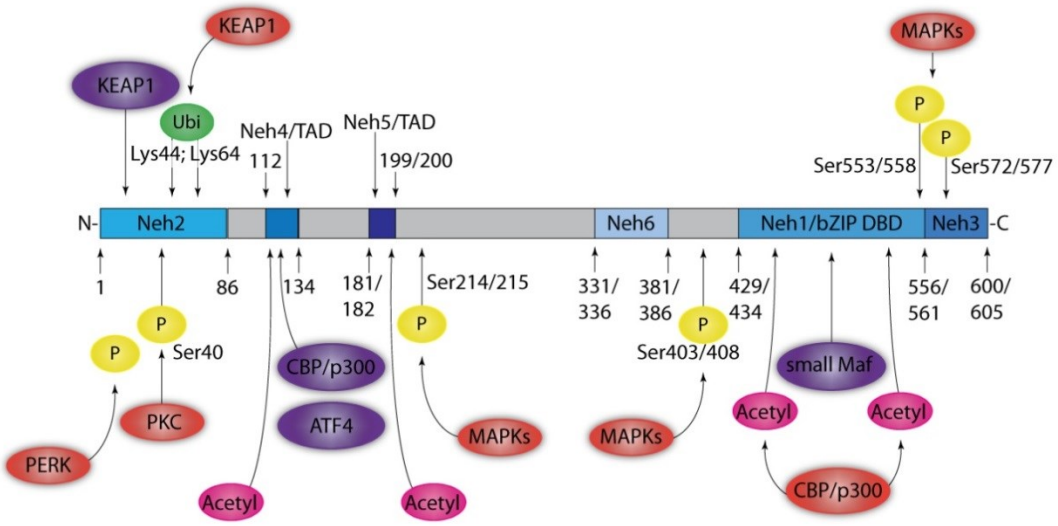

B.

Posttranslational modification	Function	References
Phospho-S40 by PKC-δ	Nrf2-Keap1 dissociation	Bloom and Jaiswal 2003
Phosphorylation in Neh2 domain by PERK	Nrf2-Keap1 dissociation and Nrf2 nuclear import	Cullinan et al. 2003
Ubi-K44 and K64 by KEAP1-Cul3	Negatively controls Nrf2 function	Zhang et al. 2004; Kim et al. 2011
Phospho-S214/215 by MAPK - ERK and JNK	Moderately induces transcription and nuclear localization	Sun et al. 2009b
Phospho-S403/408 by MAPK - ERK and JNK	Moderately induces transcription and nuclear localization	Sun et al. 2009b
Phospho-S553/558 by MAPK - ERK and JNK	Moderately induces transcription and nuclear localization	Sun et al. 2009b
Phospho-S572/577 by MAPK - ERK and JNK	Moderately induces transcription and nuclear localization	Sun et al. 2009b
Phosphorylation by PI3K	Cytoskeletal modifications which may destabilize the Nrf2-Keap1 complex	Kang et al. 2002
Acetyl-K433/K438; K438/K443; K440/K445; K457/K462; K467/K472; K482/K487; K501/K506; K503/K508; K511/K516; K513/K518; K528/K533; K531/K536; K533/K538; K536/K541; K538/K543; K543/K548; K549/K554; K550/K555 by CBP/p300	Augments promoter-specific DNA binding of Nrf2	Sun et al. 2009a
Acetyl-K591/K596; K594/K599 by CBP/p300	Augments promoter-specific DNA binding of Nrf2	Kawai et al. 2011
SUMO-Lys in bZIP domain	inhibits Nrf2-induced gene transcription	Malloy et al. 2013

Figure 4.3: Posttranslational modifications (PTMs) of Nrf2. A. Illustration of PTMs mapped to the corresponding amino acid residues; the first number indicates ground squirrel followed by the human residues. Domains of Nrf2 are represented by blue boxes including Nrf2-ECH homology (Neh) domains, transactivation domains (TAD), and basic ZIP DNA binding domains (bZIP DBD). Kinases and acetyltransferases are denoted by a red circle and proteins which make physical interactions with Nrf2 are denoted by a purple circle. PTMs are denoted as Ubi (ubiquitination), P (phosphorylation), and Acetyl (acetylation). B. Summary of PTM sites and associated kinases/acetyltransferases/ubiquitin ligase and functions.

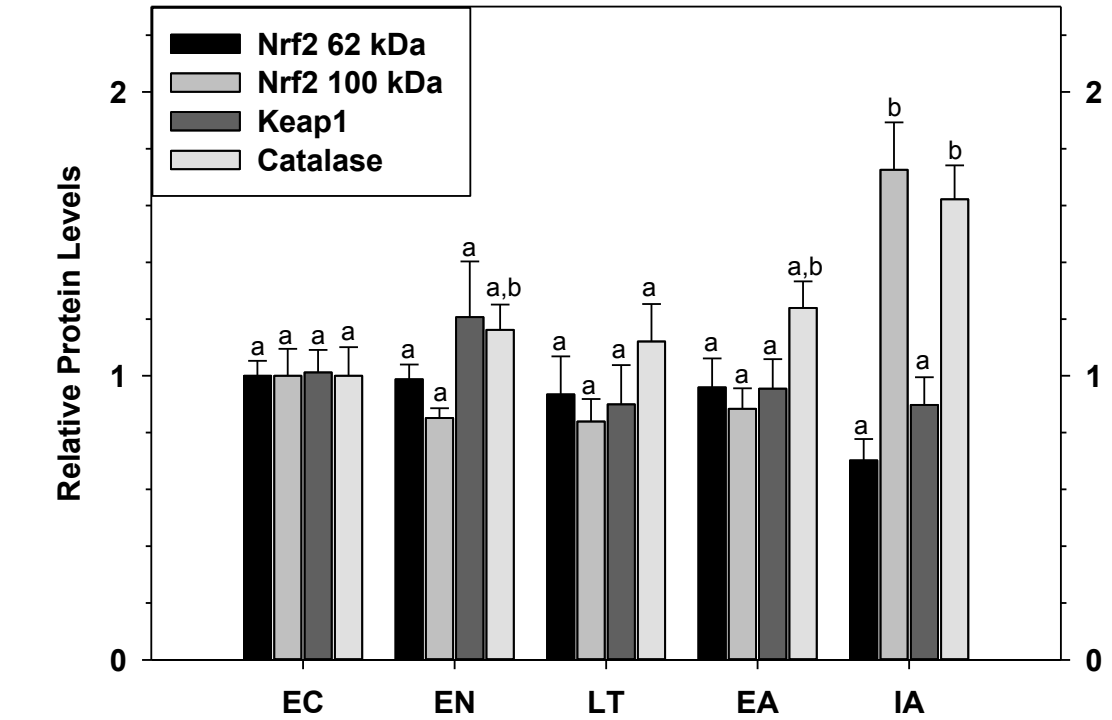

A.

B.

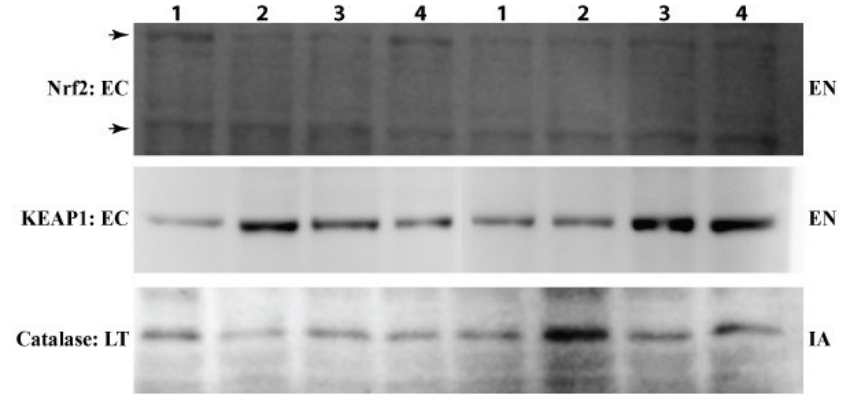

Figure 4.4: Changes in the protein levels of Nrf2 and KEAP1 over the course of the torpor–arousal cycle in skeletal muscle of *I. tridecemlineatus*. A. Histograms show means (± S.E.M., n=4 independent protein isolations from different animals) for five sampling points. B. Representative Western blots are shown for Nrf2 62 kDa/100 kDa, KEAP1, and catalase. The protein of interest and select experimental conditions are labeled to the left and right while sample numbers (lanes) are labeled along the top indicating 4 samples of one type (e.g., EC lanes 1, 2, 3, 4) and 4 samples of another (e.g. EN/IA lanes 1, 2, 3, 4). Arrows indicate Nrf2 at 100 kDa (top) and 62 kDa (bottom). Data were analyzed using analysis of variance with a post hoc Tukey test ($p<0.05$); values that are not statistically different from each other share the same letter notation.

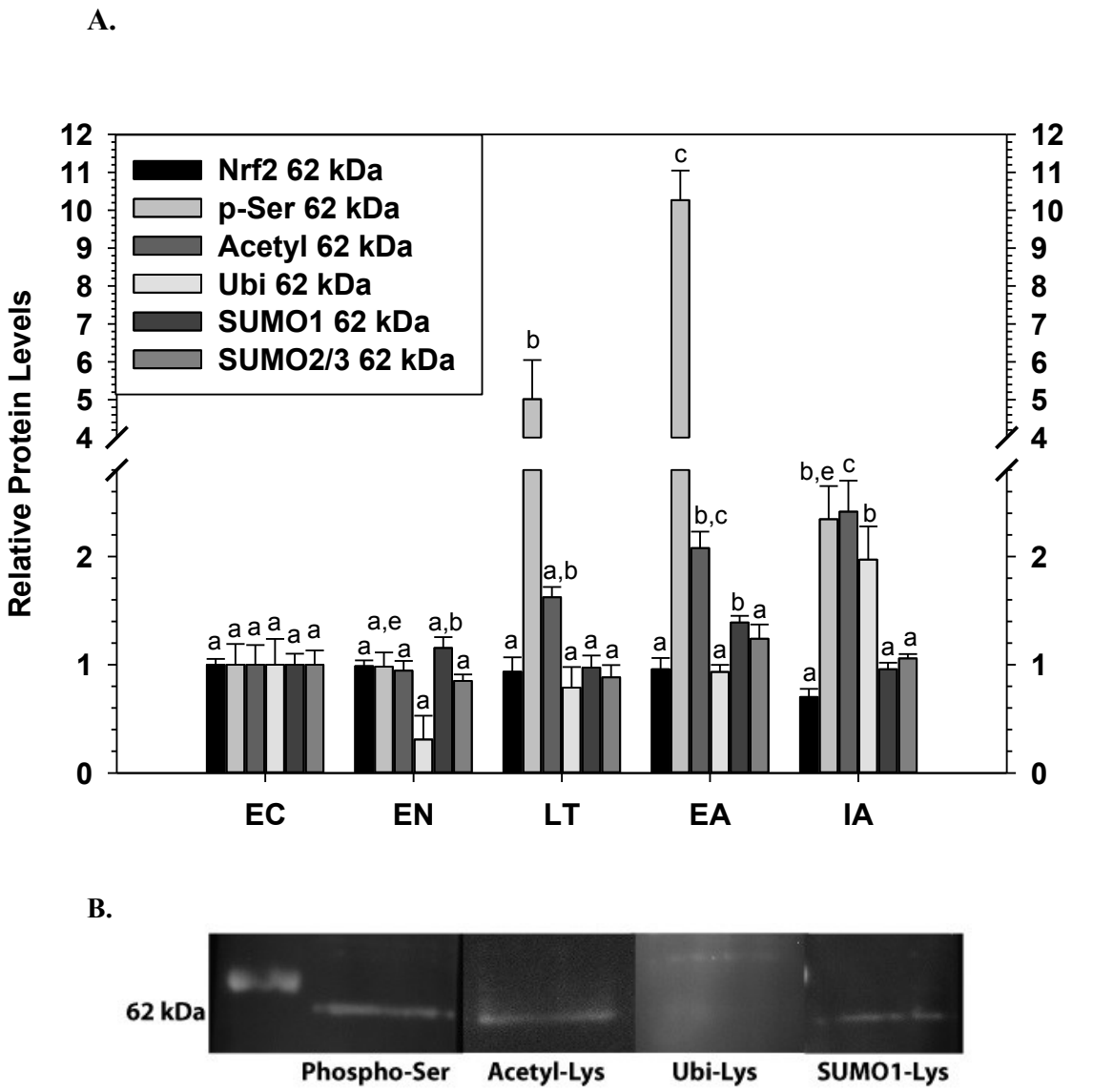

Figure 4.5: Changes in posttranslational modifications of Nrf2 (62 kDa) purified by co-immunoprecipitation from ground squirrel skeletal muscle over the torpor-arousal cycle. A. Histograms show means (± S.E.M., n=4 independent Nrf2 purifications from different animals) for five sampling points. B. Representative Western blots are shown for Nrf2 62 kDa purified from EC experimental conditions and probed with phospho-serine, acetyl-lysine, ubiquitin-lysine, and SUMO1-lysine antibodies. The molecular weight marker is labeled to the left and the antibodies are labeled along the bottom. Other information as in Figure 4.4.

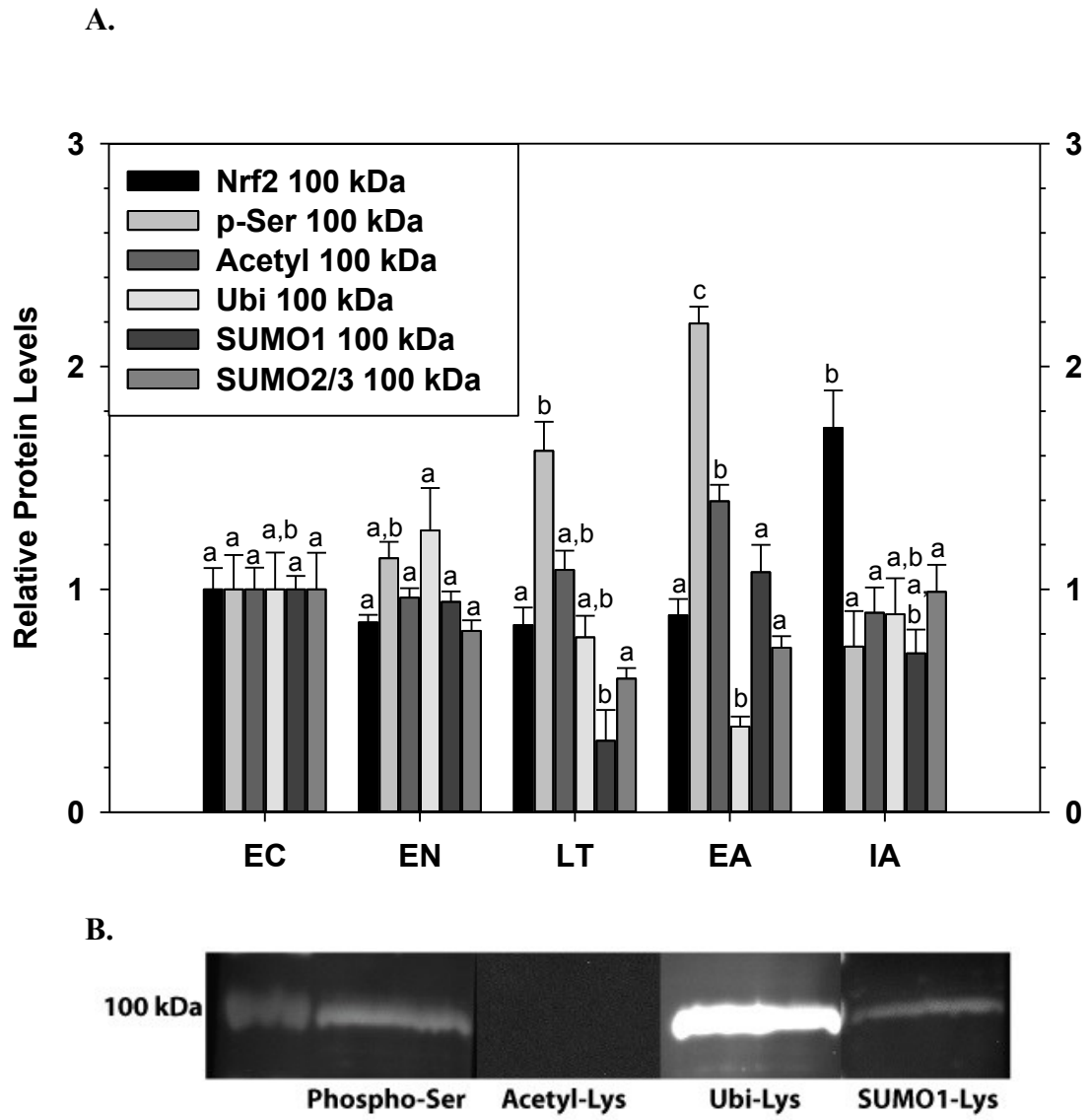

Figure 4.6: Changes in posttranslational modifications of Nrf2 (100 kDa) purified by co-immunoprecipitation from ground squirrel skeletal muscle over the torpor-arousal cycle. A. Histograms show means (± S.E.M., n=4 independent Nrf2 purifications from different animals) for five sampling points. B. Representative Western blots are shown for Nrf2 100 kDa purified from EC experimental conditions and probed with phospho-serine, acetyl-lysine, ubiquitin-lysine, and SUMO1-lysine antibodies. The molecular weight marker is labeled to the left and the antibodies are labeled along the bottom. Other information as in Figure 4.4.

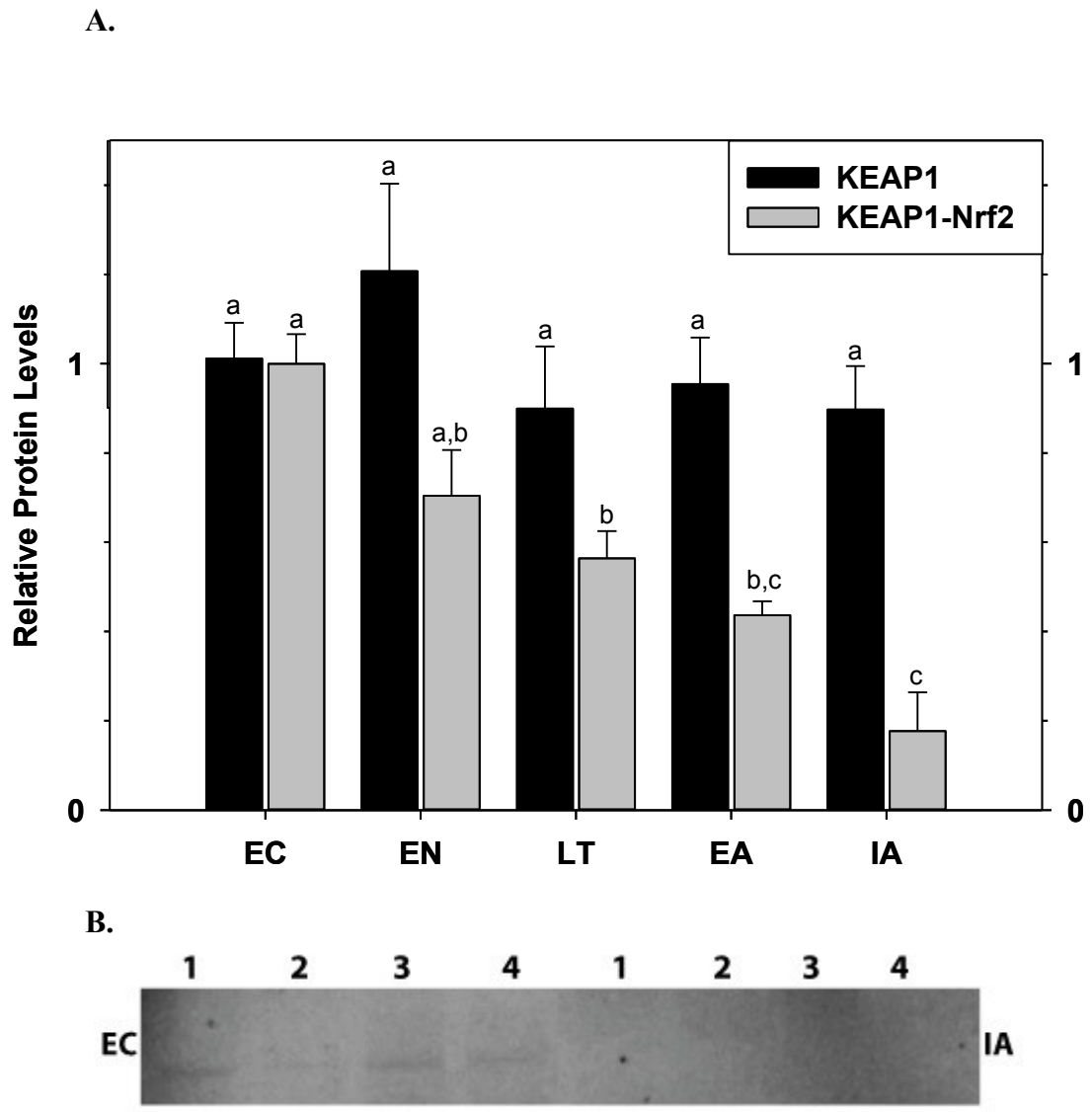

Figure 4.7: Changes in the levels of KEAP1 and KEAP1 bound to Nrf2 in ground squirrel skeletal muscle over the torpor-arousal cycle. A. Histograms show means (± S.E.M., n=4 independent total protein extracts (i.e. KEAP1) and Nrf2 Co-IP purifications (i.e. KEAP1-Nrf2) from different animals) for five sampling points. B. Representative Western blots are shown for purified Nrf2 probed with the KEAP1 antibody. The experimental conditions are labeled to the left/right and the samples (lanes) are labeled along the top. Other information as in Figure 4.4.

Discussion

The present chapter aimed at deepening our understanding of the molecular regulation of transcription factors and antioxidant responses during hibernation in the thirteen-lined ground squirrel. Common biochemical themes amongst organisms facing hypometabolic states include; (1) reversible protein phosphorylation of enzymes/proteins as a crucial mechanism that coordinates the suppression of metabolic processes [Storey and Storey 1990; Storey and Storey 2004; Storey and Storey 2007], (2) the widespread enhancement of antioxidant defenses as a means of viability extension in the hypometabolic state and of providing defense against a rapid production of reactive oxygen species (ROS) when animals return to an active state [Storey 1996; Storey 2010], and (3) the involvement of transcription factors in achieving selected upregulation of genes which will aid in meeting challenges associated the various stresses faced as a result of hypometabolism [Fahlman et al. 2000; Hittel and Storey 2001; Morin and Storey 2005; Mamady and Storey 2006; Eddy and Storey 2007; Morin and Storey 2007]. Therefore, it was of interest to discern the importance of each of these principles in the context of an established redox sensitive transcription factor (i.e. Nrf2) while also expanding the types of important regulatory factors that influence transcription factor activity to other under-studied PTMs (e.g. acetylation, ubiquitination, and sumoylation) and protein-protein interactions. These types of regulatory principles are likely crucial during hibernation since they can provide essentially “on” and “off” cellular responses with minimal impact on cellular energy status.

Previous studies have assessed the role of Nrf2 transcription factors in the regulation of antioxidant defenses in thirteen-lined ground squirrels during hibernation

with a particular focus on cardiac muscle [Morin et al. 2008; Ni and Storey 2010]. Furthermore, other studies have described changes in well-known downstream targets of the antioxidant response element in skeletal muscle including manganese superoxide dismutase (MnSOD) and heme oxygenase-1 (HO-1) [Allan and Storey 2012]. The present work expands this to include catalase. Superoxide dismutases are a class of enzymes that catalyze the dismutation of superoxide into oxygen and hydrogen peroxide [Buzadzic et al. 1990]. While this cellular reaction is a central detoxifying mechanism, cellular levels of the hydrogen peroxide product must be closely monitored. For example, accumulating levels of hydrogen peroxide in myocytes can result in increased expression levels of ubiquitin ligases such as muscle atrophy F box/atrogin-1 (MAFbx) and muscle ring finger 1 (MuRF1) [Chambers et al. 2009]. As such, intracellular levels of hydrogen peroxide are regulated by catalase which degrades hydrogen peroxide into oxygen and water [Krivoruchko and Storey 2010]. HO-1 is an inducible enzyme that is involved in heme degradation and subsequent production of biliverdin which acts as a known antioxidant [Morin and Storey 2007]. Since MnSOD protein levels increased strongly during torpor and arousal, HO-1 protein levels rose during early arousal [Allan and Storey 2012] and the relative expression of catalase increased significantly during interbout arousal (Fig. 4.4), it was predicted that the Nrf2 response would be most important during these experimental stages.

Curiously, however, Nrf2 and KEAP1 relative protein levels did not change over the torpor-arousal cycle, as illustrated in Figure 4.4. While these data were surprising at first, Nrf2 purified by co-immunoprecipitation was responsive to relative changes in posttranslational modifications which influence its transcriptional activity across the

torpor-arousal cycle. Figure 4.3B lists well-known PTMs on Nrf2, their associated amino acid residue (if known), and the enzyme responsible for catalyzing the transfer of phosphate, acetyl, ubiquitin, or SUMO groups. While the present data do not identify the specific serine that is phosphorylated across the torpor-arousal cycle, the literature reports that serine phosphorylation serves a general role in transcriptional activation [Kang et al. 2002; Bloom and Jaiswal 2003; Cullinan et al. 2003; Sun et al. 2009b] whether that be by promoting the dissociation of KEAP1 from Nrf2, enhancing nuclear translocation, or triggering a re-arrangement of actin microfilaments that influence the Nrf2-actin complex. Catalyzed by CBP/p300, many acetylation sites occurring on Nrf2 have also been reported to induce Nrf2-dependent gene expression; however, since they occur mainly in the DNA binding domain, acetylation has been proposed to be a mechanism to augment promoter-specific DNA binding by Nrf2 [Sun et al. 2009a]. The present study showed that ground squirrel Nrf2 was phosphorylated, including parallel changes in serine phosphorylation for Nrf2 62 kDa and 100 kDa (Fig. 4.5 and 4.6); relative phosphorylation of the protein begin to rise during late torpor and peaked during early arousal, before returning to levels similar to EC values (Nrf2 100 kDa) or remaining slightly elevated above EC values (Nrf2 62 kDa) during IA. Although it is not known which protein kinase (or combination thereof) is responsible for mounting this response, data presented in Chapter 3 showed that Jun amino-terminal kinase (JNK) had a parallel activation profile and, therefore, may play a role in the activation of Nrf2, especially during EA. Relative changes in serine phosphorylation were complimented by relative increases in lysine acetylation of the protein which began to rise during LT (although not statistically significant) and peaked during early arousal from torpor. The delayed

response by lysine acetylation may suggest that phosphorylation is an essential priming event and that acetylation acts as a mechanism to augment the Nrf2 transcriptional response rather than direct it. Taken together, these data suggest that the activation of Nrf2 transcription factors is maximal during early arousal from torpor when huge surges in oxygen uptake and consumption are occurring within minutes thereby making the hibernator more susceptible to attack by damaging ROS.

Ground squirrel Nrf2 was also responsive to changes in ubiquitination across the torpor-arousal cycle, albeit this response was not as strong as those signals for phosphorylation. Although further studies are required, this may be as a result of the short-life span of ubiquitinated Nrf2. KEAP1 serves as a substrate adaptor for protein ubiquitination of Nrf2 [Zhang et al. 2004; Kim et al. 2011]. Two regions of KEAP1, the DGR or Kelch domains, make physical interactions with the Neh2 domain of Nrf2 (as illustrated in Figure 4.3) and the N-terminal BTB region of KEAP1 interacts with the ubiquitination catalytic complex [Atia and Abdullah, 2014]. As a result of subsequent reactions by ubiquitin activating enzyme (Ub-E1), ubiquitin conjugating enzyme (Ub-E2), and ubiquitin ligase (Ub-E3), Nrf2 is ubiquitinated and degraded by the 26S proteasome [Kobayashi et al. 2004]. The Ub-E3 complex consists of a cullin protein which recruits its relative E2 enzyme and Keap1 displays selectivity to Cul3, one of eight cullin proteins [Kobayashi et al. 2004]. In response to changes in the redox state of the cell, the activity of the Ub-E3 ligase complex is suppressed due to chemical modifications of cysteine residues which prevent protein-protein interactions [Villeneuve et al. 2010]. For example, modification at Cys151 in the BTB domain of Keap1 leads to the disruption of Keap1 and Cul3 binding, thus impairing Nrf2 ubiquitination

[Rachakonda et al. 2008]**.** This central mode of regulation of KEAP1 is reflected in the fact that KEAP1 bound to Nrf2 was not regulated by post-translational modifications including phospho-serine, acetyl-lysine, ubiquitin-lysine, SUMO1-lysine, and SUMO2/3-lysine during hibernation. Further studies which identify PTMs of purified KEAP1 alone would hopefully elucidate the role of posttranslational modifications on KEAP1 and perhaps delineate the relative importance of PTMs versus redox-sensitive cysteines as the primary mode of KEAP1 regulation during hibernation.

As evidenced by the present study, protein-protein interactions between Nrf2 and KEAP1 decrease consistently over the torpor-arousal cycle (Fig. 4.7); statistically lower levels of KEAP1 co-purified with Nrf2 during LT and EA, stages when signals associated with enhanced Nrf2 activity (e.g. phosphorylation and acetylation) were strongest. Furthermore, a significant increase in ubiquitination levels were only observed during IA for Nrf2 62 kDa when serine phosphorylation and lysine acetylation were substantially reduced from peak values in EA, suggesting that the interbout arousal stage represents a transition from a highly activated Nrf2 response in EA to inhibition of this response in subsequent torpor-arousal cycles. Interestingly, however, the interaction between KEAP1-Nrf2 remained reduced during IA (Fig. 4.7), suggesting that KEAP1-independent Nrf2 ubiquitination was occurring during IA. Indeed, Malloy et al. (2013) has described such a mechanism whereby a SUMO-dependent degradation pathway mediated by the SUMO specific RING finger protein 4 (RNF4) E3 ubiquitin ligase promotes the ubiquitination of sumolyated Nrf2 without biologically active KEAP1 [Malloy et al. 2013]. In this capacity, modest increases of Nrf2 62 kDa SUMO-1 levels during EA may represent an essential step in the transition of activated to ubiquitinated Nrf2 which

occurs during IA. While further evidence is required in order to confirm that a KEAP1-independent ubiquitination event is in fact occurring during IA, the reason why two such pathways exist is intriguing. This may be related to differences in the regulatory mechanisms of cytoplasmic versus nuclear pools of Nrf2 or perhaps KEAP1-dependent and KEAP1-independent ubiquitination pathways result in differences in the final outcome of Nrf2 degradation pathways. Lastly, Nrf2 100 kDa significantly increased during IA, suggesting that increased association between Nrf2 and actin may possibly act to sequester Nrf2 thereby decreasing transcriptional activity.

In summary, the present data elucidates the regulation of Nrf2 transcription factors by post-translational modifications and protein-protein interactions during hibernation and implicates this regulation in counteracting the deleterious effects of oxidative stress. Nrf2 is primarily regulated by its interaction with a negative regulator (KEAP1) and via serine phosphorylation and lysine acetylation. Presumably, serine phosphorylation promotes Nrf2 nuclear localization whereas acetylation promotes Nrf2-DNA binding. In addition, ubiquitination acts as an inhibitory signal for Nrf2 activation and sumoylation may play a role in a KEAP1-independent ubiquitination event.

Chapter 5

The involvement of mRNA processing factors TIA-1, TIAR, and PABP-1 during mammalian hibernation.

The present chapter was co-authored by TE Audas (University of Ottawa), CW Wu (Carleton University), S Lee (University of Ottawa), KB Storey (Carleton University).

Author contributions:

Project conception: SNT, KBS

Data collection:
- Computational analysis: SNT
- Primer design, RNA isolation, cDNA synthesis, and PCR amplification: SNT
- Immunofluorescence and fluorescence microscopy: SNT, TEA
- Cytoplasmic/nuclear extract preparation: SNT
- Soluble-insoluble fractionation of lysates: SNT
- Western blotting: SNT, CWW

Writing: SNT

Edting: SNT, KBS, TEA, SL

Introduction

The genes that support the hibernating phenotype appear to be common among all mammals, suggesting that regulatory changes determine why some mammals can enter torpor and survive the associated stresses while others cannot. Such regulatory changes may include altered controls over mRNA transcripts. From the moment these molecules are synthesized in the nucleus to their demise following translation in the cytoplasm, eukaryotic mRNAs are subject to an intricate array of regulatory events that mediate every step of their life cycle [Moore 2005]. A host of RNA-binding proteins act as mRNA chaperones and, through these protein adaptors, individual mRNAs can respond to a multitude of inputs. TIA-1 (T-cell intracellular antigen 1), TIAR (TIA1-related), and PABP-1 [poly(A)-binding protein] are stress-responsive DNA/RNA-binding proteins that exert control over mRNA fate during transcription [Suswam et al. 2005], pre-mRNA splicing [Minvielle-Sebastia et al. 1997; Suswam et al. 2005], translation [Sachs and Davis 1989; Kedersha and Anderson 2007], mRNA stabilization (Decker and Parker 1993) and decay [Caponigro and Parker 1995]. TIA-1 and TIAR are composed of three N-terminal RNA recognition motifs (RRM1-3) and a C-terminal glutamine-rich motif (Suswam et al. 2005). The glutamine-rich motifs of TIA-1 and TIAR are structurally related to prion proteins (prion-like domains, PRD) and have the capacity to form dose-dependent, reversible aggregates [Gilks et al. 2004]. TIA-1/TIAR are expressed as two major isoforms (TIA-1a/TIA-1b, TIARa/TIARb) which regulate alternative pre-mRNA splicing of various genes (e.g. FGFR-2, msl-2, Fas) and display distinct functional properties [Izquierdo and Valcárcel 2007], while p15-TIA-1 is derived from proteolytic cleavage of the C-terminus of TIA-1 [Taupin et al, 1995; Kawakami et al, 1994]. PABP-1

contains four RNA-binding domains (RBDs) and a proline-rich C-terminal domain which associates with the 3' poly(A) tail of mRNA [Burd et al. 1991].

In the present chapter, I endeavoured to identify the role played by RNA-binding proteins in the post-transcriptional regulatory control of mRNA transcripts during hibernation in the liver of thirteen-lined ground squirrels (*Ictidomys tridecemlineatus*). Since RNA-binding proteins such as TIA-1/R and PABP-1 influence transcription and mRNA splicing as well as the localization, stability, and association of transcripts with the translation machinery I hypothesized that these factors could play a significant role in the global suppression of translation during hypometabolism. Further to this, I proposed that this response would be especially vital to the hibernating liver since this organ plays an established role in metabolism and in the maintenance of homeostasis over cycles of torpor and arousal. To address the hypothesis, a number of experimental approaches were taken. Firstly, the amino acid sequences of ground squirrel TIA-1, TIAR and PABP-1 were determined and included identification of TIA-1 and TIAR splice variants in the liver. The generation of alternative splice variants and their differential expression have the capacity to modify protein function, yet their involvement remains a largely unexplored concept in mammalian hibernation. Fluorescence microscopy, protein fractionation, and western blotting were then applied to assess the localization and relative expression of the RNA-binding proteins. Finally, solubility tests were used to assess the formation of reversible aggregates that are associated with TIA-1/R function during stress. The data presented demonstrates the presence of two major TIA-1 and TIAR isoforms in ground squirrel liver that possessed a high degree of sequence similarity with other mammals. Surprisingly, the shorter variants of both TIA-1 and

TIAR (isoforms b) displayed consistently higher expression across experimental hibernation stages. Formation of nuclear foci was observed during hibernation using immunofluorescence microscopy, complementing the observation of a relative increase in TIA-1a and TIA-1b in the nuclear fractions of torpid ground squirrels. The solubility of TIARa/b, TIA-1 p15, and PABP-1 did not change, but a relative increase in the ratio of soluble:insoluble fractions was observed for TIA-1a and TIA-1b during hibernation. The data revealed that RNA-binding proteins play a role in mRNA processing during hibernation and these proteins could provide a framework for the global reduction in translation and selective regulation of key cellular networks as well as facilitate the rapid reversal of the hibernating phenotype.

Materials & Methods

Animals

Thirteen-lined ground squirrels (*Ictidomys tridecemlineatus*) were captured, treated, and organs harvested following the same protocol as previously described in Chapter 2 [McMullen and Hallenbeck 2010]. Livers sampled from control (EC) and hibernating (LT) thirteen-lined ground squirrel were used in the present chapter.

Computational analysis

The full sequences for ground squirrel (*I. tridecemlineatus*) TIA-1, TIAR, and PABP-1 were deduced using whole genome shotgun (wgs) reads, as described in Chapter 4. Human sequences used for TIA-1, TIAR, and PABP-1 wgs BLAST (NCBI) searches had accession numbers NM_022173.2, NM_001033925.1, and NM_002568.3,

respectively. The predicted ground squirrel mRNA coding sequence was translated into amino acids and aligned with human (*Homo sapiens*), Rhesus macaque (*Mucaca mulatta*), bovine (*Bos taurus*), rat (*Rattus norvegicus*), mouse (*Mus musculus*), and African clawed frog (*Xenopus laevis*) sequences using Geneious (Biomatters Ltd) in order to determine percent homology. The domains/motifs were predicted using the Eukaryotic Linear Motif resource for Functional Sites in Proteins (ELM, http://elm.eu.org/) and compared to those predicted using the ScanProsite tool (http://prosite.expasy.org/scanprosite/).

Primer design and synthesis.

Primers for *Tia-1* and *TiaR* were designed using alignments created by Geneious (Biomatters Ltd) and online OligoAnalyzer software (Integrated DNA Technologies, Inc.) based on the deduced ground squirrel coding sequence and consensus sequences for the genes derived from several mammalian species (mouse, rat, cow, human). The *Tia-1* primer pairs span exon 5 (i.e. amplify *Tia-1* splice variants *a* and *b*), while the *TiaR* primer pairs span an alternate in-frame splice site in the coding region (i.e. amplify *TiaR* splice variants *a* and *b*). The predicted transcript size of *Tia-1a* amplified from forward/reverse primers F1R1 and F2R1 is 314 bp and 319 bp, respectively, and the predicted transcript size of *Tia-1b* amplified from the same primer pairs is 281 and 286, respectively. The predicted transcript size of *TiaRa* amplified from F1R1 and F1R2 is 290 bp and 338 bp, respectively, and the predicted transcript size of *TiaRb* amplified from the same primer pairs is 239 and 287, respectively. The primer sequences (purchased from Integrated DNA Technologies, Inc.) were as follows:

(1) *Tia-1* forward 1 (*Tia-1* F1) 5’ – GATAATGGGTAAGGAAGTCA –3’

(2) *Tia-1* forward 2 (*Tia-1* F2) 5' – CGGAAGATAATGGGTAAGGA –3'

(3) *Tia-1* reverse 1 (*Tia-1* R1) 5' – CCAGTTAGTTCTGATTTGTC –3'

(5) *TiaR* forward 1 (*TiaR* F1) 5' – GGACCCTGTAAAAGCTGTAA – 3'

(6) *TiaR* reverse 1 (*TiaR* R1) 5' – GGGCAAATGCTGATTTGATA – 3'

(7) *TiaR* reverse 2 (*TiaR* R2) 5' – GTTGCCATGTCTTTAACTAC – 3'

RNA isolation, cDNA synthesis and PCR amplification

Total RNA was extracted from liver (~100 mg) of n=4 individual animals from control (EC) and late torpor (LT) groups. Samples were homogenized using a Polytron homogenizer in 1 mL Trizol^{TM} reagent (Invitrogen), according to manufacturer's instructions and as previously described (Tessier and Storey 2010). In brief, following homogenization, chloroform was added to each sample, soluble fractions were removed, RNA was precipitated with isopropanol, and, finally, washed with 70% ethanol. RNA concentrations were determined by reading absorbance at 260 nm on a GeneQuant Pro spectrophotometer (Pharmacia) using the ratio of absorbance at 260/280 nm as an indicator of RNA purity ($A_{260/280}$ ratio = 1.8-2). RNA quality was confirmed by native gel electrophoresis with ethidium bromide staining to check the integrity of 18S and 28S ribosomal RNA (rRNA) bands (28S rRNA band was about twice as intense as the 18S rRNA band). All samples were standardized to 1 µg/µl with diethylpyrocarbonate (DEPC)-treated water.

First strand cDNA synthesis used 3 µg aliquots of total RNA from liver, according to manufacturer's instructions and as previously described (Tessier and Storey 2010). RNA aliquots were combined with 7 µl of DEPC-treated water and 1 µl of oligo-

dT (Sigma Genosys; 200 ng/ul). Following a 5 min incubation at 65°C in a PCR machine (iCycler, BioRad) and rapid chilling on ice, the following components were added to each sample: 4 µl 5× first strand buffer, 2 µl 10 mM dithiothreitol (DTT), 1 µl 10 mM dNTPs, and 1 µl Superscript II reverse transcriptase (all reagents from Invitrogen). The final mixture (19 µl) was incubated at 42°C for 1 h and then held at 4°C. Dilutions of cDNA were prepared (10^{-1}) in DEPC water and were used to amplify *Tia-1* and *TiaR* splice variants in ground squirrel liver.

PCR was performed by mixing 5 µl of cDNA (10^{-1}) with 1.25 µl of primer mixture (0.3 nmol/µl forward and 0.3 nmol/µl reverse), 13 µl of DEPC treated water, 2.5 µl of 10× PCR buffer (Invitrogen), 1.75 µl of 50 mM $MgCl_2$, 0.5 µl of 10 mM dNTPs, and 1 µl of Taq Polymerase (Invitrogen) for a total volume of 25 µl. The cycles performed for amplification consisted of an initial step of 7 min at 95˚C, followed by 35 cycles at 95°C for 1 min, annealing at 53°C (*Tia-1a/b*) or 64.6°C (*TiaRa/b*) for 1 min, 72°C for 1 min; the final step was 72°C for 10 min. PCR products containing 2 µg aliquots of xylene blue loading dye and 1× Sybr Green 1 (Invitrogen, Cat# S7563) were separated on 2.0% agarose gels (80 min, 130 V).

Immunofluorescence and fluorescence microscopy

Liver cryosections were prepared by the Morphology Unit (Department of Pathology and Laboratory Medicine, University of Ottawa) and were stored at -80°C until use. Sections were immediately fixed in ice-cold methanol (5 min), transferred to ice-cold acetone (5 min), and washed twice with 1× PBS. Sections were then incubated with Hoeschst#33342 (Invitrogen) in order to stain DNA. Sections were blocked for 1 h

in goat serum (10% v:v made up in 1× PBS) and washed twice in 1× PBS at room temperature. All primary antibodies were diluted 1:100 v:v in 10% goat serum (1× PBS) and incubated overnight at 37°C (with 5% CO_2). Antibodies for TIA-1/TIAR were purchased from Santa Cruz (D-9, sc-48371) while PABP-1 antibody was purchased from Upstate (Cat# 05-847). Before secondary antibody application, slides were washed four times in 1× PBS. Secondary Alexa488-conjugated antibodies (Invitrogen) were used at 1:200 v:v in 10% goat serum (1× PBS) and incubated for 1 h 40 min at 37°C. Glass coverslips were mounted in Fluomount G, sealed with nail polish, visualized on a Zeiss AxioImager.Z1 microscope. A 100x oil immersion lens with a 1.3 NA was controlled by Zeiss AxioVision v4.8.2 software and images were captured on an AxioCam HRm camera. Thirty nuclei stained for TIA-1/TIAR and PABP-1 were counted for the presence or absence of signal localization in four separate fields (n=120 nuclei/antibody/experimental condition). Images were prepared using Adobe Creative Suite CS4.

Cytoplasmic/nuclear extract preparation

Samples of frozen liver from n=4 individuals from EC and LT experimental conditions were used to prepare cytoplasmic and nuclear fractions as previously described by Tessier and Storey (2010). Samples of liver (~200 mg) were homogenized using a Dounce homogenizer and 400 µl of homogenization buffer (10 mM HEPES, pH 7.9, 10 mM KCl, 10 mM EDTA, 20 mM β-glycerophosphate) with 10 µl 100 mM DTT and 10 µl protease inhibitor cocktail (BioShop) added immediately before homogenization. Samples were centrifuged (10,000 rpm, 10 min, 4°C) and the

supernatant was removed as cytoplasmic fractions. Pellets were re-suspended in 147 µl of extraction buffer (20 mM HEPES, pH 7.9, 400 mM NaCl, 1 mM EDTA, 10% v:v glycerol, 20 mM β-glycerophosphate) with 1.5 µl 100 mM DTT and 1.5 µl protease inhibitor cocktail added (a total of 150 µl/g starting material). After 1 h incubation, samples were centrifuged (10,000 rpm, 10 min, 4°C) and the supernatants were collected as nuclear fractions. Protein concentration was quantified by the Coomassie blue dye-binding method using the BioRad reagent (BioRad Laboratories, Hercules, CA) at 595 nm on a MR5000 microplate reader. Samples were then adjusted to 10 µg/µl and aliquots were combined 1:1 v:v with 2× SDS loading buffer (100 mM Tris-base pH 6.8, 4% w:v SDS, 20% v:v glycerol, 0.2% w:v bromophenol blue, 10% v:v 2-mercaptoethanol), boiled, and final protein samples (5 µg/µl) were stored at -40°C until use. Identical protein amounts of each sample (15-25 µg) were loaded onto SDS-polyacrylamide gels or 15% Tris-Tricine gels (to enhance resolving power).

Soluble-insoluble fractionation of lysates

Samples of frozen liver from n=4 individuals from each experimental condition were separately extracted in order to assess total protein solubility (protocol adapted from Ripaud et al. 2003). The basic method involved tissue homogenization using mechanical/physical cell disruption thereby releasing proteins from both cytoplasmic and nuclear compartments as well as separating soluble and insoluble proteins using a suspension (i.e. aqueous) and solubilizing (i.e. containing detergent) buffer, respectively. Samples were quickly weighed, crushed into small pieces under liquid nitrogen, and then homogenized 1:5 w:v using a Polytron PT10 in ice-cold suspension buffer (1× PBS pH

7.4, 100 mM NaCl, 0.2% Triton-X) with 10 µl/mL protease inhibitor cocktail (Bioshop) added immediately before homogenization. Homogenates were incubated with gentle agitation for 20 min at room temperature and then centrifuged at 11,000 rpm (20 min, 4°C). The supernatant was transferred to a clean Eppendorf tube (soluble fraction) and the pellet was washed twice with water (500 µl/wash) to minimize cross-contamination. Using equivalent volumes to the suspension buffer, the pellet was then resuspended in SDS solubilization buffer (1× PBS pH 7.4, 300 mM NaCl, 2% v:v SDS, 1% v:v Triton-X) with 2 mM DTT and 10 µl/mL protease inhibitor cocktail. Samples were then centrifuged at 11,000 rpm (30 min, room temperature) and the supernatant was collected as the insoluble fraction. Total protein control samples were used in order to ensure that the composition of total protein was preserved in each experimental condition. Total protein control samples were prepared using 1:10 v:v solubilization buffer (1× PBS pH 7.4, 300 mM NaCl, 2% v:v SDS, 1% v:v Triton-X) with 2 mM DTT and 10 µl/mL protease inhibitor cocktail. Control homogenates were incubated with gentle agitation for 1 h at room temperature and then centrifuged at 11,000 rpm (30 min, room temperature). The supernatant was removed, transferred to a clean Eppendorf tube, and saved as total protein controls. All samples (control and soluble/insoluble fractions) were combined 1:1 v:v with 2× SDS loading buffer, boiled, and stored at -20°C until use. Identical volumes of each sample (3 µl of soluble/insoluble fractions and controls) were loaded onto SDS-polyacrylamide gels or 15% Tris-Tricine gels.

Western blotting

Western blotting was performed as described in Chapter 2. Equal amounts from each sample were loaded onto 10-12% SDS-polyacrylamide gels and run at 180 V for 45-60 min. Membranes were blocked with milk (2-5% w:v) in TBST and incubated with the membrane on a rocker for 20 min. Antibodies specific for mammalian TIA-1 (C-20, sc-1751) and TIAR (C-18, sc-1749) were purchased from Santa Cruz Biotechnologies, TIA-1 p15 was purchased from Abcam (ab2712), and PABP-1 was purchased from GeneTex (GTX101515). Antibodies for TIA-1a/TIA-1b and TIARa/TIARb cross-reacted with bands on the immunoblots at molecular masses of 43/41 kDa and 41/40 kDa, respectively, whereas antibodies for TIA-1 p15 and PABP-1 cross-reacted with bands on the immunoblots at molecular masses of 15 kDa and 70 kDa, respectively. Antibodies were used at 1:1000 v:v dilution in TBST. Membranes that had been probed with TIA-1 p15 were probed with HRP-linked anti-mouse IgG secondary antibody (1:4000 v:v dilution), PABP-1 were probed with HRP-linked anti-rabbit IgG secondary antibody (1:5000 v:v dilution), and TIA-1 and TIAR were probed with HRP-linked anti-goat IgG secondary antibody (1:10,000 v:v dilution). All membranes were washed three times between incubation periods in 1× TBST for ~10 minutes/wash. Bands were visualized by enhanced chemiluminescence and restained using Coomassie blue.

Quantification and statistics

Band densities on chemiluminescent immunoblots were visualized using a Chemi-Genius BioImaging system (Syngene, Frederick, MD) and quantified using the associated Gene Tools software. Immunoblot band density in each lane was standardized against the summed intensity of a group of Coomassie stained protein bands in the same

lane (except for solubility data); these were chosen because they did not show variation between different experimental states and were not located close to the protein bands of interest. Solubility data are expressed as the ratio of soluble:insoluble fractions. Data are expressed as means ± SEM, n = 4 independent samples from different animals. Statistical testing of standardized band intensities used the Student's t-test.

Results

Characterization of thirteen-lined ground squirrel TIA-1, TIAR, and PABP-1

Human and mouse mRNA coding sequences were used in whole genome shotgun NCBI BLAST analysis to deduce the *I. tridecemlineatus* TIA-1, TIAR, and PABP-1 mRNA sequences. The encoded ground squirrel RNA-binding proteins were translated from the *in silico* derived open reading frames and motifs in the proteins were identified using online software (ELM and ScanProsite) (Fig. 5.1a and Table 5.1). As expected, protein alignment scores revealed that the ground squirrel amino acid sequences were highly conserved when compared to other species; (1) TIA-1 was 99%, 97%, 96%, and 85%, (2) TIAR was 99%, 93%, 98%, and 68%, (3) PABP-1 was 100%, 99%, 99%, 93% identical to human, bovine, mouse, and African clawed frog sequences, respectively (note the very close identity as compared with other mammals) (Table 5.2). RT-PCR with primers designed to amplify *Tia-1* and *TiaR* confirmed the presence of the alternative splice variants of both proteins in ground squirrel liver (Fig. 5.1b). These splicing variants were also detected as mature proteins via western blotting, with antibodies targeting TIA-1 identifying two bands in the 42 kDa range, TIA-1a (top) and TIA-1b

(bottom), wheras TIAR antibodies detected two bands in the 41 kDa range, TIARa (top) and TIARb (bottom).

Relative expression and nuclear localization of RNA-binding proteins

To better understand the functions of the mRNA processing factors during hibernation, immunohistochemistry was used visualize their subcellular distribution in euthermic control (EC) and torpor (LT) animals (Fig. 5.2). While a large pool of TIA-1/TIAR and PABP-1 was found in the cytoplasm, a population of these molecules was also present in subnuclear bodies within the nuclei of LT ground squirrels but not in EC (Fig. 5.2a). These large (~48 μm) structures appeared as a single foci rather than the multiple, speckled domains as is sometimes observed for other types of nuclear bodies. Targeting of TIA-1/TIAR and PABP-1 to nuclear foci was observed in approximately 98% and 90% of liver nuclei during LT, respectively (Fig. 5.2b, Table 5.3). Conversely, EC ground squirrels possessed subnuclear TIA-1/TIAR and PABP-1 in less than 3% of liver nuclei visualized (Fig. 5.2b).

Subcellular fractionation and immunoblotting was also used to determine the relative expression of TIARa/b, TIA-1 p15, TIA-1a/b, and PABP-1 in the cytoplasmic and nuclear fractions of ground squirrel liver, during EC and LT experimental conditions (Fig. 5.3). No change was observed in the protein levels of TIAR isoforms when comparing nuclear fractions across experimental conditions (Fig. 5.3a); however, TIARa and TIARb decreased significantly in the cytoplasm during torpor to levels that were 46% and 59%, respectively, of EC values. As shown in Fig. 5.3b, TIARa was predominantly localized in the cytoplasm with negligible amounts in the nuclei under

both EC and LT conditions, whereas TIARb was present in both fractions. TIA-1a and TIA-1b showed parallel, statistically significant changes in relative protein expression levels whereby 7- and 3.7-fold increases were observed in the nuclear fractions from torpid ground squirrels as compared to EC, respectively (Fig. 5.3a). This increased nuclear population agreed with the immunohistochemistry results observed in Fig. 5.2. In contrast, neither TIA-1 isoform changed in cytoplasmic fractions between EC and LT. TIA-1 p15 and PABP-1 showed no significant changes in either cytoplasmic or nuclear fractions across experimental conditions. Representative Western blots corresponding to those quantified to produce histograms depicted in Fig. 5.3a are shown in Figure 5.3c.

Relative expression of TIA-1a/b and TIARa/b isoform expression

Immunoblotting was also used to compare the relative protein abundance of each TIA-1 or TIAR isoform in EC versus LT stages. Expression levels of the b isoforms are expressed relative to the corresponding a isoforms in both the nuclear and cytoplasmic fractions (Fig. 5.4). Interestingly, when assessing the relative expression of TIARa versus TIARb in the nucleus, consistently higher levels of TIARb were observed in liver during both EC (4.7 fold) and LT (3.3 fold) stages (Fig. 5.4a). TIA-1b expression was also consistently higher than TIA-1a in the nucleus of both EC (1.9 fold) and LT (2.9 fold) (Fig. 5.4a) animals. When comparing the relative levels of TIARa/b and TIA-1a/b in the cytoplasmic fractions the b isoform of both proteins was regularly higher than the a isoform. TIARb was 2.4- and 3.3 fold higher in EC and LT, respectively, than was TIARa; comparable values for TIA-1b were 1.9- and 2.2 fold higher (Fig. 5.4b).

Together, these data suggest that the b isoform of both proteins is the predominant splice variant.

Detergent solubility test of RNA-binding proteins

Soluble and insoluble protein fractions were collected through classic methods used to isolate pathological protein aggregates present in brain tissues of subjects with neurodegenerative diseases [Wolozin 2012]. However, the soluble versus insoluble forms of TIA-1 are associated specific functions [Gilks et al. 2004] and, by extension, may be used a means to learn more about their cellular function. The present study tested for differences in solubility of RNA-binding proteins, particularly those with the glutamine-rich prion-related domain (PRD) such as TIA-1 and TIAR (Fig. 5.5). The solubility of TIARa/b, TIA-1 p15, and PABP-1 did not change when comparing the ratio of soluble:insoluble fractions between euthermic and torpid conditions. However, a relative increase in the ratio of soluble:insoluble fractions was observed for TIA-1a and TIA-1b during torpor; the relative amount of soluble protein during LT was 1.8- and 1.7-fold higher than EC for TIA-1a and TIA-1b, respectively. That is, relatively more TIA-1a and TIA-1b proteins were recovered in the soluble fractions during torpor as compared to euthermic controls.

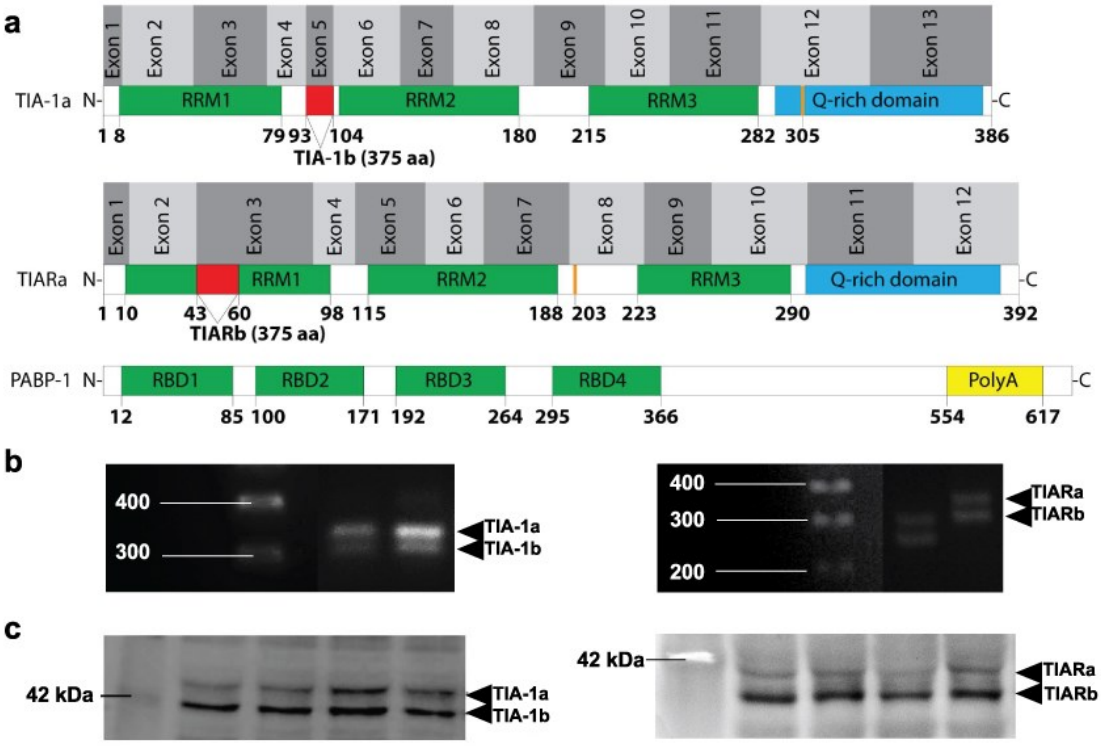

Figure 5.1: Alternative isoform expression of RNA-binding proteins in the liver of hibernating thirteen-lined ground squirrel (*I. tridecemlineatus*). (a) Illustration of alternative splice sites. Patterns of alternative splicing are represented by a line and a red box, exons are denoted by alternating light and dark gray boxes, RNA Recognition Motifs (RRMs) are represented by green boxes, the Q-rich domain is represented by a blue box, the Poly-A-tail binding domain is represented by a yellow box, the location of ground squirrel amino acid substitutions (as compared to the human sequence) are represented by thick yellow lines, and numbers indicate amino acid residues. (b) Representative bands on agarose gels are shown for *Tia-1* and *TiaR* splice variants amplified by primers spanning exon 5 and an alternate in-frame splice site in the coding region, respectively. The DNA ladder is labeled to the left and the isoform to the right of the gel. (c) Representative Western blots are shown for TIA-1 and TIAR protein isoforms with the protein ladder labeled to the left and the isoform to the right of the gel.

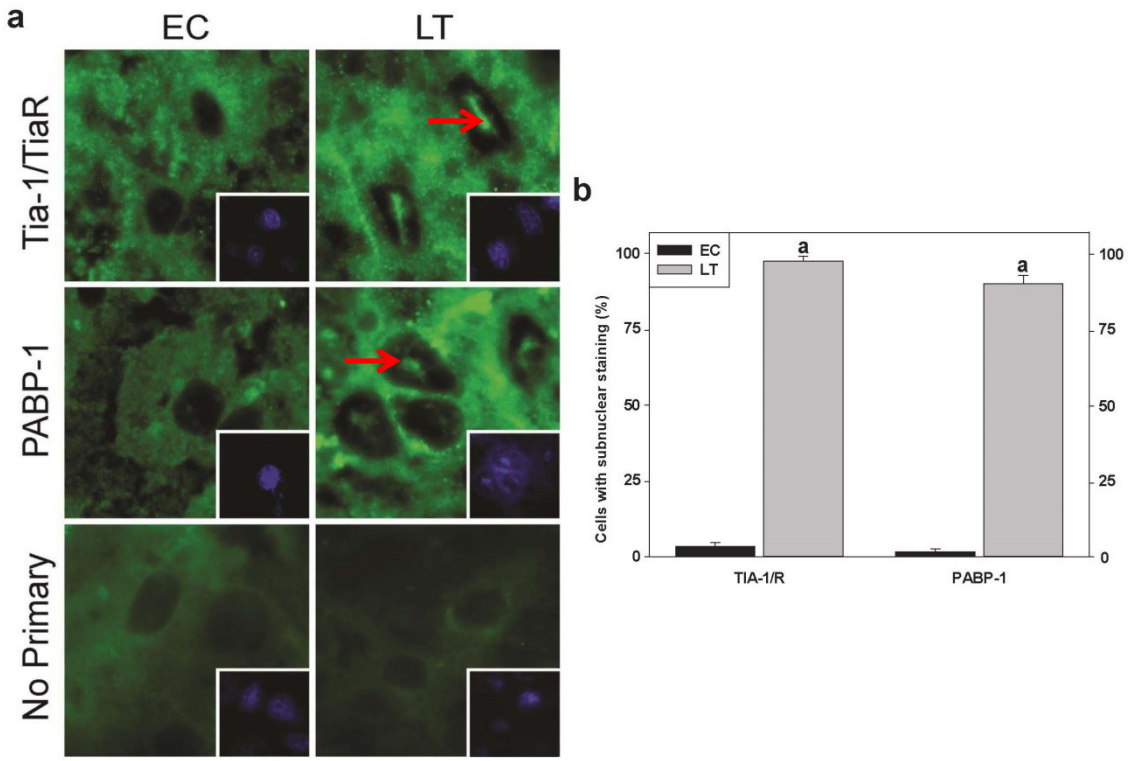

Figure 5.2: Localization of RNA-binding proteins to the nucleus in the liver of torpid thirteen-lined ground squirrels (*I. tridecemlineatus*). (a) Immunostaining of endogenous TIA-1/R and PABP-1. Fluorescent signals from TIA-1/R and PABP-1 were distributed in the cytoplasm and nucleus during EC, but displayed distinct nuclear foci (shown by red arrows) during LT. Shown are representative cryosections immunostained with TIA-1/R and PABP-1 as well as Hoeschst stained nuclei (depicted in the bottom right quadrant) from EC and LT liver samples. (b) Number of cells possessing subnuclear foci averaged across four fields comparing euthermic control (EC) and late torpor (LT) conditions. Data were analyzed using the Student's t-test; "a" denotes values are significantly different from EC, $p<0.05$.

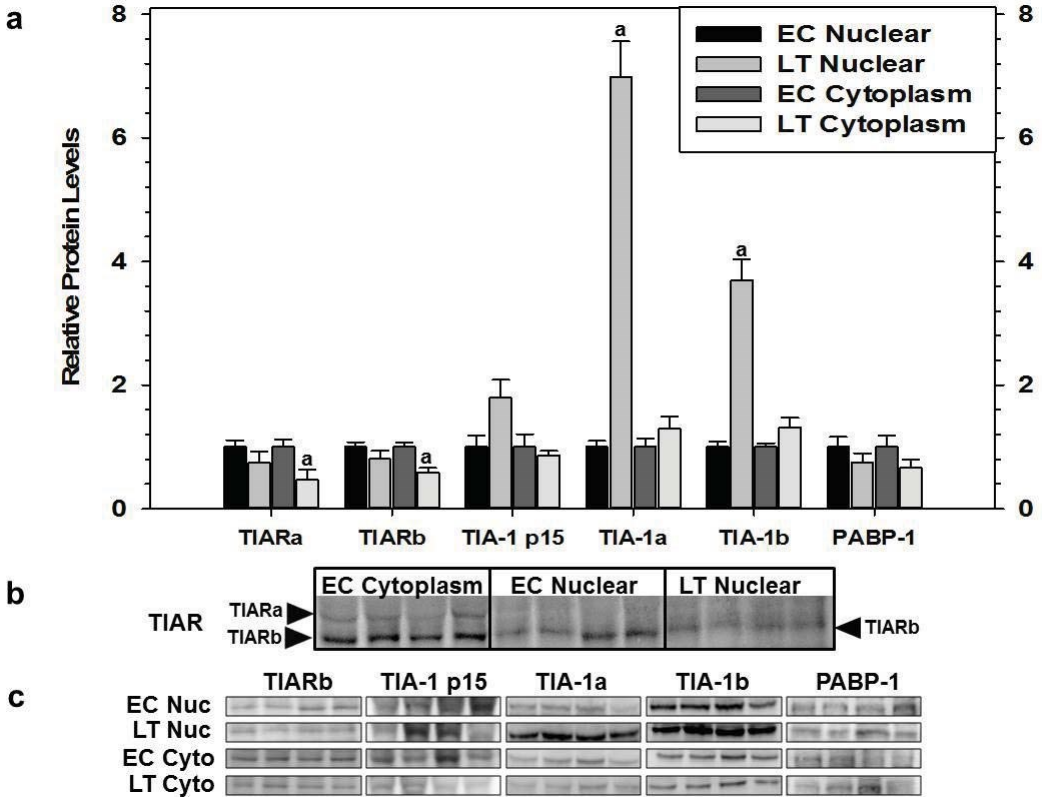

Figure 5.3: Subcellular distribution of RNA-binding proteins in cytoplasmic and nuclear fractions sampled from liver of thirteen-lined ground squirrels (*I. tridecemlineatus*) comparing euthermic control (EC) and late torpor (LT) conditions. (a) Histogram showing mean relative expression of TIARa/b, TIA-1 p15, TIA-1a/b, and PABP-1 (± S.E.M., n=4 independent protein isolations from different animals). (b) Representative Western blots are shown of the cytoplasmic and nuclear distribution of TIAR with the subcellular fraction and experimental conditions labeled at the top of the gel and the TIAR isoform labeled to the left of the gel. (c) Representative Western blots are shown with the experimental conditions labeled to the left of the gel and the protein target labeled at the top of the gel. Data were analyzed using the Student's t-test; "a" denotes values are significantly different from EC, $p<0.05$.

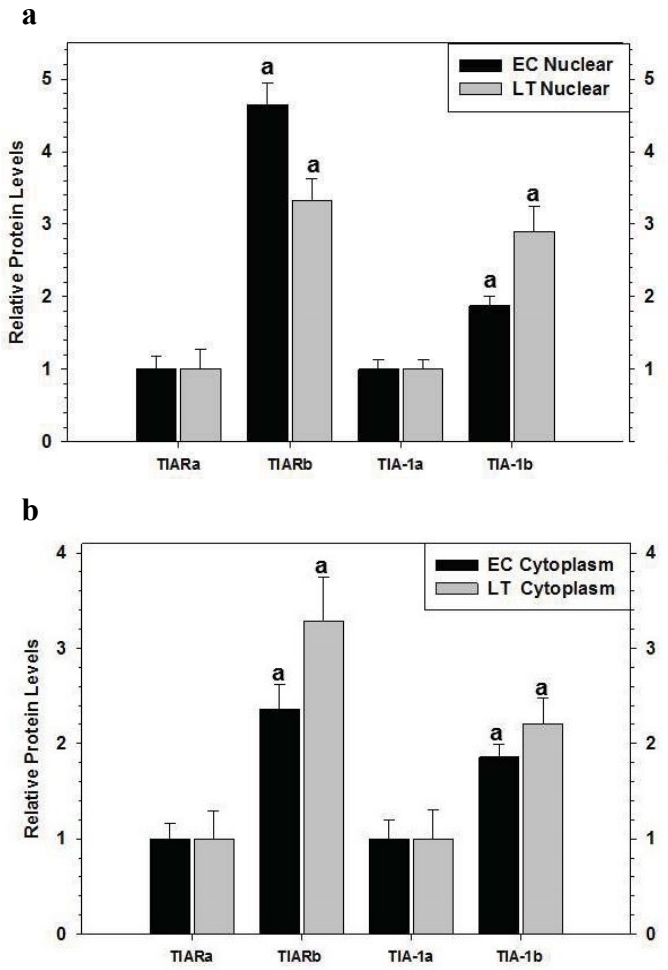

Figure 5.4: The expression levels of isoforms of RNA-binding proteins in liver of thirteen-lined ground squirrels (*I. tridecemlineatus*) comparing euthermic control (EC) and late torpor (LT) conditions as well as their subcellular distribution. (a) Histogram showing mean relative expression levels of TIARa vs. TIARb and TIA-1a vs. TIA-1b in nuclear fractions (± S.E.M., n=4 independent protein isolations from different animals). (b) Histogram showing mean relative expression of TIARa vs. TIARb and TIA-1a vs. TIA-1b in cytoplasmic fractions (± S.E.M., n=4 independent protein isolations from different animals). *Other information as in Figure 5.3.

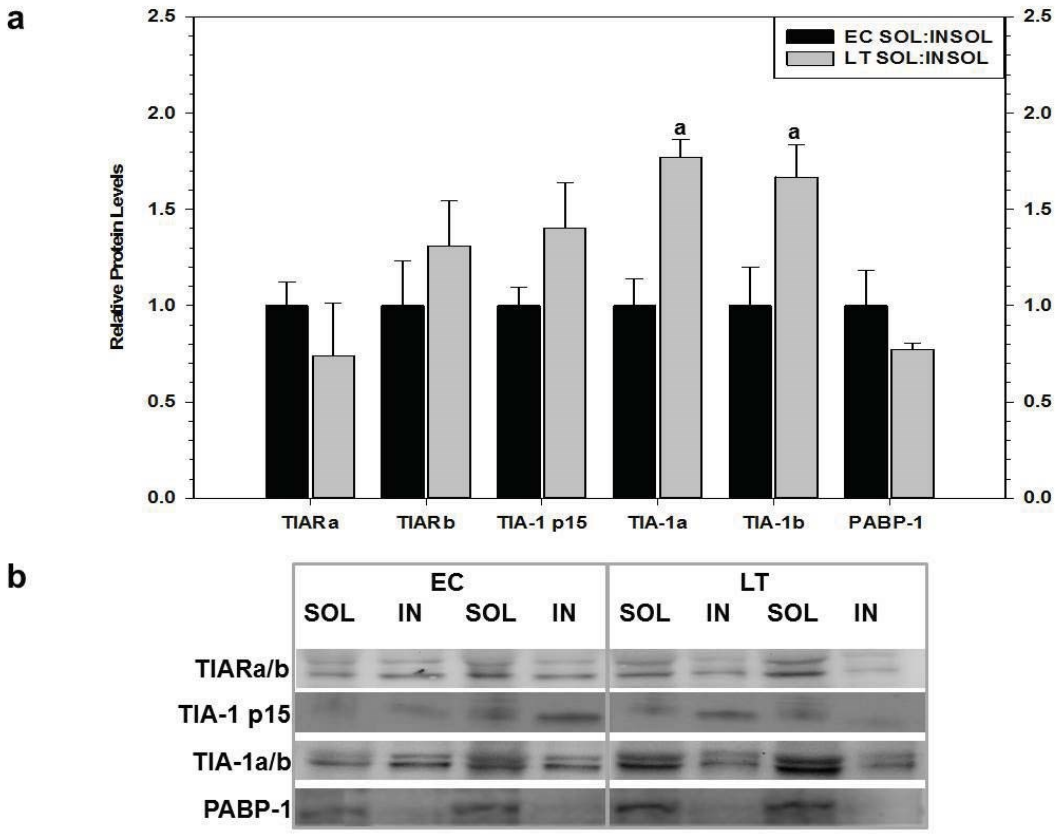

Figure 5.5: The relative expression of RNA-binding proteins in soluble and insoluble protein fractions isolated from the liver of thirteen-lined ground squirrels (*I. tridecemlineatus*) comparing euthermic control (EC) and late torpor (LT) conditions. (a) Histogram showing mean relative protein levels in soluble vs. insoluble fractions for TIARa/b, TIA-1 p15, TIA-1a/b, and PABP (± S.E.M., n=4 independent protein isolations from different animals). (b) Representative Western blots are shown with the protein targets labeled to the left of the gel and the experimental conditions labeled at the top of the gel. *Other information as in Figure 5.3.

Table 5.1: The predicted thirteen-ground squirrel mRNA coding sequences for TIA-1, TIAR, and PABP-1 were translated into amino acids and the domains/motifs were predicted using the Eukaryotic Linear Motif resource for Functional Sites in Proteins (ELM) and compared to those predicted using the ScanProsite tool.

13LGS TIA-1a	**ELM**	**ScanProsite**
RRM1	8-79	7-83
RRM2	107-180	106-184
RRM3	215-282	214-286
Q-rich domain		295-366
13LGS TIAR	**ELM**	**ScanProsite**
RRM1	10-98	9-102
RRM2	115-188	114-192
RRM3	223-290	222-294
13LGS PABP-1	**ELM**	**ScanProsite**
RRM1	12-85	11-89
RRM2	100-171	99-175
RRM3	192-264	191-268
RRM4	295-366	294-370
PolyA	554-617	542-619

Table 5.2: Alignment scores comparing TIA-1, TIAR and PABP-1 protein sequences of thirteen-lined ground squirrel to human, bovine, mouse and African clawed frog sequences. NCBI accession numbers are included.

	Human (*Homo sapiens*)	Bovine (*Bos taurus*)	Mouse (*Mus musculus*)	African Clawed Frog (*Xenopus laevis*)
TIA-1	99% (NP_071505.2)	97% (NP_001069577.1)	96% (NP_035715.1)	85% (NP_001087561.1)
TIAR	99% (NP_001029097.1)	93% (NP_001179985.1)	98% (NP_033409.1)	68% (NP_001167497.1)
PABP-1	100% (NP_002559.2)	99% (NP_776993.1)	99% (NP_032800.2)	93% (NP_001080204.1)

Table 5.3: The number of cells possessing subnuclear foci as viewed by immunofluorescence of cryosections obtained from thirteen-lined ground squirrel liver stained for TIA-1/R and PABP-1. Across 4 separate fields (30 nuclei/field), a total of 120 nuclei were counted for either the presence or absence of signal localization comparing control (EC) and hibernating (LT) conditions.

Field		1	2	3	4
TIA-1/R	EC	1	1	0	2
	LT	30	30	28	29
PABP-1	EC	1	0	0	1
	LT	27	29	27	25
No 1° AB	EC	0	0	0	0
	LT	0	0	0	0
No. of nuclei counted/antibody		30	30	30	30

Discussion

The present chapter investigates the presence of alternative isoforms, localization and solubility of protein targets involved in mRNA processing in the liver of control (EC) and hibernating (LT) thirteen-lined ground squirrels. Hibernating ground squirrels are an excellent model system for uncovering mechanisms involved in mRNA processing in response to stress since they demonstrate a marked global decrease in transcription [Morin and Storey 2006] and translation [Frerichs et al. 1998] during torpor, yet show increases in the levels of selected mRNA/protein species [Pan and van Breukelen 2011]. While a suite of transcriptional and post-transcriptional controls vital to achieving this molecular restructuring have been described [Hittel and Storey 2002; Storey and Storey 2004; Morin and Storey 2009; Kornfeld et al. 2012; Wu and Storey 2012], many regulatory mechanisms remain to be elucidated during hibernation. To further understand the mechanisms that direct mRNA fate, a selection of DNA/RNA-binding proteins that are stress-responsive and involved in guiding gene transcription, mRNA processing, and the formation of stress granules were analyzed.

It has been established previously that RNA binding proteins have different roles when present in the cytoplasm versus nucleus [Suswam et al. 2005; Zhang et al. 2005]; therefore, the subcellular distribution and localization of TIA-1/TIAR and PABP-1 in both cytoplasm and nucleus of euthermic and torpid animals was analyzed. In the cytoplasm, RNA-binding proteins such as TIA-1/R and PABP-1 are localized to stress granules, which store stalled translational pre-initiation complexes when cells are under stress [Zhang et al. 2005; Kedersha and Anderson 2007]. While an attractive candidate for involvement in the hibernating liver, the current study did not reveal evidence of

cytoplasmic stress granule formation using indirect-fluorescence microscopy (Fig. 5.2a). Furthermore, the formation of cytoplasmic stress granules tend to be dependent on the concentration of TIA proteins [Gilks et al. 2004]; however, in the present study, the relative expression of cytoplasmic TIA-1 and TIAR did not change or decreased significantly during LT, respectively. Nonetheless, recent evidence suggests that RNA binding proteins such as TIAR may play a more generalized role in translational repression which is not exclusively linked with the presence of cytoplasmic stress granules [Mazan-Mamczarz et al. 2006]. Additionally, when ribosomal fractions from ground squirrel kidney were separated on sucrose gradients, TIA-1 was restricted to monosome fractions (i.e. translationally silent) during control and torpor [Hittel and Storey 2002]. Taken together, these data suggest that cytoplasmic RNA binding proteins may play a generalized role in translational suppression in ground squirrels.

In contrast to the diffuse signals observed for cytoplasmic pools of RNA binding proteins, the use of fluorescence microscopy revealed strong localization of these proteins in nuclei during LT. Antibodies directed towards TIA-1/TIAR and PABP-1 cross-reacted with proteins that localized to relatively large (~48 μm) subnuclear foci during LT with a 27 to 29-fold increase in the numbers of these nuclear foci (Fig. 5.2b). The appearance of subnuclear structural components has also been observed as a response to torpor or hibernation in the hazel dormouse (*Muscardinus avellanarius*) and the edible dormouse (*Glis glis*) [Malatesta et al. 1994, 1999, 2001, 2008]. However, the subnuclear structures observed by Malatesta and colleagues were numerous and diffuse whereas in the ground squirrel each nucleus showed only one of these with distinct characteristics, including size. Since nuclear TIA-1 and TIAR perform a range of functions including rendering

mRNA translationally silent, modulating the rates of gene transcription, and regulating constitutive and alternative pre-mRNA splicing [Förch et al. 2000; López de Silanes et al. 2005; Suswam et al. 2005], further studies were performed in order to better understand the function of subnuclear foci during torpor.

Using subcellular fractionation and western blotting, up to a 7-fold increase in relative protein expression of TIA-1a and TIA-1b was observed in the nucleus during LT, compared with EC (Fig. 5.3). By contrast, the TIARa isoform was largely restricted to the cytoplasmic fraction and there was no relative change in the expression of the TIARb isoform and PABP-1 in the nucleus between EC and LT. These data suggest that TIA-1 isoforms are major components of the nuclear foci observed by fluorescence microscopy during torpor. It has been shown using both experimental and bioinformatics approaches that approximately 3,000 mRNAs interact with TIA-1 spanning a range of cellular processes and, when bound by TIA-1, these mRNAs are translationally repressed [Piecyk et al. 2000; López de Silanes et al. 2005]. Consequently, it is possible that, when ground squirrels enter torpor, nuclear TIA-1 associates with target mRNAs destined for translational suppression while the mRNA is still in the nucleus. It should also be noted that whereas the localization of TIA-1 into subnuclear structures was correlated with significant increases in relative protein levels during torpor, this was not the case for TIAR and PABP-1 whereby signal localization occurred despite a lack of observed changes in nuclear protein expression levels. These data suggest that TIAR/PABP-1 proteins undergo a re-organization of the nuclear pool during LT and protein localization to subnuclear structures is not necessarily dose-dependent.

While a case has been made for the role TIA-1 in ground squirrel subnuclear foci during LT, proposed roles for nuclear TIAR and PABP-1 may also be gleaned from the present data. In the nucleus, TIAR binds single-stranded DNA (ssDNA) and ssDNA conformations occur in chromatin undergoing active transcription [Suswam et al. 2005]. Given that 1) the TIARa isoform occurred mostly in the cytoplasm (Fig. 5.3), 2) there was no change in relative expression of TIARb in the nucleus between EC and LT conditions, and 3) that a state of enhanced transcription does not agree with the general energy conservation strategy of the hypometabolic state [Morin and Storey 2006], it is unlikely that TIAR associates with ssDNA during hibernation but further evidence is required in order to confirm. Instead, TIAR in the nucleus during hibernation may be related to other tasks such as regulating mRNA processing and/or enhancing mRNA stability, which are also functions associated with TIA-1 and PABP-1 activity [Minvielle-Sebastia et al. 1997; Afonina et al. 1998; Förch et al. 2000; Suswam et al. 2005]. In this capacity, nuclear TIA proteins and PABP-1 may represent stalled mRNA processing factors and, in hibernating hazel dormice, the accumulation of pre-mRNAs at the splicing/cleavage stage has been demonstrated [Malatesta et al. 2008]. It should be noted, however, that some level of active pre-mRNA processing may be critical during torpor since a small subset of genes are selectively activated in order to support the torpid phenotype. Consequently, whereas a generalized global repression of mRNA processing occur during torpor, a selected subpopulation of mRNA species responds oppositely with increased expression of selected genes whose protein products are essential for mitigating stresses associated with hibernation. In summary, the nuclear functions of RNA binding proteins described above would be highly advantageous during torpor since mRNA could

be held in highly organized storage centers, selectively processed when needed, and possibly gain benefits of enhanced stability. Indeed, all of these proposed functions would support an overall suppression of translation during torpor, while also permitting a rapid resumption of protein synthesis when animals arouse back to euthermia.

Further to containing distinct functional roles in the cytoplasm versus nucleus, structural transitions mediated by the prion-like domains of TIA-1 and TIAR have been associated with their function during stress [Gilks et al. 2004]. TIA-1/R proteins are composed of a RNA recognition motif (RRM) and a glutamine-rich prion-related domain (PRD), which have been shown to be important for RNA recruitment and assembly of stress granules, respectively [Anderson and Kedersha 2002]. Similar to infectious prion proteins, the PRD of TIA-1 displays conformation-dependent changes of function which are related to differences in physical properties, especially solubility [Gilks et al. 2004]. Furthermore, the soluble form of TIA proteins has been suggested to function as a translational silencer while aggregated forms promote stress-induced translational arrest via stress granule formation [Gilks et al. 2004]. As such, the solubility of RNA-binding proteins was assessed in the liver of ground squirrels (Fig. 5.5) in order to determine if these interchangeable forms were responsive to torpor. During LT, TIA-1a/TIA-1b showed a shift towards the soluble fraction and all other targets showed no change, suggesting that regulated protein aggregation was not present during torpor. While the functional consequences of this shift towards the soluble fraction are not clear, the data support the role of RNA binding proteins, especially TIA-1, as translational suppressors during torpor.

To characterize ground squirrel RNA-binding proteins the amino acid sequences

of TIA-1, TIAR, and PABP-1 were deduced using sequencing information available as whole genome shotgun reads (Fig. 5.1a). All RNA-binding proteins analyzed were highly conserved in comparison to the sequences from other mammals (Table 5.2). For example, compared with human TIA-1 and TIAR there were only single amino acid substitutions located within the Q-rich domain (residue 305) of TIA-1 or the linker region between RRM2 and RRM3 (residue 203) in TIAR. The full length TIA-1 protein is proteolytically cleaved in order to derive the C-terminus TIA-1 p15 [Kawakami et al. 1994; Taupin et al. 1995] and, in the human gene, TIA-1a and TIA-1b are generated by alternative splicing surrounding exon 5 [Izquierdo and Valcárcel 2007]. Exon 5 is located between RRM1 and RRM2 and its inclusion generates the longer TIA-1a isoform, whereas exon skipping generates the shorter TIA-1b isoform (Fig, 5.1a). The full length TIAR protein (TIARa) uses an alternate in-frame splice site in the coding region, resulting in a longer protein compared to TIARb. Overall, the a isoforms of TIA-1 and TIAR are larger than their corresponding b forms by 11 and 17 amino acids, respectively. The present study detected the presence of the two TIA-1 and TIAR isoforms in the liver of ground squirrels, which was confirmed by RT-PCR and SDS-PAGE (Fig. 5.1b and 5.1c). The presence of alternate isoforms not only agrees with data obtained by Izquierdo and Valcárcel (2007), but also supports the possibility that alternative splicing may indeed be occurring in ground squirrel liver and/or play a role during hibernation.

Izquierdo and Valcárcel (2007) observed that the relative expression of TIA isoforms differed in human tissues and cell lines. For example, overall protein levels of TIA-1 were higher in HeLa than NRK cells, with isoform a being dominant in HeLa cells and isoform b being the only detectable species in NRK cells. TIAR was expressed at

roughly the same level in the two cell lines but whereas HeLa cells expressed TIARa and b equally, TIARb was the dominant isoform in NRK cells. In thirteen-lined ground squirrel liver the relative expression of isoforms a and b were analyzed in both cytoplasmic and nuclear fractions (Fig. 5.4). When comparing the relative expression of TIA-1a to TIA-1b and TIARa to TIARb, a consistently higher expression level of isoform b was observed for both proteins across experimental conditions in both cytoplasmic and nuclear fractions (Fig. 5.4). The TIA-1 isoforms appear to have overlapping roles, yet exhibit functional differences in splicing activity. For example, TIA-1 isoforms exhibit identical subcellular distribution and RNA-binding properties, but TIA-1b displayed enhanced splicing activity [Izquierdo and Valcárcel 2007]. Previous results have shown that TIAR can regulate the levels of mRNA isoforms of TIA-1a versus TIA-1b; thus, a reduction in the levels of TIAR resulted in increases in the TIA-1 isoform b in comparison to isoform a [Izquierdo and Valcárcel 2007]. While stable levels of TIAR were observed in nuclear fractions across experimental conditions in the present study, the selective localization of TIARa to cytoplasmic fractions may have influenced the relative expression of TIA-1b in the nucleus. Nonetheless, more evidence will be required to further elucidate the relationship between TIAR and TIA-1 isoforms in ground squirrel liver.

In summary, the present chapter provides insight into the regulation of RNA-binding proteins in the liver of hibernating thirteen-lined ground squirrels. Torpor-specific subnuclear structures were observed by fluorescence microscopy and RNA-binding proteins such as TIA-1, TIAR, and PABP-1 showed selective increases in relative expression in the nuclear compartment as evidenced by subcellular fractionation

and western blotting. These data suggest a role for these proteins in reducing translational rates, regulating mRNA processing, and/or enhancing mRNA stability during torpor. In addition, a case has been made for the presence of alternate splice variants of TIA-1 and TIAR in ground squirrel liver, opening up the field to further studies that would elucidate a role for alternative gene variants during hibernation. An important future milestone would involve delineating the dynamic (i.e. playing an active role in mRNA processing and/or splicing) versus static (i.e. acting primarily as storage/sequestering molecules) nature of subnuclear structures during torpor. This may be achieved by characterizing the interactions of RNA binding proteins with specific mRNA species and tracking their movement between subcellular compartments. Since selective increases in gene/protein expression must be balanced with an overall reduction in transcriptional and translational rates, the hibernating ground squirrel provides a unique opportunity to study nuclear dynamics and post-transcriptional control under changing environmental conditions.

Chapter 6

General Discussion

The set of genes/proteins expressed in a cell largely define it and documentation of these expression signatures has helped us to understand innumerable physiological and pathological states while also having significant impacts on diagnostics, clinical care and outcome. However, much more remains to be learned. While a global understanding of all the genes/proteins responsible for shaping a particular phenotype is an exciting goal, the real breakthrough will involve the capacity to selectively manipulate gene/protein expression profiles in order improve health and treat disease. Crucial advancements in our understanding of the cellular regulatory mechanisms which drive the global make-up of cells are therefore required. One particular piece of the puzzle that is needed is a better understanding of the cellular machinery responsible for directing gene and protein expression programs, including a vast array of proteins and non-coding RNAs whose complex interplay drives gene expression, mRNA transcript handling, protein synthesis, and posttranslational processing to create the final functional protein and place it in the correct subcellular destination. A particularly interesting model to use to examine the regulation of gene/protein expression in response to environmental stress is mammalian hibernation. Hibernating mammals use a suite of molecular and biochemical mechanisms to cope with environmental conditions that are known to be harmful or lethal for nonhibernating mammals. For example, hibernators survive hypothermia (core body temperatures as low as 4-5°C), ischemia-reperfusion, restricted nutritional resources, and demonstrate regulatory mechanisms which enhance cellular preservation and ensure seamless transitions to and from the hypometabolic state. Consequently, the induction of a hibernation-like state which is resistant to parallel stresses holds immense clinical promise in diverse fields including increasing the functional shelf-life of excised human

organs for transplant.

To investigate the mechanisms that regulate cycles of torpor-arousal without injurious effects, I surveyed targets across a range of cellular processes including epigenetics, signal transduction and cellular survival, transcription factors, and RNA binding proteins in thirteen-lined ground squirrels (*Ictidomys tridecemlineatus*). As a result, I identified key targets that were responsive to hibernation with involvement in: 1) reversible, global controls on transcription including a particular important role for histone modifications, 2) signal transduction pathways which stimulate changes in gene expression with emphasis on the activation of mitogen-activated protein kinases (MAPKs) during early arousal, 3) the regulation of the antioxidant response by Nrf2 and the role of posttranslational modifications and protein-protein interactions, and 4) guiding posttranscriptional processing by TIA-1, TIAR, and PABP-1 through localization to subnuclear structures. The data show that while global molecular controls that inhibit ATP-expensive cellular processes are central to achieving a hypometabolic state during torpor, arousal from torpor most likely relies on the complex coordination of cytoprotective strategies. In this capacity, the present thesis has newly identified a group of proteins – RNA binding proteins – that appear crucial not just to the overall suppression of translation during torpor, but are hypothesized to be involved in the rapid resumption of protein synthesis when animals arouse back to euthermia (Chapter 5). Furthermore, these RNA binding proteins displayed differential regulation of alternative gene variants thereby representing the first torpor-responsive isoforms to be described in thirteen-lined ground squirrels. Data collected on the regulation of MAPKs (e.g. ERK, JNK, p38) demonstrated selectivity for downstream substrates (Chapter 3), while

transcription factors (e.g. Nrf2) most likely rely on the integration of multiple signals in order to achieve a highly specific outcome (Chapter 4). Collectively, therefore, Chapters 3 and 4 define a new set of molecular targets in the area of stress resistance which help support arousal from torpor. Finally, epigenetic mechanisms identified in the present thesis showed that lysine acetylation was particularly important during arousal and identified novel protein modifications on histone H2B, attesting to the complexity of chromatin structure during hibernation (Chapter 2).

DNA methylation and histone modifications

Recently, there has been a growing interest in the idea that mechanisms associated with epigenetic regulation may also be used to achieve global, reversible suppression of transcription [Morin and Storey 2009; Storey 2014]. Early studies on histones revealed that actively transcribed genes were associated with hyperacetylated histones [Pogo et al. 1966]. Moreover, this response occurred broadly on multiple lysine residues within the tail region of histone proteins and was not specific to a particular gene [Martin et al. 2004]. The suggested mechanism involves neutralization of positively charged lysine residues through addition of an acetyl group that weakens the charge-dependent interaction between histone and DNA. Furthermore, it has been proposed that a cumulative effect exists since the addition of multiple acetyl groups acting on the same or surrounding histone can achieve enhanced charge neutralization [Zentner and Henikoff 2013]. While charge neutralization of lysines is often associated with promoting gene expression, it is also important for relaxing histone-DNA contacts for efficient DNA replication and also occurs at DNA double-stranded breaks in order to increase DNA

access to repair factors [Zentner and Henikoff 2013]. While acetylation may be viewed as having the general effect of increasing access to DNA, the "histone code" hypothesis suggests that specific histone modifications or combinations of modifications confer unique biological functions [Strahl and Allis 2000] and provides a mechanism to resolve these differing effects on chromatin relaxation.

In the present thesis, posttranslational modifications on histone proteins including phosphorylation, acetylation and methylation were of particular interest since reversible protein phosphorylation is already a well-established mechanism of achieving hypometabolism and, by extension, may also provide a framework for dynamically controlling chromatin structure. Furthermore, acetylation has also been shown to be differentially regulated on transcription factors such as Nrf2 (presented in Chapter 4), and may alter Nrf2 binding to upstream promoter regions in DNA. Therefore, acetylation may prove to be another broadly important reversible protein modification during hypometabolism, possibly rivaling the importance of phosphorylation. Initial data obtained from mammalian hibernators suggested that coordinated controls on histone proteins (mediated by histone deacetylases) and RNA Pol II occurred during torpor [Morin and Storey 2006]. Data from the present thesis confirmed that reductions in H3 phosphorylation at Ser 10 and acetylation at Lys 23 were uniquely associated with late torpor (LT) and concerted increases in H3 acetylation at K14, K18, and K27 were shown during early arousal. According to the histone code hypothesis these sites are thought to be primarily involved in controlling gene expression and, as a result, these data suggest that posttranslational modifications acting on histones may have an inhibitory effect on transcription during torpor, yet this response is flexible and readily reversible during

arousal.

At least eleven types of PTMs have been reported at over 60 different amino acid residues on histones [Tan et al. 2011]. These modifications include acetylation, phosphorylation, methylation, and ubiquitination which have been extensively described in the literature as well as more exotic modifications such as crotonylation [Tan et al. 2011]. Indeed, the information collected in this thesis adds to this data set with the discovery of unique modifications on histone H2B proteins in thirteen-lined ground squirrels. One of these modifications (i.e. methylation of arginine 6) has particularly interesting characteristics since 1) it is located within the protruding H2B tail thereby potentially interacting with the surrounding environment, 2) the peptide housing the modification is also found in the naked mole rat perhaps reflecting parallels in their physiology (e.g. hypoxia tolerance or heterothermic capacity), and 3) the modified residue is an amino acid substitution which, in the human protein, is a well-known regulatory lysine. Consequently, these characteristics may have substantial cellular consequences and warrant further investigation. Since there are no antibodies available at present to assess this arginine-containing peptide, one particularly interesting future direction would be a mass spectrometry approach which would allow the quantification of posttranslational modifications of the specific arginine-containing peptide comparing control and other time points over the torpor-arousal cycle.

Signal transduction and transcription factor regulation

The ability of cells to respond to extrinsic and intrinsic cues depends on the transmission of signals along highly ordered signalling networks, leading to changes in

cell metabolism, gene/protein expression, intracellular trafficking, etc. Understanding the mechanisms which provide the cell with the information required to react appropriately to its environment is essential to our understanding of human health and disease. In recent years, research has begun to illuminate how these intracellular networks are coordinated and, even further, how cells direct a highly specific response based on the integration of multiple signals. Reversible phosphorylation of intracellular proteins carried out by protein kinases and protein phosphatases is a vital regulatory mechanism responsible for activating/inhibiting many specific cellular responses which modulate the cellular environment and return the cell to its preferred homeostatic milieu. While it is widely accepted that signal transduction pathways and transcription factors play a vital role in the overall health of the cell [Rose et al. 2010; Akazawa and Komuro 2003], the underlying molecular mechanisms which connect signaling to gene expression are not well understood. The impact of this gap in knowledge is therapeutic targets with inconsistent results and difficulties delineating protective versus injurious molecular cascades [Rose et al. 2010]. As a result, the points at issue are how extracellular stimuli are perceived, how these are converted into intracellular signals, and how these signals change the transcriptional program.

Mitogen-activated protein kinases (MAPKs) are seemingly promiscuous Ser/Thr kinases with the capacity to respond to diverse stimuli, relay this information to intracellular responses, and yet achieve specific cellular outcomes. The best known MAPK enzymes, or conventional MAPKs, include ERK1/2, JNK1/2/3, p38 α, β, γ, δ, and ERK5; however, other understudied MAPKs also exist (e.g. atypical MAPKs including ERK3/4, ERK7/8, and Nemo-like kinase, NLK) [Cargnello and Roux 2011]. Similarly,

transcription factors respond to incredibly diverse stimuli and contain binding sites for the promoter/enhancer regions of a large number of genes. This characteristic implies that understanding how transcription factor activation is translated into a cell-type, tissue-specific, disease-specific, and stress-specific response would be vital to understanding the initiation program that directs gene expression. A growing number of well-studied transcription factors have already allowed large strides to be made in our understanding of the regulatory mechanisms that govern the specific activity of important transcription factors [e.g. Oeckinghaus and Ghosh, 2009; Zhang et al, 2011]; however, the data remains incomplete. Hibernation in ground squirrels represent an opportunity to understand the role transcription factors play in activating a subset of stress-responsive pathways and their regulation by upstream signal transduction pathways, aimed at overcoming the stresses associated with the hibernating phenotype.

In light of this, I chose to identify the activation profile of conventional signal transduction pathways (e.g. ERK, JNK, p38) and trace this down to selected transcription factors (e.g. CREB1, ELK1, c-Jun, ATF2, p53, Nrf2) which may aid in meeting challenges associated with hibernation. Importantly, I proposed that these signal transduction pathways and transcription factors would be regulated by fine cellular controls (e.g. post-translational modifications and protein-protein interactions) which require very little ATP expenditure, result in a rapid response and directed changes in gene transcription during hypometabolism. Additionally, through a combinatorial mechanism, transcription factor complexes and their PTMs will ensure the expression of select genes/proteins at the optimal time, concentration and in the optimal cellular compartment. Indeed, the data showed that MAPKs and select transcription factors are

subject to differential phosphorylation during hibernation. Additionally, other understudied posttranslational modifications including acetylation, ubiquitination, and sumoylation are also important regulatory mechanisms on Nrf2 as well as changes in its physical interactions with its binding partner protein, KEAP1.

Of particular interest was the capacity to achieve a highly specific response during hibernation; JNK2/3 was activated, whereas JNK1 and all other MAPKs studied were not responsive to torpor-arousal in muscle. In heart, there was a much more concerted response in MAPK activation during arousal; however, similar to skeletal muscle, many of the transcription factors and heat shock proteins presently studied did not respond to torpor-arousal in muscle or heart. Taken together, these data support the capacity of MAPKs to direct highly specific cellular effects. A particularly relevant lead which may be activated by JNK2/3 in the muscle is the Nrf2 transcription factor since parallel activation patterns were observed between them during hibernation; JNK2/3 and Nrf2 phosphorylation was enhanced during early arousal. Nrf2 can be regulated by phosphorylation from many kinases; however, Nrf2 activation by MAPKs is thought to aid in nuclear localization, although MAPKs only moderately induces Nrf2 transcription on their own. As a result, it may be hypothesized that Nrf2 may be phosphorylated during late torpor by kinases which are known to disrupt the inhibitory action of KEAP1 (e.g. PKC) and the mounting signal observed in early arousal (phosphorylation levels peaked during early arousal) may be as a result of JNK2/3 activation. This response is also correlated with enhanced levels of lysine acetylation during early arousal. Consequently, this proposed mechanism would rely on the integration of multiple signaling pathways (i.e. at least two kinases and one acetyltransferase) and may provide a framework for

achieving a directed cellular response.

Of course, further data are required in order to confirm or deny the direct regulation of Nrf2 by JNK2/3 during early arousal, but the general concept of kinase specificity would nonetheless be an interesting future direction. In fact, JNK is a particularly fascinating example in the field of kinase specificity since it displays differential regulation of its isoforms [Waetzig and Herdegen 2005] and interacts uniquely with scaffold proteins depending on the cellular stimuli/stress [Dhanasekaran et al. 2007]. The JNK family is known to consist of ten isoforms derived from three genes; JNK1 (four isoforms), JNK2 (four isoforms), and JNK3 (two isoforms). JNK isoforms have differential expression patterns in select tissues; JNK1 and JNK2 are ubiquitously expressed whereas JNK3 is present primarily in the heart, brain and testis [Waetzig and Herdegen 2005]. JNK isoforms exhibit downstream preferences for subsets of JNK targets. For example, JNK1 and JNK2 differ in their ability to interact with c-Jun, a transcription factor which is tightly linked with survival [Kallunki et al. 1994]. JNK2 binds to c-Jun 25-times more efficiently than JNK1 and the reason for this was traced to a small, β-strand-like region (near the catalytic site of the enzyme) which serves as a docking site that effectively increases the concentration of c-Jun near JNK2 [Kallunki et al. 1994].The binding affinity of JNK1β1, JNK2α1 and JNK2α2 for c-Jun is twofold higher than that for ATF2, whereas the affinity of JNK2β1 and JNK2β2 for ATF2 is twofold higher than that for c-Jun [Gupta et al. 1996]. These differences in substrate affinities lead to differentially regulated sets of target genes [Chen et al. 2002]. Indeed, the isoform variation of JNKs in ground squirrels may shed light on how this kinase specificity achieves such selectivity during hibernation.

Scaffold proteins have been shown to play a role in diverse signaling pathways and MAPKs provide an elegant example of how scaffold proteins can promote kinase specificity by organizing closely related kinases in microdomains [Dhanasekaran et al. 2007; Morrison 2001; Waetzig and Herdegen 2005; Tao et al. 2010]. By organizing the cell in microdomains, the diversity of substrates for a given kinase may be severely limited since a kinase may come into contact with only a subset of these targets resulting in a directed response. For example, a critical scaffold protein for the organization of the ERK1/2 cascade is the Kinase Suppressor of Ras (KSR) protein [Morrison 2001]. KSR ensures both kinase specificity and efficiency of signal propagation through recruitment of all 3-tiers of the ERK cascade (i.e. MAPKKK, MEK, ERK). Activation of other MAPK modules, such as JNK and p38, are mediated by different, yet overlapping, scaffold proteins [Waetzig and Herdegen 2005]. The JNK-interacting proteins (JIPs) form an important family of JNK scaffolds. The scaffold protein JLP (a variant of the JIP4 scaffold protein) assembles MEKK3-MKK4-JNK leading to cellular differentiation, JIP3 recruits MLK/MEKK1-MKK4/MKK7-JNK under growth factor withdrawal, and JIP1 recruits MLK-MKK7-JNK upon excitotoxic stress and obesity [Waetzig and Herdegen 2005]. Furthermore, JNK is activated by two other scaffold proteins, plenty of SH3 (POSH), which upon apoptosis stimuli or growth factor withdrawal activates the Rac1/MLKs-MKK4/7-JNK module and the Connector Enhancer of KSR-1 (CNK1) that links MLK3-MKK7-JNK for gene regulation [Waetzig and Herdegen 2005]. The p38 MAPK, on the other hand, can be activated by JIP2, JIP4, and JLP; JIP4 provides a platform for activating p38 that requires MKK3 and MKK6 whereas JLP requires signaling input from the novel scaffold BNIP-2/Cdc42 perhaps acting as a mechanism to

distinguish JNK -JLP vs. p38-JLP pathways [Waetzig and Herdegen 2005].

In summary, much remains to be explored as it pertains to MAPKS and transcription factor regulation during hibernation. As result, a long list of future directions for analysis of MAPK regulatory involvement in hibernation may include: 1) expanding the involvement of conventional MAPKS to include ERK5 in muscle and heart, while also investigating MAPK responses in additional tissues, 2) looking at the atypical MAPKs including ERK3/4, ERK7/8, and Nemo-like kinase (NLK), 3) identifying the specific MAPK isoform(s) which are activated during torpor including 4) evaluating possible links between MAPK regulation and epigenetic mechanisms including the involvement of p300/CBP , 5) identifying the interactions of MAPKs with scaffold proteins and their organization in subdomains, and 6) identifying the specific *in vivo* targets and cellular consequences of MAPK activation during hibernation. Similarly, future directions for transcription factor regulation may include: 1) examining the changes in and consequences of additional PTMs (e.g. threonine and tyrosine phosphorylation, arginine and lysine methylation) and protein-protein interactions (e.g. small Mafs for Nrf2) for transcriptional control in hibernation, 2) performing analogous studies on other transcription factors known to play a role in hibernation (e.g. MEF2, FOXO, PGC-1α), 3) using co-immunoprecipitation studies on cytoplasmic and nuclear fractions in order to assess regulatory mechanisms which define each subcellular compartment, and 4) performing mass spectrometry in order to determine the specific amino acid sites containing PTMs. Analysis of the mechanisms of selective regulation through this comparative approach will shed light on the context-dependent selectivity of kinases for downstream substrates and the resulting changes which alleviate the stresses

associated with extreme environmental conditions.

Subdomains during hibernation

Cytoplasmic stress granules have been shown to form in response to hypoxia [Gottschald et al. 2010], heat/cold shock [Kramer et al. 2008; Hofmann et al. 2012], oxidative stress [Emara et al. 2012], viral infection [Lindquist et al. 2010], and nutrient deprivation [reviewed in Anderson and Kedersha 2008; Jones et al. 2013]. Nuclear bodies respond to cell stress of many kinds including heat shock, apoptosis, senescence, heavy metal exposure, viral infection, and DNA damage, and are involved in multiple human disease pathologies such as neurodegenerative diseases and cancer [reviewed in Zimber et al 2004; Morris 2008; Busà et al. 2010]. These nuclear structures are thought to represent highly organized subdomains that comprise the nucleus of metazoan cells [Denegri et al. 2001], yet their function has remained enigmatic despite being the focus of intense research. One way in which the cellular functions of these subdomains can be delineated involves characterizing the residing constituents. Consequently, I was greatly interested in the involvement of RNA binding proteins that have known roles in translational suppression as well as in forming subcellular compartments. The present thesis identified a novel subcellular body during deep torpor in thirteen-lined ground squirrels (Chapter 5). This subnuclear body consists of RNA-binding proteins such as TIA-1, TIAR, and PABP-1 which are also markers of cytoplasmic stress granules. While further evidence is required to associate these hibernating-specific subnuclear foci with a specific function, I hypothesized the following possible roles; 1) the enhancement of mRNA stability, 2) sites of transcript storage while mRNA is still in the nucleus, and/or

3) selective processing of pre-mRNA essential to the stress response. All of these functions likely support the overall suppression of translation during torpor, while also promoting a rapid resumption of protein synthesis when animals arouse back to euthermia.

While research on nuclear dynamics as it pertains to hibernating thirteen-lined ground squirrels remains quite sparse, significant advances have been made through studies of hibernating edible and hazel dormice and these are summarized herein. Firstly, the general morphology of cell nuclei does not change substantially between euthermia and torpor [Malatesta et al. 1994a], although the cell nucleus undergoes an important structural reorganization in the hypometabolic state [Malatesta et al. 1999; Malatesta et al. 2008]. In this capacity, nuclear bodies including fibro-granular material, amorphous bodies, coiled bodies, perichromatin granule-like granules and nucleoplasmic fibrils have been shown to be strictly correlated with hibernation [Malatesta et al. 1999]. Furthermore, these nuclear structures are present across different species, although nuclear bodies were less frequent in edible versus hazel dormice and displayed morphological differences [Malatesta et al. 1999]. Whereas tissue specific differences in the distribution of nuclear bodies have been shown, most contain some mRNA splicing or processing factors (except for nucleoplasmic fibrils for which the composition remains unknown) suggesting that post-transcriptional regulatory mechanisms during torpor-arousal are quite complex. While sensitive to low body temperatures, the presence of nuclear bodies is correlated with strongly reduced metabolic rate [Malatesta et al. 1999; Malatesta et al. 2001]. Finally, structures including coiled bodies (CBs) and amorphous bodies (ABs) are suggested to represent storage sites for splicing factors that can be

rapidly used upon arousal, nucleoplasmic fibrils are hypothesized to play a role in the dynamics of the associated structural components, and fibro-granular material (FGM) is thought to be involved in transcription and processing of pre-mRNA during hibernation [Malatesta et al. 2001].

In addition to nuclear dynamics, well-studied cytoplasmic foci/granules also appear to be involved in RNA silencing during mammalian hibernation. Cytoplasmic stress granules and processing bodies are both non-membranous, ribonucleoprotein containing structures that each recruit distinct proteins during stress which are reflective of their cellular roles. The core components of stress granules are small ribosomal subunits and translation initiation factors (eIF4E, eIF3, eIF4A, eIFG), RNA-binding proteins (HuR, TIA-1, TIAR), and other components of mRNA metabolism [Kedersha and Anderson 2007]. By contrast, processing bodies contain components of the RNA decay machinery (DCP1/DCP2, Hedls/GE-1, SMG5/7, UPF1) and RNA-induced silencing machinery (GW182, microRNA, argonaute) [Kedersha and Anderson 2007]. As a result, stress granules are generally considered to be sites of mRNA storage whereas processing bodies are places for mRNA degradation. Moreover, it has been proposed that mRNAs selected for degradation are passed from stress granules to processing bodies. While an attractive candidate for involvement in the hibernation state, there was no evidence of stress granules in hepatocytes of hibernating thirteen-lined ground squirrels (Chapter 5). However, given tissue specific mechanisms employed by each tissue to repress translation, the involvement of stress granules nonetheless remains a plausible hypothesis in other tissues, especially in the kidney. Hittel and Storey (2002) analyzed protein and ribosome distributions in a sucrose gradient between euthermic and torpid

states. They found a redistribution of PABP within a sucrose gradient changing from association with monosome fractions (fractions 8–10) in euthermia to PABP presence in fractions 4, 5, and 7 during hibernation, fractions apparently associated with stress granules. This suggested that stress granules play a role in the inhibition and stabilization of mRNA during hibernation. While stress granules were not verified by immunofluorescence and fluorescence microscopy, further research in this area will clarify the functional significance of data obtained from these polysome profiles.

Alternative splicing during hibernation

Adding to the amazing complexity of mRNA processing, it is estimated that alternative splicing occurs in about 60-80% of human genes [Johnson et al. 2003; Lander et al. 2001]. Alternative splicing can affect the untranslated region (UTR) of mRNA that plays a major role in the control of transcript fate; therefore, alternative splicing may provide a mechanism to evade stress-induced repression of translation. Furthermore, alternative splicing may also occur within the coding sequence of mRNA, effectively diversifying the functional properties of proteins with potential for significant cellular consequences. Indeed, various forms of stress induce a large spectrum of modifications in alternative splicing [Muñoz et al. 2009] and the misregulation of pre-mRNA splicing has been associated with various human disease states [Faustino and Cooper 2003; Singh and Cooper 2012]. While the regulation of alternative splicing has been extensively studied in a tissue- and developmental stage-specific manner, data on the role of alternative splice variants in mammalian hibernation is very limited. Studies of the American black bear (*Ursus americanus*) aimed at the development of genomic resources was able to gain a

perspective on the proportion of alternatively spliced genes through in-depth analysis of large scale Expressed Sequence Tags (ESTs) [Zhao et al. 2010]. The data revealed that alternative 5'splice sites had the highest occurrence (35%), followed by alternative 3'sites (29%), exon skipping (24%), and intron retention (12%). The frequency of each category was not significantly different from the distribution of splicing events in other mammalian species but the order of each category from highest to lowest was different; e.g. in humans, the order was exon skipping (42%), alternative 3'sites (26%), alternative 5'splice sites (24%), and intron retention (8%). Although these data do not comment on the importance of alternative splicing events to torpor-arousal, other groups have begun to describe these changes.

Accumulating data have identified hibernators including arctic ground squirrels, Syrian hamsters, and black bears as models for understanding the pathobiology of neurodegenerative diseases such as Alzheimer's [Stieler et al. 2011]. The pathogenesis of neurodegenerative disease is thought to be related to Tau proteins whereby increased Tau phosphorylation is a pivotal aspect for aggregation and formation of neurofibrillary tangles [Iqbal et al. 2005]. Consequently, studies with these hibernators have focused on Tau proteins and microtubule assembly/stability as well as changes in Tau phosphorylation. Tau exhibits six alternatively spliced mRNA isoforms that differ in the number of N-terminal inserts and their differential expression, in combination with protein modifications by phosphorylation, influences their affinity to microtubules. In arctic ground squirrels, mRNA isoform expression data revealed two distinct PCR products resulting from an alternative splicing event surrounding exon 10 that encodes for an additional microtubule binding repeat. Moreover, the results showed a significantly

altered Tau isoform expression pattern during hibernation whereby the tau isoforms including exon 10 were significantly decreased during torpor and following arousal. Exon 10 encodes for an additional microtubule binding repeat [Stieler et al. 2011], suggesting that alternative splicing events surrounding exon 10 may alter the binding capacity of Tau with microtubules during hibernation. Similarly, results from the greater horseshoe bat, obtained from a suppression subtractive hybrizidation library, revealed that the bat brain calcium/calmodulin-dependent protein kinase kinase β1 (CaMKKβ1) gene has four transcript isoforms differing primarily in exons b and d [Yuan et al. 2007]. CaMKKβ1 was of particular interest because it plays an important role in calcium mediated neurotransmission and normal brain activity [Hsu et al. 2001]. Interestingly, the authors showed that the functional and non-functional splicing isoform of CaMKKβ1 displays distinct expression patterns between hibernating and active states whereby the non-functional isoform was selectively upregulated. Furthermore, the authors suggest that this differential regulation may represent a novel neuroprotective strategy adopted by bats to avoid tissue damage during hibernation by decreasing the sensitivity of neurons to calcium influx. Consequently, these studies determined that alternative splice variants are responsive to hibernation and, moreover, suggest that changes in alternative splice variants could have significant functional consequences.

Hibernator brains are not the only tissue to show evidence of alternative splicing in response to hibernation since additional data from the liver of the greater Egyptian jerboa (*Jaculus orientalis*) and thirteen-lined ground squirrel have also recently been described. The peroxisome proliferator-activated receptor (PPAR) family of transcription factors play a key role in lipid metabolism and controlled regulation of lipid metabolism

is integral to mammalian hibernation [Eddy et al. 2005]. While PPARgamma and the PPARgamma co-activator (PGC-1alpha) have been shown to respond to hibernation in thirteen-lined ground squirrels [Eddy et al. 2005], PPARα also plays a role in *J. orientalis* liver during hibernation [El Kebbaj et al. 2009]. The data showed that jerboa liver expressed an active wild-type form of PPARα (PPARα1wt) and a truncated PPARα (PPARα2tr) and the ratio of wt:tr was differentially regulated during hibernation. As a result of a posttranscriptional exon-skipping event, PPARα2tr lacks the ligand-binding domain and is thought to repress the activity of PPARα1wt by competing with essential coactivators [Gervois et al. 1999]. During hibernation, the level of the active PPARα1wt did not vary significantly but PPARα2tr nearly disappeared so that the wt:tr ratio rose by 3.74-fold as compared with liver of active jerboas.

In the present thesis, I described data whereby alternative TIA-1 and TIAR gene variants were detected in the liver of thirteen-lined ground squirrels (Chapter 5). T cell intracellular antigen 1 (TIA-1) and TIA1-related (TIAR) are RNA-binding proteins that play a role in pre-mRNA splicing [Minvielle-Sebastia et al. 1997; Suswam et al. 2005], translation [Sachs and Davis 1989; Kedersha and Anderson 2007], mRNA stabilization [Decker and Parker 1993], and decay [Caponigro and Parker 1995]. The data revealed that TIA-1a and TIA-1b isoforms were significantly enhanced in nuclear fractions during torpor, as compared with controls, suggesting that both isoforms were responsive to hibernation. TIAR isoforms a and b also exhibited parallel changes in response to torpor; however, the subcellular distribution of these isoforms differed whereby TIARa was mostly restricted to cytoplasmic fractions. Another interesting point was the prevalence of the TIA-1b isoform relative to the TIA-1a isoform in both nuclear and cytoplasmic

fractions across control and torpid conditions. Studies of the functional consequences of TIA-1 alternative processing indicate that isoform b has higher splicing activity [Izquierdo and Valcárcel_2007], supporting the possibility that alternative splicing may be occurring during torpor (albeit at low levels) or that pre-mRNA preloaded with TIA-1b during torpor may help to fuel the rapid reversal of the hibernating phenotype. While the above mentioned data gives us a first glimpse into the role of alternative gene variants as significant biological processes during mammalian hibernation, I anxiously await further studies in the area since much remains incompletely understood.

mRNA stability

In comparison to proteins, mRNA is significantly less stable with half-lives of different transcripts ranging from a just few minutes to 12 hours [Hargrove and Schmidt 1989]. Hence, multiple regulatory mechanisms have evolved that enhance mRNA stability. These involve interactions with RNA binding proteins which protect mRNA from decay pathways and sequester mRNA into cytoplasmic stress granules, structural transitions, and/or alterations to the length of the poly(A) tail [Ross 1995]. Given the instability of mRNA relative to protein, the length of a torpor bout (as long as 3 weeks), and the low transcriptional rates during torpor, one could predict that gene products would become limiting during torpor. This could hold true despite low body temperatures which would passively slow mRNA decay pathways during deep torpor. Surprisingly, data from several mammalian hibernators have shown that the total pool of mRNA remains constant through a torpor bout [Srere et al. 1995; Frerichs et al. 1998; O'Hara et al. 1999], suggesting that global reductions in degradation pathways and enhanced mRNA stability may be components of torpor. Since changes in mRNA half-life may

play a direct role in mRNA abundance without any change to transcription, this regulatory mechanism could have significant consequences for torpor when energy conservation is critical. Indeed, studies with mammalian hibernators are beginning to identify mechanisms that prolong mRNA half-life and enhance stability.

Pathways involved in mRNA decay include removal of the poly(A) tail prior to nucleolytic cleavage; therefore, the length of the poly(A) tail can be used as a measure of mRNA stability [Korner and Wahle 1997]. As such, studies in arctic ground squirrels used the length of the poly(A) tail as a proxy for mRNA stability [Knight et al. 2000]. The data revealed that poly(A) tail lengths are conserved during torpor, suggesting that mRNA is stabilized during hibernation. Further to this, when the distribution of poly(A) tail lengths were plotted as a function of torpor bout progression, the distribution pattern was consistent with the binding of poly(A)-binding protein (PABP), indicating a possible role of PABP in mRNA stability, as has been shown in other studies [Bernstein et al. 1989; Korner and Wahle 1997]. While the interaction between mRNA and PABP-1 has not been fully described, I also suggested a role for PABP-1 as an mRNA stabilizer in hepatocytes of thirteen-lined ground squirrels during deep torpor (Chapter 5). The data showed that despite a lack of observed change in the relative expression levels of PABP-1 in nuclear fractions from liver of euthermic versus torpid ground squirrels, RNA binding proteins including PABP-1 and TIA-1/R localized to subnuclear structures during torpor. It may be proposed that this nuclear localization has a role to play in enhancing the stability of mRNA transcripts during torpor. Hence, taken together, studies in arctic and thirteen-lined ground squirrels suggest that PABP and other RNA binding proteins play a prominent role in enhancing mRNA stability during torpor.

Concluding remarks

In conclusion, my thesis offers insights into some of the mechanisms which regulate gene expression including epigenetics, signal transduction pathways, transcription factors, and RNA binding proteins. When a stress occurs, it is converted into various biological signals following cell signaling pathways and leading to modifications of the properties of existing enzymes/proteins and gene transcriptional/translational events that change the numbers and types of cell proteins. While global changes to gene transcription may rely on epigenetic mechanisms, select genes are strategically upregulated by transcription factors which are subject to complex regulatory mechanisms (e.g. PTMs and protein-protein interactions). Finally, posttranscriptional processing of mRNA by RNA binding proteins allows mRNA to respond to a multitude of inputs and play a role in nuclear dynamics. In particular, I show that histone modifications on histone H3 are important in muscle, responding during late torpor and early arousal. Additionally, I have identified novel modifications and amino acid substitutions at important regulatory sites on histone H2B and further studies into their biological significance are surely warranted. I found that MAPK activation is particularly significant during arousal from torpor, likely coordinating essential cellular functions and places new interest in the importance of the transitory phases of hibernation. Nrf2 transcription factors are regulated primarily by phosphorylation, acetylation, and interactions with KEAP1, and the integration of multiple signals allows the transcription factor to achieve a highly specific outcome. Finally, this thesis is the first to look at the subcellular distribution of RNA binding proteins during torpor and has identified a novel subcellular structure.

Appendix A: Publication List

Luu BE, **Tessier SN**, Duford DL, Storey KB (2014) The regulation of troponins I, C and ANP by GATA4 and Nkx2-5 in heart of hibernating thirteen-lined ground squirrels. PLOS ONE, Submitted, PONE-D-14-25708.

Tessier SN, Storey KB (2014) To be or not to be: the regulation of mRNA fate as a survival strategy during mammalian hibernation. Cell Stress & Chaperones, Accepted, CSAC-D-14-00041.

Rouble AN, **Tessier SN**, Storey KB (2014) Characterization of adipocyte stress response pathways during hibernation in thirteen-lined ground squirrels. Mol Cell Biochem, Accepted, MCBI-D-14-00129.

Tessier SN, Audas TE, Wu CW, Lee S, Storey KB (2014) The involvement of mRNA processing factors TIA-1, TIAR, and PABP-1 during mammalian hibernation. Cell Stress & Chaperones, Epub ahead of print.

Seibel BA, Häfker NS, Trübenbach K, Zhang J, **Tessier SN**, Portner HO, Rosa R, Storey KB (2014) Metabolic suppression during protracted exposure to hypoxia in the jumbo squid, *Dosidicus gigas*, living in an oxygen minimum zone. J Exp Biol, Accepted, JEXBIO/2013/100487.

James RS, Staples JF, Brown JCL, **Tessier SN**, Storey, KB (2013) The effects of hibernation on the contractile and biochemical properties of skeletal muscles in the thirteen-lined ground squirrel, *Ictidomys tridecemlineatus*. J Exp Biol 216:2587-2594.

Rouble AN, Helfer J, Mamady H, Storey KB, **Tessier SN** (2013) Anti-apoptotic signaling as a cytoprotective mechanism in mammalian hibernation. Peer J 1:e29.

Tessier SN, Storey KB (2012) Myocyte enhancer factor-2 and cardiac muscle gene expression during hibernation in thirteen-lined ground squirrels. Gene 501:8-16.

De la Roche M, **Tessier SN**, Storey KB (2012) Structural and functional properties of glycerol-3-phosphate dehydrogenase from a Mammalian hibernator. Protein J, 31: 109-19.

Zhang J, **Tessier SN**, Storey KB (2011) PI3K-Akt regulation as a molecular mechanism of the stress response during aerobic dormancy, in: Nowakowska A, Caputa M (Eds.), Hypometabolism: Strategies of Survival in Vertebrates and Invertebrates. Research Signpost, Kerala, pp. 147-182.

Morin M, Dickson D (2010) Leading Matters, An Inspirational and Practical Approach for High-Performance Leaders. General Store Publishing House. Renfrew, Ontario. Leaders who collaborated and contributed their experience and insights to the book include: Gerry Arial, General Jean Boyle, Jim Durrell, Roger

Greenberg Franklin Holtforster, Jacquelin Holzman, France Jacovella, Jan Kaminski Jr., Rosemarie Leclair, Rob Lindsay, Jim Orban, J.P Soublier, **Shannon Tessier**, John Watts. http://www.kwapartnersottawa.com/leading-matters

Tessier SN, Storey KB (2010) Expression of myocyte enhancer factor-2 and downstream genes in ground squirrel skeletal muscle during hibernation. Mol Cell Biochem 344:151-62.

Appendix B: Communication at scientific meetings

Talks

Tessier SN, Storey KB (2014) Lessons from mammalian hibernators: surviving the adverse effects of hypothermia and ischemia-reperfusion. ACCryo2014, Key Largo, Florida, January 15-19, 2014.

Tessier SN, Storey KB (2013) Linking signaling pathways to gene expression during mammalian hibernation. CRYO2013, 50th Annual Meeting, Society for Cryobiology, Bethesda, Maryland, July 28-31, 2013.

Tessier SN (2011) Enterprising Women: Networking, Leadership, and Experience. Carleton Entrepreneur Association. Ottawa, October 27, 2011.

Tessier SN, Holden HA (2011) Life in the Cold and Beyond. Celebration of Women in Science and Engineering, hosted by Carleton University Women in Science and Engineering (CU-WISE), Ottawa, April 6th, 2011.

Tessier SN (2011) The Art of Social Exchange: Basic Networking Etiquette. Carleton Entrepreneur Association. Ottawa, March 3, 2011.

Posters

Tessier SN, Storey KB (2012) Modulating Nrf2 transcription factor activity by posttranslational modifications and protein-protein interactions: revealing the regulatory mechanisms of antioxidant defenses during hibernation. 19th Methods in Protein Structure Analysis (MPSA 2012), Ottawa, June 25th-28th, 2012; CRYO2013, 50th Annual Meeting, Society for Cryobiology, Bethesda, Maryland, July 28-31, 2013.

James RS, Staples JF, **Tessier SN**, Storey KB (2012) Does hibernation affect skeletal muscle performance in 13 lined ground squirrels? Society for Experimental Biology meeting. Salzburg, Austria**,** June 29 – July 2, 2012.

Tessier SN, Luu B, Storey KB (2011) Adaptations of cardiac muscle function during mammalian hibernation. Carleton Institute for Biology Symposium, Ottawa, April 28-29th, 2011; 50th annual Canadian Society of Zoologists, Ottawa, May 12-16, 2011; CRYO2013, 50th Annual Meeting, Society for Cryobiology, Bethesda, Maryland, July 28-31, 2013; ACCryo2014, Key Largo, Florida, January 15-19, 2014.

Rouble A, **Tessier SN**, Storey KB (2011) Antiapoptotic signaling as a cytoprotection mechanism during mammalian hibernation. 50th annual Canadian Society of Zoologists, Ottawa, May 12-16, 2011; 26th Annual meeting, Federação de Sociedades de Biologia Experimental, Rio de Janeiro, Brazil, August 24-27, 2011; ACCryo 2013, Miami, Florida, USA. January 2-7, 2013.

Hefler J, **Tessier SN**, Storey KB (2011) Role of antiapoptotic signaling in mammalian hibernation. 50th annual Canadian Society of Zoologists, Ottawa, May 12-16, 2011; 26th Annual meeting, Federação de Sociedades de Biologia Experimental, Rio de Janeiro, Brazil, August 24-27, 2011; ACCryo2014, Key Largo, Florida, January 15-19, 2014.

Tessier SN, Storey KB (2010) Pioneering muscle plasticity: molecular adaptations of structural proteins in striated muscle of the Thirteen-lined ground squirrel during hibernation. 7th annual Ottawa-Carleton Institute for Biology Symposium, Ottawa, April 14th, 2010.

Tessier SN (2010) Conquering adversity: amazing tales of winter survival by hibernating mammals and the biomedical secrets they hold. Women in Science and Engineering (CU-WISE), Ottawa, April 8th, 2010.

Tessier SN, Storey KB (2009) Muscle Disuse Atrophy: The expression of Myocyte Enhancer Factor-2 in the skeletal muscle of *Spermophilus tridecemlineatus* during hibernation. 11th Annual Chemistry and Biochemistry Graduate Research Conference, Montreal, November 21-22, 2008; 6th annual Ottawa-Carleton Institute for Biology Symposium, Ottawa, April 30th, 2009; 48th annual Canadian Society of Zoologists, Toronto, May 12-16, 2009; 26th Annual meeting, Federação de Sociedades de Biologia Experimental (FeSBE), Rio de Janeiro, Brazil, August 24-27, 2011; ACCryo 2013, Miami, Florida, USA. January 2-7, 2013.

Appendix C: List of GenBank submissions

LuuBE, Tessier SN, Duford D, Storey KB (2013) Natriuretic peptide A (NPPA) mRNA, *Spermophilus tridecemlineatus*, partial cds, 206 bp linear mRNA, Accession: KC466329.1.

LuuBE, Tessier SN, Duford D, Storey KB (2013) GATA binding protein 4 (Gata4) mRNA, *Spermophilus tridecemlineatus*, partial cds, 441 bp linear mRNA, Accession: KC466328.1

LuuBE, Tessier SN, Duford D, Storey KB (2013) NK2 homeobox 5 (Nkx2-5) mRNA, *Spermophilus tridecemlineatus*, partial cds, 413 bp linear mRNA, Accession: KC466327.1

LuuBE, Tessier SN, Duford D, Storey KB (2013) Troponin I (TnI) mRNA*, Spermophilus tridecemlineatus*, partial cds, 421 bp linear mRNA, Accession: KC466326.1

LuuBE, Tessier SN, Duford D, Storey KB (2013) Troponin C (TnC) mRNA, *Spermophilus tridecemlineatus*, partial cds, 219 bp linear mRNA, Accession: KC466325.1

Tessier SN, Storey KB (2012) Myomesin 1 (MYOM1) mRNA, Ictidomys tridecemlineatus, partial cds, 507 bp linear mRNA, Accession: JQ362355.1

Tessier SN, Storey KB (2012) Desmin (DES) mRNA, Ictidomys tridecemlineatus, partial cds, 346 bp linear mRNA, Accession: JQ362354.1

Tessier SN, Storey KB (2010) Myogenic differentiation 1 (MyoD1) mRNA, *Spermophilus tridecemlineatus*, partial cds, 337 bp linear mRNA, Accession: GU434273.1

Tessier SN, Storey KB (2010) Myocyte enhancer factor 2C (Mef2C) mRNA, *Spermophilus tridecemlineatus*, partial cds, 352 bp linear mRNA, Accession: GU434272.1

Tessier SN, Storey KB (2010) Glucose transporter 4 (Glut4) mRNA*, Spermophilus tridecemlineatus*, partial cds, 290 bp linear mRNA, Accession: GU434271.1

Tessier SN, Storey KB (2010) Myocyte enhancer factor 2A (Mef2A) mRNA, *Spermophilus tridecemlineatus*, partial cds, 310 bp linear mRNA, Accession: GU434270.1

References

Abnous K, Dieni CA, Storey KB (2012) Suppression of MAPKAPK2 during mammalian hibernation. Cryobiology 65:235-241.

Afonina E, Stauber R, Pavlakis GN (1998) The human poly(A)-binding protein 1 shuttles between the nucleus and the cytoplasm. J Biol Chem 273:13015-13021. doi: 10.1074/jbc.273.21.13015

Akazawa H, Komuro I (2003) Roles of cardiac transcription factors in cardiac hypertrophy. Circ Res 92:1079-1088.

Allan ME, Storey KB (2012) Expression of NF-κB and downstream antioxidant genes in skeletal muscle of hibernating ground squirrels, *Spermophilus tridecemlineatus*. Cell Biochem Funct 30:166-174.

Anderson P, Kedersha N (2002b). Visibly stressed: the role of eIF2, TIA-1, and stress granules in protein translation. Cell Stress Chaperones 7: 213–221.

Anderson P, Kedersha N (2008) Stress granules: the Tao of RNA triage. Trends Biochem Sci 33:141-150.

Armstrong SC, Delacey M, Ganote CE (1999) Phosphorylation state of hsp27 and p38 MAPK during preconditioning and protein phosphatase inhibitor protection of rabbit cardiomyocytes. J Mol Cell Cardiol 31:555-567.

Atia1 A, Abdullah A (2014) The Nrf2-Keap1 Signalling pathway: mechanisms of ARE transcription regulation in antioxidant cellular defence. Int J Pharm Tech Res 6:154-167.

Audas TE, Jacob MD, Lee S (2012) Immobilization of proteins in the nucleolus by ribosomal intergenic spacer noncoding RNA. Mol Cell 45:147-157.

Azuma Y, Arnaoutov A, Dasso M. (2003) SUMO-2/3 regulates topoisomerase II in mitosis. J Cell Biol.163:477–487.

Barnes BM (1989) Freeze avoidance in a mammal: body temperatures below 0°C in an Arctic hibernator. Science 244*:* 1593-*1595.*

Bentley D (2002) The mRNA assembly line: transcription and processing machines in the same factory. Curr Opin Cell Biol 14:336-342.

Bernstein PS, Peltz W, Ross J (1989) The poly(A)-poly(A)-binding protein complex is a major determinant of mRNA stability in vitro. Mol Cell Biol 9:659–670.

Biamonti G, Caceres JF (2009) Cellular stress and RNA splicing. Trends Biochem Sci 34:146–153.

Biggar KK, Storey KB (2011) The emerging roles of microRNAs in the molecular responses of metabolic rate depression. J Mol Cell Biol 3: 167-175.

Bloom DA, Jaiswal AK (2003) Phosphorylation of Nrf2 at Ser40 by protein kinase C in response to antioxidants leads to the release of Nrf2 from INrf2, but is not required for Nrf2 stabilization/accumulation in the nucleus and transcriptional activation of antioxidant response element-mediated NAD(P)H:quinone oxidoreductase-1 gene expression. J Biol Chem 278:44675-44682.

Bönisch C, Hake SB (2012) Histone H2A variants in nucleosomes and chromatin: more or less stable? Nucleic Acids Res 40:10719-10741.

Boros J, Donaldson IJ, O'Donnell A, Odrowaz ZA, Zeef L, Lupien M, Meyer CA, Liu XS, Brown M, Sharrocks AD (2009) Elucidation of the ELK1 target gene network reveals a role in the coordinate regulation of core components of the gene regulation machinery. Genome Res 19:1963–1973.

Bouma HR, Verhaag EM, Otis JP, Heldmaier G, Swoap SJ, Strijkstra AM, Henning RH, Carey HV (2012) Induction of torpor: mimicking natural metabolic suppression for biomedical applications. J Cell Physiol 227:1285-1290.

Brooks NE, Myburgh KH, Storey KB (2011) Myostatin levels in skeletal muscle of hibernating ground squirrels. J Exp Biol 214:2522-2527.

Buffenstein R (2008) Negligible senescence in the longest living rodent, the naked mole-rat: insights from a successfully aging species. J Comp Physiol B 178:439-445.

Burd CG, Matunis EL, Dreyfuss G (1991) The multiple RNA-binding domains of the mRNA poly(A)-binding protein have different RNA-binding activities. Mol Cell Biol 11:3419-3424.

Busà R, Geremia R, Sette C (2010) Genotoxic stress causes the accumulation of the splicing regulator Sam68 in nuclear foci of transcriptionally active chromatin. Nucleic Acids Res 38:3005-3018.

Buzadzic B, Spasic MB, Saicic ZS, Radojicic R, Petrovic VM, Halliwell B (1990) Antioxidant defenses in the ground squirrel *Citellus citellus*. 2. The effect of hibernation. Free Rad Biol Med 9:407-413.

Cai D, McCarron RM, Hallenbeck J (2004) Cloning and characterization of a forkhead transcription factor gene, FoxO1a, from thirteen-lined ground squirrel. Gene 343:203-209.

Caiafa P, Zampieri M (2005) DNA methylation and chromatin structure: the puzzling CpG islands. J Cell Biochem 94:257-265.

Canagarajah BJ, Khokhlatchev A, Cobb MH, Goldsmith EJ (1997) Activation mechanism of the MAP kinase ERK2 by dual phosphorylation. *Cell,* 90(5): 859-69.

Caponigro G, Parker R (1995) Multiple functions for the poly(A)-binding protein in mRNA decapping and deadenylation in yeast. *Genes Dev* 9:2421-2432.

Carey HV, Andrews MT, Martin SL (2003) Mammalian hibernation: cellular and molecular responses to depressed metabolism and low temperature. Physiol Rev 83:1153-1181.

Carey HV, Frank CL, Seifert JP (2000) Hibernation induces oxidative stress and activation of NK-kappaB in ground squirrel intestine. J Comp Physiol B 170:551-559.

Cargnello M, Roux PP (2011) Activation and function of the MAPKs and their substrates, the MAPK-activated protein kinases. Microbiol Mol Biol Rev 75:50-83.

Chambers MA, Moylan JS, Reid MB (2009) Physical inactivity and muscle weakness in the critically ill. Crit Care Med 37:S337-S346.

Chan K, Kan YW (1999) Nrf2 is essential for protection against acute pulmonary injury in mice. *Proc* Natl Acad Sci USA 96: 12731-12736.

Chen N, She QB, Bode AM, Dong Z (2002) Differential gene expression profiles of Jnk1- and Jnk2-deficient murine fibroblast cells. Cancer Research 62:1300-1304.

Cheung P, Allis CD, Sassone-Corsi P (2000) Signaling to chromatin through histone modifications. Cell 103:263-271.

Choi H, Selpides PJ, Nowell MM, Rourke BC (2009) Functional overload in ground squirrels plantaris muscle fails to induce myosin isoform shifts. Am J Physiol Regul Integr Comp Physiol 297:R578–R586.

Chung D, Lloyd GP, Thomas RH, Guglielmo CG, Staples JF (2011) Mitochondrial respiration and succinate dehydrogenase are suppressed early during entrance into a hibernation bout, but membrane remodeling is only transient. J Comp Physiol B 181:699–711.

Cowan KJ, Storey KB (2003) Mitogen-activated protein kinases: new signaling pathways functioning in cellular responses to environmental stress. J Exp Biol 206:1107-1115.

Cuesta R, Laroia G, Schneider RJ (2000) Chaperone hsp27 inhibits translation during heat shock by binding eIF4G and facilitating dissociation of cap-initiation complexes. Genes Dev 14:1460-1470.

Cullinan SB, Diehl JA (2004) PERK-dependent activation of Nrf2 contributes to redox homeostasis and cell survival following endoplasmic reticulum stress. J Biol Chem 279: 20108-20117.

Cullinan SB, Zhang D, Hannink M, Arvisais E, Kaufman RJ, Diehl JA (2003) Nrf2 is a direct PERK substrate and effector of PERK-dependent cell survival. Mol Cell Biol 23:7198-7209.

Dark J (2005) Annual lipid cycles in hibernators: integration of physiology and behavior. Annu Rev Nutr 25:469-497.

Dave KR, Christian SL, Perez-Pinzon MA, Drew KL (2012) Neuroprotection: lessons from hibernators. Comp Biochem Physiol B Biochem Mol Biol 162:1–9.

Decker CJ, Parker R (1993) A turnover pathway for both stable and unstable mRNAs in yeast: evidence for a requirement for deadenylation. Genes Dev 7:1632–1643.

Denegri M, Chiodi I, Corioni M, Cobianchi F, Riva S, Biamonti G (2001) Stress-induced nuclear bodies are sites of accumulation of pre-mRNA processing factors. Mol Biol Cell 12:3502-3514.

Dhanasekaran DN, Kashef K, Lee CM, Xu H, Reddy EP (2007) Scaffold proteins of MAP-kinase modules. Oncogene 26:3185-3202.

Eddy SF, McNally JD, Storey KB (2005) Up-regulation of a thioredoxin peroxidase-like protein, proliferation-associated gene, in hibernating bats. Arch Biochem Biophys 435:103-111.

Eddy SF, Morin P Jr, Storey KB (2005) Cloning and expression of PPAR-gamma and PGC-1alpha from the hibernating ground squirrel, *Spermophilus tridecemlineatus*. Mol Cell Biochem 269:175-182.

Eddy SF, Storey KB (2007) P38 MAPK regulation of transcription factor targets in muscle and heart of the hibernating bat, *Myotis lucifugus*. Cell Biochem Funct 25:759–765.

El Kebbaj Z, Andreoletti P, Mountassif D, Kabine M, Schohn H, Dauça M, Latruffe N, El Kebaj MS, Cherkaoui-Malki M (2009) Differential regulation of peroxisome proliferator-activated receptor (PPAR)-alpha1 and truncated PPARalpha2 as an adaptive response to fasting in the control of hepatic peroxisomal fatty acid beta-oxidation in the hibernating mammal. Endocrinology 150:1192-1201.

Emara MM, Fujimura K, Sciaranghella D, Ivanova V, Ivanov P, Anderson P (2012) Hydrogen peroxide induces stress granule formation independent of eIF2α phosphorylation. Biochem Biophys Res Commun 423:763-769.

Epperson LE, Rose JC, Carey HV, Martin SL (2010) Seasonal proteomic changes reveal molecular adaptations to preserve and replenish liver proteins during ground squirrel hibernation. Am J Physiol 298:R329-R340.

Fahlman A, Storey JM, Storey KB (2000) Gene up-regulation in heart during mammalian hibernation. Cryobiology 40: 332-342.

Faustino NA, Cooper TA (2003) Pre-mRNA splicing and human disease. Genes Dev 17:419-437.

Figueroa C, Vojtek AB (2003) Akt negatively regulates translation of the ternary complex factor Elk-1. Oncogene 22:5554-5561.

Frerichs KU, Smith CB, Brenner M, DeGracia DJ, Krause GS, Marrone L, Dever TE, Hallenbeck JM (1998) Suppression of protein synthesis in brain during hibernation involves inhibition of protein initiation and elongation. Proc Natl Acad Sci USA 95:14511-14516.

Förch P, Puig O, Kedersha N, Martínez C, Granneman S, Séraphin B, Anderson P, Valcárcel J (2001) The apoptosis-promoting factor TIA-1 is a regulator of alternative pre-mRNA splicing. Mol Cell 6:1089-1098.

Fujiwara Y, Shiomi K (2006) Distinct effects of different temperatures on diapause termination, yolk morphology and MAPK phosphorylation in the silkworm, *Bombyx mori*. J Insect Physiol 52:1194–1201.

Gervois P, Torra IP, Chinetti G, Grötzinger T, Dubois G, Fruchart JC, Fruchart-Najib J, Leitersdorf E, Staels B (1999) A truncated human peroxisome proliferator-activated receptor alpha splice variant with dominant negative activity. Mol Endocrinol 13:1535-1549.

Geiser F (2004) Metabolic rate and body temperature reduction during hibernation and daily torpor. Annu Rev Physiol 66:239–274.

Gething MJ, Sambrook J (1992) Protein folding in the cell. Nature 355:33–45.

Gilks N, Kedersha N, Ayodele M, Shen L, Stoecklin G, Dember LM, Anderson P (2004) Stress granule assembly is mediated by prion-like aggregation of TIA-1. Mol Biol Cell 15:5383-5398.

Giudice A, Montella M (2006) Activation of the Nrf2-ARE signaling pathway: a promising strategy in cancer prevention. Bioessays 28:169-181.

Glozak MA, Sengupta N, Zhang X, Seto E (2005) Acetylation and deacetylation of non-histone proteins. Gene. 363:15-23.

Goldman BD[1], Goldman SL, Lanz T, Magaurin A, Maurice A (1999) Factors influencing metabolic rate in naked mole rats (*Heterocephalus glaber*). Physiol Behav 66:447-459.

Gottschald OR, Malec V, Krasteva G, Hasan D, Kamlah F, Herold S, Rose F, Seeger W, Hänze J (2010) TIAR and TIA-1 mRNA-binding proteins co-aggregate under conditions of rapid oxygen decline and extreme hypoxia and suppress the HIF-1α pathway. J Mol Cell Biol 2:345-56.

Goto H, Tomono Y, Ajiro K, Kosako H, Fujita M, Sakurai M, Okawa K, Iwamatsu A, Okigaki T, Takahashi T, Inagaki M (1999) Identification of a novel phosphorylation site on histone H3 coupled with mitotic chromosome condensation. J Biol Chem 274:25543-25549.

Gupta S, Barrett T, Whitmarsh AJ, Cavanagh J, Sluss HK, Dérijard B, Davis RJ (1996) Selective interaction of JNK protein kinase isoforms with transcription factors. EMBO Journal 15:2760-2770.

Halliwell B, Gutteridge J (2007) Free Radicals in Biology and Medicine, 4th ed., Oxford University Press, Oxford, UK.

Hargrove JL, Schmidt FH (1989) The role of mRNA and protein stability in gene expression. FASEB J 3:2360–2370.

Havlis J, Thomas H, Sebela M, Shevchenko A (2003) Fast-response proteomics by accelerated in-gel digestion of proteins. Anal Chem 75:1300–1306.

Heldmaier G, Ortmann S, Elvert R (2004) Natural hypometabolism during hibernation and daily torpor in mammals. Respir Physiol Neurobiol 141:317–329.

Hindle AG, Karimpour-Fard A, Epperson LE, Hunter LE, Martin SL (2011) Skeletal muscle proteomics: carbohydrate metabolism oscillates with seasonal and torpor-arousal physiology of hibernation. Am J Physiol Regul Integr Comp Physiol 301:R1440-R1452.

Hittel D, Storey KB (2001) Differential expression of adipose and heart type fatty acid binding proteins in hibernating ground squirrels. Biochim Biophys Acta 1522: 238-243.

Hittel D, Storey KB (2002) The translation state of differentially expressed mRNAs in the hibernating thirteen-lined ground squirrel (*Spermophilus tridecemlineatus)*. Arch Biochem Biophys 401: 244-254.

Hsu LS, Chen GD, Lee LS, Chi CW, Cheng JF, Chen JY (2001) Human Ca^{2+}/calmodulin-dependent protein kinase kinase β gene encodes multiple isoforms that display distinct kinase activity. J Biol Chem 276:31113-31123.

Huang HC, Nguyen T, Pickett CB (2000) Regulation of the antioxidant response element by protein kinase C-mediated phosphorylation of NF-E2-related factor 2. Proc Natl Acad Sci USA 97:12475-12480.

Iqbal K, Alonso AC, Chen S, Chohan MO, El-Akkad E, Gong CX, Khatoon S, Li B, Liu F, Rahman A, Tanimukai H, Grundke-Iqbal I (2005) Tau pathology in Alzheimer disease and other tauopathies. Biochim Biophys Acta 1739:198-210.

Izquierdo JM, Valcárcel J (2007) Two isoforms of the T-cell intracellular antigen 1 (TIA-1) splicing factor display distinct splicing regulation activities. Control of TIA-1 isoform ratio by TIA-1-related protein. J Biol Chem 282:19410-19417.

Jin SG, Kadam S, Pfeifer GP (2010) Examination of the specificity of DNA methylation profiling techniques towards 5-methylcytosine and 5-hydroxymethylcytosine. Nucleic Acids Res 38:e125.

Jirtle RL, Skinner MK (2007) Environmental epigenomics and disease susceptibility. Nat Rev Genet 8:253-262.

Jones BL, VanLoozen J, Kim MH, Miles SJ, Dunham CM, Williams LD, Snell TW (2013) Stress granules form in *Brachionus manjavacas* (Rotifera) in response to a variety of stressors. Comp Biochem Physiol A Mol Integr Physiol 166:375-384.

Johnson JM, Castle J, Garrett-Engele P, Kan Z, Loerch PM, Armour CD, Santos R, Schadt EE, Stoughton R, Shoemaker DD (2003) Genome-wide survey of human alternative pre-mRNA splicing with exon junction microarrays. Science 302:2141-2144.

Katoh Y, Itoh K, Yoshida E, Miyagishi M, Fukamizu A, Yamamoto M (2001) Two domains of Nrf2 cooperatively bind CBP, a CREB binding protein, and synergistically activate transcription. Genes Cells 6:857-868.

Kallunki T, Su B, Tsigelny I, Sluss HK, Dérijard B, Moore G, Davis R, Karin M (1994) JNK2 contains a specificity-determining region responsible for efficient c-Jun binding and phosphorylation. Genes Dev 8:2996-3007.

Kang KW, Lee SJ, Park JW and Kim SG (2002) Phosphatidylinositol 3-kinase regulates nuclear translocation of NF-E2-related factor 2 through actin rearrangement in response to oxidative stress.
Mol Pharmacol 62: 1001-1010.

Kawai Y, Garduño L, Theodore M, Yang J, Arinze IJ (2011) Acetylation-deacetylation of the transcription factor Nrf2 (nuclear factor erythroid 2-related factor 2) regulates its transcriptional activity and nucleocytoplasmic localization. J Biol Chem 286: 7629-7640.

Kawakami A, Tian Q, Streuli M, Poe M, Edelhoff S, Disteche CM, Anderson P (1994) Intron-exon organization and chromosomal localization of the human TIA-1 gene. J Immunol 152:4937-4945.

Kayahara M, Wang X, Tournier C (2005) Selective regulation of c-jun gene expression by mitogen-activated protein kinases via the 12-o-tetradecanoylphorbol-13-acetate-responsive element and myocyte enhancer factor 2 binding sites. Mol Cell Biol 25:3784-3792.

Kedersha N, Anderson P (2007) Mammalian stress granules and processing bodies. Methods Enzymol 431:61-81.

Kellinger MW, Song C-X, Chong J, Lu X-Y, He C, Wang D (2012) 5-Formyl- and 5-carboxyl-cytosine reduce the rate and substrate specificity of RNA polymerase II transcription. Nat Struct Mol Biol 19:831–833.

Kim EB, Fang X, Fushan AA, Huang Z, Lobanov AV, Han L, Marino SM, Sun X, Turanov AA, Yang P, Yim SH, Zhao X, Kasaikina MV, Stoletzki N, Peng C, Polak P, Xiong Z, Kiezun A, Gladyshev VN (2011) Genome sequencing reveals insights into physiology and longevity of the naked mole rat. Nature 479:223-227.

Kim W, Bennett EJ, Huttlin EL, Guo A, Li J, Possemato A, Sowa ME, Rad R, Rush J, Comb MJ, Harper JW, Gygi SP (2011) Systematic and quantitative assessment of the ubiquitin-modified proteome. Mol Cell 44:325-340.

Knight JE, Narus EN, Martin SL, Jacobson A, Barnes BM, Boyer B (2000) mRNA stability and polysome loss in hibernating Arctic ground squirrels (*Spermophilus parryii*). Mol Cell Biol 20:6374-6379.

Kobayashi A, Kang MI, Okawa H, Ohtsuji M, Zenke Y, Chiba T, Igarashi K, Yamamoto M (2004) Oxidative stress sensor Keap1 functions as an adaptor for Cul3-based E3 ligase to regulate proteasomal degradation of Nrf2. Mol Cell Biol 24:7130–7139.

Kohli RM, Zhang Y (2013) TET enzymes, TDG and the dynamics of DNA demethylation. Nature. 502:472-479.

Korner CG, Wahle E (1997) Poly(A) tail shortening by a mammalian poly(A)-specific 3'-exoribonuclease. J Biol Chem 272:10448–10456.

Kornfeld SF, Biggar KK, Storey KB (2012) Differential expression of mature microRNAs involved in muscle maintenance of hibernating little brown bats, *Myotis*

lucifugus: a model of muscle atrophy resistance. Genomics Proteomics Bioinformatics 10:295-301.

Kouzarides T (2007) Chromatin modifications and their function. Cell 128:693-705.

Kramer S, Queiroz R, Ellis L, Webb H, Hoheisel JD, Clayton C, Carrington M (2008) Heat shock causes a decrease in polysomes and the appearance of stress granules in trypanosomes independently of eIF2(alpha) phosphorylation at Thr169. J Cell Sci 121:3002-3014.

Krivoruchko A, Storey KB (2010) Forever young: mechanisms of anoxia tolerance in turtles and possible links to longevity. Oxid Med Cell Longevity 3: 186-198.

Kyriakis JM, Avruch J (2001) Mammalian mitogen-activated protein kinase signal transduction pathways activated by stress and inflammation. Physiol Rev 81:807–869.

Lander ES, Linton LM, Birren B et al (2001) Initial sequencing and analysis of the human genome. Nature 409:860-921.

Lee CC (2008) Is human hibernation possible? Annu Rev Med 59:177-186.

Lee M, Choi I, Park K (2002) Activation of stress signaling molecules in bat brain during arousal from hibernation. J Neurochem 82:867–873.

Lee K, Park JY, Yoo W, Gwag T, Lee JW, Byun MW, Choi I (2008) Overcoming muscle atrophy in a hibernating mammal despite prolonged disuse in dormancy: proteomic and molecular assessment. J Cell Biochem 104:642-656.

Lee YJ, Miyake S, Wakita H, McMullen DC, Azuma Y, Auh S, Hallenbeck JM (2007) Protein SUMOylation is massively increased in hibernation torpor and is critical for the cytoprotection provided by ischemic preconditioning and hypothermia in SHSY5Y cells. J Cereb Blood Flow Metab 27:950-962.

Lewis KN, Mele J, Hornsby PJ, Buffenstein R (2012) Stress resistance in the naked mole rat: the bare essentials - a mini-review. Gerontology 58:453-462.

Li J, Johnson D, Calkins M, Wright L, Svendsen C, Johnson J (2005) Stabilization of Nrf2 by tBHQ confers protection against oxidative stress-induced cell death in human neural stem cells. Toxicol Sci 83:313–328.

Ling C, Groop L (2009) Epigenetics: a molecular link between environmental factors and type 2 diabetes. Diabetes 58:2718-2725.

Lindquist ME, Lifland AW, Utley TJ, Santangelo PJ, Crowe JE Jr (2010) Respiratory syncytial virus induces host RNA stress granules to facilitate viral replication. J Virol 84: 12274–12284.

Liu Y, Hu W, Wang H, Lu M, Shao C, Menzel C, Yan Z, Li Y, Zhao S, Khaitovich P, Liu M, Chen W, Barnes BM, Yan J (2010) Genomic analysis of miRNAs in an extreme mammalian hibernator, the Arctic ground squirrel. Physiol Genomics 42A:39-51.

López de Silanes I, Galbán S, Martindale JL, Yang X, Mazan-Mamczarz K, Indig FE, Falco G, Zhan M, Gorospe M (2005) Identification and functional outcome of mRNAs associated with RNA-binding protein TIA-1. Mol Cell Biol 25: 9520–9531.

MacDonald JA (2004) Signal transduction pathways and the control of cellular responses to external stimuli. In: Storey KB, editor. Functional Metabolism: Regulation and Adaptation. Wiley-Liss: New York (pp. 87-123).

MacDonald JA, Storey KB (2005) Mitogen-activated protein kinases and selected downstream targets display organ-specific responses in the hibernating ground squirrel. Int J Biochem Cell Biol 37:679–691.

Maistrovski Y, Biggar KK, Storey KB (2012) HIF-1α regulation in mammalian hibernators: role of non-coding RNA in HIF-1α control during torpor in ground squirrels and bats. J Comp Physiol B 182:849-859.

Malatesta M, Biggiogera M, Baldelli B, Barabino SM, Martin TE, Zancanaro C (2008) Hibernation as a far-reaching program for the modulation of RNA transcription. Microsc Res Tech 71: 564-572.

Malatesta M, Cardinali A, Battistelli S, Zancanaro C, Martin TE, Fakan S, Gazzanelli G (1999) Nuclear bodies are usual constituents in tissues of hibernating dormice. Anat Rec 254: 389–395.

Malatesta M, Gazzanelli G, Battistelli S, Martin TE, Amalric F, Fakan S (2000) Nucleoli undergo structural and molecular modifications during hibernation. Chromosoma 109: 506–513.

Malatesta M, Luchetti F, Marcheggiani F, Fakan S, Gazzanelli G (2001) Disassembly of nuclear bodies during arousal from hibernation: an in vitro study. Chromosoma 110: 471-477.

Malatesta M, Zancanaro C, Marcheggiani F, Cardinali A, Rocchi MBL, Capizzi D, Vogel P, Fakan S, Gazzanelli G (1998) Ultrastructural morphometrical and immunocytochemical analyses of the exocrine pancreas in a hibernating dormouse. Cell Tissue Res 292:531–541.

Malatesta M, Zancanaro C, Martin TE, Chan EKL, Almaric F, Luhrmann R, Vogel P, Fakan S (1994a) Cytochemical and immunocytochemical characterization of nuclear bodies during hibernation. Eur J Cell Biol 65: 82–93.

Malatesta M, Zancanaro C, Martin TE, Chan EKL, Almaric F, Luhrmann R, Vogel P, Fakan S (1994b) Is the coiled body involved in nucleolar functions? Exp Cell Res 211: 415–419.

Malatesta M, Zancanaro C, Tamburini M, Martin TE, Fu X-D, Vogel P, Fakan S (1995) Novel nuclear ribonucleoprotein structural components in the dormouse adrenal cortex during hibernation. Chromosoma 104:121–128.

Malloy MT, McIntosh DJ, Walters TS, Flores A, Goodwin JS, Arinze IJ (2013) Trafficking of the transcription factor Nrf2 to promyelocytic leukemia-nuclear bodies: implications for degradation of NRF2 in the nucleus. J Biol Chem 288:14569-14583.

Mamady H, Storey KB (2006) Up-regulation of the endoplasmic reticulum molecular chaperone GRP78 during hibernation in thirteen-lined ground squirrels. Mol Cell Biochem 292:89-98.

Mamady H, Storey KB (2008) Coping with the stress: expression of ATF4, ATF6, and downstream targets in organs of hibernating ground squirrels. Arch Biochem Biophys 477:77-85.

Mao YS, Zhang B, Spector DL (2011) Biogenesis and function of nuclear bodies. Trends Genet 27:295-306.

Martin SL, Maniero GD, Carey C, Hand SC (1999) Reversible depression of oxygen consumption in isolated liver mitochondria during hibernation. Physiol Biochem Zool 72:255–264.

Martin AM, Pouchnik DJ, Walker JL, Wyrick JJ (2004) Redundant roles for histone H3 N-terminal lysine residues in subtelomeric gene repression in *Saccharomyces cerevisiae*. Genetics 167:1123–1132.

Martín-Subero JI (2011) How epigenomics brings phenotype into being. Pediatr Endocrinol Rev 9:506-510.

Mazan-Mamczarz K, Ashish L, Martindale JL, Kawai T, Gorospe M (2006) Translational Repression by RNA-Binding Protein TIAR. Mol Cell Biol 26: 2716–2727.

McArthur MD, Milsom WK (1991) Changes in ventilation and respiratory sensitivity associated with hibernation in Columbian (*Spermophilus columbianus*) and golden-mantled (*Spermophilis lateralis*) ground squirrels. Physiol Zool 64:940–959.

McMullen DC, Hallenbeck JM (2010) Regulation of Akt during torpor in the hibernating ground squirrel, *Ictidomys tridecemlineatus.* J Comp Physiol B 180:927-934.

Michaelidis B, Hatzikamari M, Antoniou V, Anestis A, Lazou A (2009) Stress activated protein kinases, JNKS and p38 MAPK, are differentially activated in ganglia and heart of land snail *Helix lucorum* (L.) during seasonal hibernation and arousal. Comp Biochem Physiol A 153:149–153.

Minvielle-Sebastia L, Preker PJ, Wiederkehr T, Strahm Y, Keller W (1997) The major yeast poly(A)-binding protein is associated with cleavage factor IA and functions in premessenger RNA 3'-end formation. Proc Natl Acad Sci USA 94:7897–7902.

Moore MJ (2005) From birth to death: The complex lives of eukaryotic mRNAs. Science 309: 1514-1518.

Morin P Jr, Dubuc A, Storey KB (2008a) Differential expression of microRNA species in organs of hibernating ground squirrels: a role in translational suppression during torpor. Biochim Biophys Acta 1779:628-633.

Morin P Jr, Ni Z, McMullen DC, Storey KB (2008b) Expression of Nrf2 and its downstream gene targets in hibernating 13-lined ground squirrels, *Spermophilus tridecemlineatus*. Mol Cell Biochem 312:121-129. doi: 10.1007/s11010-008-9727-3

Morin P, Storey KB (2005) Cloning and expression of hypoxia-inducible factor 1α from the hibernating ground squirrel, *Spermophilus tridecemlineatus*. Biochim Biophys Acta 1729:32-40.

Morin P Jr, Storey KB (2006) Evidence for a reduced transcriptional state during hibernation in ground squirrels. Cryobiology 53:310-318.

Morin P, Storey KB (2007) Antioxidant defense in hibernation: cloning and expression of peroxiredoxins from hibernating ground squirrels, *Spermophilus tridecemlineatus*. Arch Biochem Biophys 461:59-65.

Morin P Jr, Storey KB (2009) Mammalian hibernation: differential gene expression and novel application of epigenetic controls. Int J Dev Biol 53:433-442.

Morris GE (2008) The Cajal body. Biochim Biophys Acta 1783:2108-2115.

Morrison DK (2001) KSR: a MAPK scaffold of the Ras pathway? Journal of Cell Science 114:1609-1612.

Muñoz MJ, Pérez Santangelo MS, Paronetto MP, de la Mata M, Pelisch F, Boireau S, Glover-Cutter K, Ben-Dov C, Blaustein M, Lozano JJ, Bird G, Bentley D, Bertrand E, Kornblihtt AR (2009) DNA damage regulates alternative splicing through inhibition of RNA polymerase II elongation. Cell 137:708–720.

Nadeau SI, Landry J (2007) Mechanisms of activation and regulation of the heat shock-sensitive signaling pathways. Adv Exp Med Biol 594:100-113.

Nathaniel TI, Saras A, Umesiri FE, Olajuyigbe F (2009) Tolerance to oxygen nutrient deprivation in the hippocampal slices of the naked mole rats. J Integr Neurosci 8:123-136.

Ni J, Storey KB (2010) Heme oxygenase expression and Nrf2 signaling during hibernation in ground squirrels. Can J Physiol Pharmacol 88:379-381.

Nishimoto S, Nishida E (2006) MAPK signalling: ERK5 versus ERK1/2. EMBO Rep 7:782–786.

O'Connor TP, Lee A, Jarvis JU, Buffenstein R (2002) Prolonged longevity in naked mole rats: age-related changes in metabolism, body composition and gastrointestinal function. Comp Biochem Physiol A Mol Integr Physiol 133:835-842.

O'Hara BF, Watson FL, Srere HK, Kumar H, Wiler SW, Welch SK, Bitting L, Heller HC, Kilduff TS (1999). Gene expression in the brain across the hibernation cycle. J Neurosci 19:3781–3790.

Pan P, van Breukelen F (2011) Preference of IRES-mediated initiation of translation during hibernation in golden-mantled ground squirrels, *Spermophilus lateralis*. Am J Physiol Regul Integr Comp Physiol 301:R370-R377.

Peterson CL, Laniel M-A (2004) Histone and histone modifications. Curr Biol 14:R546-551.

Pi J, Bai Y, Reece JM, Williams J, Liu D, Freeman ML, Fahl WE, Shugar D, Liu J, Qu W, Collins S, Waalkes MP (2007) Molecular mechanism of human Nrf2 activation and degradation: role of sequential phosphorylation by protein kinase CK2. Free Radic Biol Med 42:1797–1806.

Piecyk M, Wax S, Beck ARP, Kedersha N, Gupta M, Maritim B, Chen S, Gueydan C, Kruys V, Streuli M, Anderson P (2000) TIA-1 is a translational silencer that selectively regulates the expression of TNF-α. EMBO J 19: 4154-4163.

Pogo BG, Allfrey VG, Mirsky AE (1966) RNA synthesis and histone acetylation during the course of gene activation in lymphocytes. Proc Natl Acad Sci USA 55:805–812.

Proud CG (2002) Control of the translational machinery in mammalian cells. Eur J Biochem 269: 5337.

Qi M, Elion EA (2005) MAP kinase pathways. J Cell Sci 118:3569–3572.

Rachakonda G, Xiong Y, Sekhar KR, Stamer SL, Liebler DC, Freeman ML (2008) Covalent modification at Cys151 dissociates the electrophile sensor Keap1 from the ubiquitin ligase CUL3. Chem Res Toxicol 21:705-710.

Ramos JW (2008) The regulation of extracellular signal-regulated kinase (ERK) in mammalian cells. Int J Biochem Cell Biol 40:2707–2719.

Reichard JF, Petersen DR (2006) Involvement of phosphatidylinositol 3-kinase and extracellular regulated kinase in hepatic stellate cell antioxidant response and myofibroblastic trans differentiation. Arch Biochem Biophys 446: 111–118.

Ripaud L, Maillet L, Cullin C (2003) The mechanisms of [URE3] prion elimination demonstrate that large aggregates of Ure2p are dead-end products. EMBO J 22:5251-5259.

Rose BA, Force T, Wang Y (2010) Mitogen-activated protein kinase signaling in the heart: angels versus demons in a heart-breaking tale. Physiol Rev. 90:1507-1546.

Ross J (1995) mRNA stability in mammalian cells. Microbiol Rev 59:423-450.

Rouble AN, Helfer J, Mamady H, Storey KB, Tessier SN (2013) Anti-apoptotic signaling as a cytoprotective mechanism in mammalian hibernation. Peer J 1:e29.

Sachs AB, Davis RW (1989) The poly(A) binding protein is required for poly(A) shortening and 60S ribosomal subunit-dependent translation initiation. Cell 58:857-867.

Saitoh H, Hinchey J. (2000) Functional heterogeneity of small ubiquitin-related protein modifiers SUMO-1 versus SUMO-2/3. J Biol Chem. 275:6252–6258.

Shan YX, Liu TJ, Su HF, Samsamshariat A, Mestril R, Wang PH (2003) Hsp10 and Hsp60 modulate Bcl-2 family and mitochondria apoptosis signaling induced by doxorubicin in cardiac muscle cells. J Mol Cell Cardiol 35:1135-1143.

Shao C, Liu Y, Ruan H, Li Y, Wang H, Kohl F, Goropashnaya AV, Fedorov VB, Zeng R, Barnes BM, Yan J (2010) Shotgun proteomics analysis of hibernating arctic ground squirrels. Mol Cell Proteomics 9:313-326.

Shevchenko A, Wilm M, Vorm O, Mann M (1996) Mass spectrometric sequencing of proteins from silver-stained polyacrylamide gels. Analytical Chemistry 68:850–858.

Shveygert M, Kaiser C, Bradrick SS, Gromeier M (2010) Regulation of eukaryotic initiation factor 4E (eIF4E) phosphorylation by mitogen-activated protein kinase occurs through modulation of Mnk1-eIF4G interaction. Mol Cell Biol 30:5160-5167.

Singh RK, Cooper TA (2012) Pre-mRNA splicing in disease and therapeutics. Trends Mol Med 18:472-482.

Staples JF (2011) Maintaining metabolic balance in mammalian hibernation and daily torpor. In: Nowakowska A, Caputa M (eds) Hypometabolism: Strategies of Survival in Vertebrates and Invertebrates. Research Signpost, Kerala, pp 95-115.

Stieler JT, Bullmann T, Kohl F, Tøein Ø, Brückner MK, Härtig W, Barnes BM, Arendt T (2011) The physiological link between metabolic rate depression and tau phosphorylation in mammalian hibernation. PLoS One 6:e14530.

Srere HK, Wang LC, Martin SL (1992) Central role for differential gene expression in mammalian hibernation. Proc Natl Acad Sci USA 89:7119-7123.

Storey KB (1996) Oxidative stress: animal adaptations in nature. Braz J Med Biol Res 29: 1715-1733.

Storey KB (2003) Mammalian hibernation: transcriptional and translational controls. Adv Exp Med Biol 543:21-38.

Storey KB (2010) Out cold: biochemical regulation of mammalian hibernation - a mini-review. Gerontology 56:220-230.

Storey KB (2014) Regulation of hypometabolism: insights into epigenetic controls. J Exp Biol Submitted

Storey KB, Storey JM (1990) Facultative metabolic rate depression: molecular regulation and biochemical adaptation in anaerobiosis, hibernation, and estivation. Quart Rev Biol 65:145-174.

Storey KB, Storey JM (2004a) Mammalian hibernation: biochemical adaptation and gene expression. In: Storey KB (ed) Functional metabolism: regulation and adaptation. John Wiley & Sons, New Jersey, pp 442-471.

Storey KB, Storey JM (2004) Metabolic rate depression in animals: transcriptional and translational controls. Biol Rev Camb Philos Soc 79: 207-233.

Storey KB, Storey JM (2007) Putting life on 'pause' – molecular regulation of hypometabolism. J Exp Biol 210: 1700-1714.

Storey KB, Storey JM (2010) Metabolic rate depression: the biochemistry of mammalian hibernation. Adv Clin Chem 52:77-108.

Storey KB, Storey JM (2011) Heat shock proteins and hypometabolism: adaptive strategy for proteome preservation. Res. Rep. Biol. 2:57-68.

Strahl BD, Allis CD (2000) The language of covalent histone modifications. Nature 403:41-45.

Strange RC, Jones PW, Fryer AA (2000) Glutathione S-transferase: genetics and role in toxicology. Toxicol Lett 112-113: 357-363.

Sun Z, Chin YE, Zhang DD (2009a) Acetylation of Nrf2 by p300/CBP augments promoter-specific DNA binding of Nrf2 during the antioxidant response. Mol Cell Biol 29:2658-2672.

Sun Z, Huang Z, Zhang DD (2009b) Phosphorylation of Nrf2 at multiple sites by MAP kinases has a limited contribution in modulating the Nrf2-dependent antioxidant response. PLoS One 4:e6588.

Suswam EA, Li YY, Mahtani H, King PH (2005) Novel DNA-binding properties of the RNA-binding protein TIAR. Nucleic Acids Res 33:4507-4518.

Taguchi K, Motohashi H, Yamamoto M (2011) Molecular mechanisms of the Keap1–Nrf2 pathway in stress response and cancer evolution. Genes Cells 16:123-140.

Tamburini M, Malatesta M, Zancanaro C, Martin TE, Fu X-D, Vogel P, Fakan S (1996) Dense granular bodies: a novel nucleoplasmic structure in hibernating dormice. Histochem Cell Biol 106: 581–586.

Tan M, Luo H, Lee S, Jin F, Yang JS, Montellier E, Buchou T, Cheng Z, Rousseaux S, Rajagopal N, Lu Z, Ye Z, Zhu Q, Wysocka J, Ye Y, Khochbin S, Ren B, Zhao Y (2011) Identification of 67 histone marks and histone lysine crotonylation as a new type of histone modification. Cell 146:1016-1028.

Tao J, Wang HY, Malbon CC (2010) AKAR2-AKAP12 fusion protein "biosenses" dynamic phosphorylation and localization of a GPCR-based scaffold. Journal of Molecular Signaling 5:3.

Taupin JL, Tian Q, Kedersha N, Robertson M, Anderson P (1995) The RNA-binding protein TIAR is translocated from the nucleus to the cytoplasm during Fas-mediated apoptotic cell death. Proc Natl Acad Sci USA 92: 1629–1633. doi: 10.1073/pnas.92.5.1629

Tessier SN, Storey KB (2010) Expression of myocyte enhancer factor-2 and downstream genes in ground squirrel skeletal muscle during hibernation. Mol Cell Biochem 344:151-162.

Tessier SN, Storey KB (2012) Myocyte enhancer factor-2 and cardiac muscle gene expression during hibernation in thirteen-lined ground squirrels. Gene 501:8-16.

Theodore M, McIntosh D, Kawai Y, Arinze IJ (2010) Sumoylation impacts the transcriptional activity of Nrf2 and is necessary for its localization to promyelocytic leukemia nuclear bodies. FASEB J Supplement 859.4.

Thomas MC, Chiang CM (2006) The general transcription machinery and general cofactors. Crit Rev Biochem Mol Biol 41:105-178.

Tøien Ø[1], Blake J, Edgar DM, Grahn DA, Heller HC, Barnes BM (2011) Hibernation in black bears: independence of metabolic suppression from body temperature. Science 331:906-909.

Turjanski AG, Vaque JP, Gutkind JS (2007) MAP kinases and the control of nuclear events. Oncogene 26: 3240–3253.

Van Breukelen F, Sonenberg N, Martin SL (2004) Seasonal and state-dependent changes of eIF4E and 4E-BP1 during mammalian hibernation: implications for the control of translation during torpor. Am J Physiol Regul Integr Comp Physiol 287:R349-R353.

Van Breukelen F, Sonenberg N, Martin SL (2004) Seasonal and state-dependent changes of eIF4E and 4E-BP1 during mammalian hibernation: implications for the control of translation during torpor. Am J Physiol Regul Integr Comp Physiol 287:R349-R353.

Villeneuve NF, Lau A, Zhang DD (2010) Regulation of the Nrf2–Keap1 antioxidant response by the ubiquitin proteasome system: an insight into cullin-ring ubiquitin ligases. Antioxid Redox Signal 13:1699-1712.

Vucetic M, Stancic A, Otasevic V, Jankovic A, Korac A, Markelic M, Velickovic K, Golic I, Buzadzic B, Storey KB, Korac B. (2013) The impact of cold acclimation and hibernation on antioxidant defenses in the ground squirrel (*Spermophilus citellus*): An update. Free Radic Biol Med 65C:916-924.

Waetzig V, Herdegen T (2005) Context-specific inhibition of JNKs: overcoming the dilemma of protection and damage. Trends Pharmacol Sci 26:455-461.

Wang LCH, Lee TF (1996) Torpor and hibernation in mammals: metabolic, physiological, and biochemical adaptations. In: Fregley MJ, Blatteis CM (eds) Handbook of Physiology: Environmental Physiology. Oxford University Press, New York, pp 507-532.

Whitmarsh AJ, Davis RJ (1996) Transcription factor AP-1 regulation by mitogen-activated protein kinase signal transduction pathways. J Mol Med 74:589-607.

Whitmarsh AJ, Shore P, Sharrocks AD, Davis RJ (1995) Integration of MAP kinase signal transduction pathways at the serum response element. Science 269:403–407.

Wolozin B (2012) Regulated protein aggregation: stress granules and neurodegeneration. Mol Neurodegener 7:56.

Wu CW, Storey KB (2012) Regulation of the mTOR signaling network in hibernating thirteen-lined ground squirrels. J Exp Biol 215:1720-1727.

Wu GS (2004) The functional interactions between the p53 and MAPK signaling pathways. Cancer Biol Ther 3:156-161.

Xu F, Mao C, Ding Y, Rui C, Wu L, Shi A, Zhang H, Zhang L, Xu Z (2010) Molecular and enzymatic profiles of mammalian DNA methyltransferases: structures and targets for drugs. Curr Med Chem 17:4052-4071.

Yan J, Barnes BM, Kohl F, Marr TG (2008) Modulation of gene expression in hibernating arctic ground squirrels. Physiol Genom 32:170-181.

Yang SH, Sharrocks AD, Whitmarsh AJ (2003) Transcriptional regulation by the MAP kinase signaling cascades. Gene 27:320:321.

Yang SH, Whitmarsh AJ, Davis RJ, Sharrocks AD (1998). Differential targeting of MAP kinases to the ETS-domain transcription factor Elk-1. EMBO J 17:1740–1749.

Yu R, Chen C, Mo YY, Hebbar V, Owuor ED, Tan TH, Kong AN (2000) Activation of mitogen-activated protein kinase pathways induces antioxidant response element-mediated gene expression via a Nrf2-dependent mechanism. J Biol Chem 275: 39907-39913.

Yuan L, Chen J, Lin B, Liang B, Zhang S, Wu D (2007) Up-regulation of a non-kinase activity isoform of Ca(2+)/calmodulin-dependent protein kinase kinase beta1 (CaMKKbeta1) in hibernating bat brain. Comp Biochem Physiol B Biochem Mol Biol 146:438-444.

Zancanaro C, Malatesta M, Vogel P, Osculati F, Fakan S (1993) Ultrastructural and morphometrical analyses of the brown adipocyte nucleus in a hibernating dormouse. Biol Cell 79: 55–61.

Zatzman ML (1984) Renal and cardiovascular effects of hibernation and hypothermia. Cryobiology 21:593–614.

Zentner GE, Henikoff S (2013) Regulation of nucleosome dynamics by histone modifications. Nat Struct Mol Biol 20:259-266.

Zhang DD, Lo SC, Cross JV, Templeton DJ, Hannink M (2004) Keap1 is a redox-regulated substrate adaptor protein for a Cul3-dependent ubiquitin ligase complex. Mol Cell Biol 24:10941-10953.

Zhang T, Delestienne N, Huez G, Kruys V, Gueydan C (2005) Identification of the sequence determinants mediating the nucleo-cytoplasmic shuttling of TIAR and TIA-1 RNA-binding proteins. J Cell Sci 118:5453-5463.

Zhao S, Shao C, Goropashnaya AV, Stewart NC, Xu Y, Tøein Ø, Barnes BM, Fedorov VB, Yan J (2010) Genomic analysis of expressed sequence tags in American black bear *Ursus americanus*. BMC Genomics 11:201.

Zheng C, Lin Z, Zhao ZJ, Yang Y, Niu H, Shen X (2006) MAPK-activated protein kinase-2 (MK2)-mediated formation and phosphorylation-regulated dissociation of the signal complex consisting of p38, MK2, Akt, and Hsp27. J Biol Chem 281:37215-37226.

Zhu X, Smith MA, Perry G, Wang Y, Ross AP, Zhao HW, LaManna JC, Drew KL (2005) MAPKs are differentially modulated in arctic ground squirrels during hibernation. J Neurosci Res 80:862–868.

Zimber A, Nguyen QD, Gespach C (2004) Nuclear bodies and compartments: functional roles and cellular signalling in health and disease. Cell Signal 16:1085-104.